

**DESIGN OF
STRUCTURAL CONCRETE USING STRUT-AND-
TIE MODEL AND APPLICATION TO SOME
SPECIAL STRUCTURES**

**BY
AZIZ MOHAMMED**

**A THESIS
SUBMITTED TO
THE SCHOOL OF GRADUATE STUDIES OF
ADDIS ABABA UNIVERSITY**

**IN
PARTIAL FULFILLMENT OF THE REQUIREMENTS
FOR THE DEGREE OF MASTER OF SCIENCE IN
CIVIL ENGINEERING (STRUCTURES)**

SEPTEMBER 2004

**ADDIS ABABA UNIVERSITY
SCHOOL OF GRADUATE STUDIES**

**LITERATURE REVIEW: DESIGN OF
STRUCTURAL CONCRETE USING STRUT-AND-
TIE MODEL AND APPLICATION TO SOME
SPECIAL STRUCTURES**

BY

AZIZ MOHAMMED

APPROVED BY BOARD OF EXAMINERS

ADVISOR

EXTERNAL EXAMINER

INTERNAL EXAMINER

CHAIRMAN

DECLARATION

This Thesis is my original work and has not been presented for a degree in any university and that all sources of material used in the Thesis have been dually acknowledged.

Candidate

Name

Signature

ACKNOWLEDGEMENTS

I would like to take this opportunity to express my sincere appreciation to my advisor Dr-Ing Girma Z/Yohannes, Addis Ababa University, Faculty of Technology, for his supervision and guidance during the period I was carrying out this research. I am also deeply grateful to Dr-Ing Adil Zekeria, for his guidance and excellent comments on the contents of this thesis.

Particular thanks also go to Ato Girmay Kahsaay of the Ethiopian Airports Enterprise for his willingness to assist me so that the research work may be carried out on time. Finally, I would like to express my sincere appreciation for my dear brother Ato Abdulwasie Rashid who has been a constant source of encouragement in my life, and to all my friends who have been supportive in this venture. I am deeply grateful to all of them.

TABLE OF CONTENTS

I	Acknowledgements	iii
II	Table of contents	iv
III	List of tables	vii
IV	List of figures	viii
V	Abstract	xiii
CHAPTER 1		
1.1	Introduction to the Thesis	1
1.2	The Study Issues	2
1.2.1	Statement of the Problem	2
1.2.2	Objectives of the Thesis	3
1.2.3	The Study Design and Methodology	4
1.2.4	Application of the Study	4
1.2.5	Scopes and Limitations of the Study	4
CHAPTER 2		
2.1	Literature Review: Brief History of Design Development	6
2.2	Truss Analogy	6
2.3	Development of the Strut-and-Tie Model	9
CHAPTER 3		
3.1	Design Of Structural Concrete Using Strut-and-Tie Model	10
3.2	Definition of Application of Strut-and-tie model	11
3.2.1	B-regions	13

3.2.2	D-regions	14
3.2.3	Steps in Identification and Analysis of B and D regions	16
3.3	General Analysis Procedure	18
3.4	Stresses in Members (Stress Trajectories)	20
3.5	Constructing the Strut-and-Tie models using the Load Path Method	22
3.6	Selection of Optimal model	24
3.7	Typical Representation Strut-and-Tie Model of Regions	26
3.7.1	Typical B-regions	26
3.7.2	Typical D-region Models	33
3.8	Design Criteria of Strut-and-Tie Model members	47
3.8.1	Ties Members	48
3.8.2	Strut or Compression Members	48
3.8.3	Nodes	55
CHAPTER 4		62
4.1	Application of Strut-and-Tie Model – Example 1	62
4.2	Data of the deep Beam	62
4.2.1	Design Procedure	62
4.3	Application of STM-Example 2	69
4.3.1	Corbel	69
4.3.2	Design Procedure	71
4.3.3	Some Typical Corbel STM models	77
CHAPTER 5		78
5.1	Design of Special Structures Using Strut-and-Tie Model	78

5.2	System Description	78
5.3	Design and Analysis Assumptions	82
5.4	Loading on the structure	82
5.5	Structural Modeling and Applied Loading	85
5.6	Input data	90
5.6.1	Loading	90
5.6.2	Geometry	91
5.7	Overall Analysis of the Monument	92
5.8	Analysis and Design Using the Strut-and-Tie model	93
5.8.1	Boundary forces determined as initial step	94
5.8.2	Disc Region: STM modeling	99
5.8.3	Statical Calculation for Disc Region	101
5.8.4	Inclined Column STM model and Statical Calculation	114
5.8.5	Reinforcement Summary	118
Chapter 6		119
6.1	Conclusion	119
6.2	Recommendation	120
Annex		121
Annex 1		121
References		127
Signed Declaration Sheet		129

List of Tables

Table 5.1 Coefficient of wind load, magnification factor and wind loads at different height.....	84
Table 5.2 Forces acting on the PP section, forces acting at top of disk	98
Table 5.3 Forces acting on the section KK, forces at the bottom of disk	98
Table 5.4 Forces acting on section MM, or the bottom of the inclined column	98
Table 5.5 Reinforcement layouts for the Disk and Column regions	118

List of Figures

Fig 2.1 A simple beam with cantilever loaded at top with truss analogy model	7
Fig 2.2 Internal forces of a cracked beam Shear transfer in beam	8
Fig. 3.1 Stress trajectory for one half a deep beam and classification into B and D-region	10
Fig. 3.2 A simplified stress direction for the half-deep beam	11
Fig 3.3 Stress distribution variation for a point load on a section	12
Fig 3.4 D-regions (a) geometrical discontinuities (b) statical and/or geometrical Discontinuities	15
Fig 3.5 Detail showing limits of D-regions (1) in deep beam (2) in dapped-end beam	17
Fig 3.6 Frame structure divided into B- and D-regions, loading and bending moments	18
Fig 3.7 D-region with boundary actions a) beam-column connection b) stress on footing / deep beam c) Equivalent axial forces	19
Fig 3.8 A typical D-region: a) elastic trajectories, elastic stresses and STM model b) diagram of internal forces, internal lever arm z and strut angle θ	21
Fig 3.9 Load path and STM model a) boundary pressure replaced by equivalent load b) single point force eccentrically loaded	22
Fig 3.9 Two STM models with identical boundary load: (a) oblique & (b) orthogonal reinforcement	23
Fig. 3.11 Half of a deep beam with point load a) simplified model b) refined model	25
Fig 3.12 Trial models for deep beam a) good model b) bad model with considerable tie ...	26
Fig. 3.13 B1 region a) the boundary forces b) tie inclination α c) reinforcement layout d) with vertical tie e) reinforcement layout	27
Fig. 3.14 B2-region a) the boundary forces b) truss model c) reinforcement layout	28
Fig. 3.15 B3 region a) the boundary forces b) two STM and the sum	

c) reinforcement layout	29
Fig. 3.16 B4 region a) the boundary forces b) STM model c) reinforcement layout d) B4 in structure	30
Fig. 3.17 B5 region a) the boundary forces b) STM model c) reinforcement	31
Fig. 3.18 B6 region a) boundary forces b) resultant compression C_w c) refined STM model d) reinforcement layout	32
Fig 3.19 Region D1 region a) principal stress pattern b) transverse stress distribution for different a/l c) STM for large depth d) for short depth	34
Fig. 3.20 Region D2 region a) the stresses diagram b) the STM model	36
Fig. 3.21 Region D3 region a) principal stress pattern b) stress distribution for different c) refined model d) strut-and-tie	37
Fig. 3.22 Region D4 a) principal stress trajectory b) stress distribution c) & d) the STM model	38
Fig. 3.23 Region D5 a) principal stress trajectory b) stress distribution c) & d) strut and tie model	39
Fig. 3.24 Type D6 a) principal stress trajectory b) stress distribution c) & d) the strut and tie model	40
Fig 3.25 Type D7 a) principal stress trajectory b) stress distribution c) simplified d) refined STM	41
Fig 3.26 Type D8 a) principal stress pattern b) stress distribution c) & d) STM model ...	42
Fig. 3.27 Region D9 a) principal stress pattern b) stress distribution c) STM model d) location of D9 [2]	43
Fig. 3.28 Region D10 a) the principal stress pattern b) stress distribution c) the strut and tie model	44
Fig. 3.29 a) location of D11 & D12 in the structure b) STM models c) the refined STM model	45
Fig. 3.30 Region D12 a) location in structure b) STM model	46
Fig 3.31 Prismatic strut stress distribution.....	49
Fig 3.32 Illustration of compressive stress field with their fan stress flow	50

Fig 3.33	Bottle shaped strut a) confined to the width b) unconfined section	51
Fig 3.34	Diagonal compression strut a) prismatic strut b) bottle shaped model c) STM model	52
Fig 3.35	Reinforcement ratio for concrete& bold curve for plain concrete a) confined to the width b) bottle shaped stress distribution c) two b) phases of concrete strength d) STM model e) reinforcement layout	54
Fig 3.36	Simply supported deep beam a1) STM model a2) stress distribution a3) refined tie layout	55
Fig 3.37	Node N2 with two different idealizations, detail as N2a and N2b	56
Fig 3.38	Node N6 a) single tie with anchorage at the mid of the node b) single layer tie with full node anchorages c) multiple layer of ties with full anchorage	57
Fig 3.39	Node N2l, narrower load area of N2, STM model and reinforcement layout	59
Fig 3.40	Node N6l a) STM with moved node b) narrower width c) transverse force reinforcement	61
Fig 3.41	Node N11, beam-column connection b) STM model c) reinforcement	61
Fig 4.1	Simply supported deep beam, dimensions and loading	62
Fig 4.2	Deep beam, division of the section into D-regions	63
Fig 4.3	Half of deep beam and boundary forces	64
Fig 4.4	Half-Deep beam a) STM trial model 1 b) STM trial model 2	65
Fig 4.5	Half of deep beam a) refined STM model b) Reinforcement layout (main and transverse force)	67
Fig. 4.6	Corbel, dimensions and loadings	70
Fig. 4.7	Corbel with preliminary dimensions	71
Fig 4.8	Strut-and-tie model of a corbel for the loading and dimensions	73
Fig 4.9	Corbel with the width of the struts and tie reinforcement layout.....	76
Fig. 4.10	Three typical corbels STM for different loading and possible	77
Fig 5.1	Architectural features of the monument a) four elevations b) two elevations	81

Fig 5.2	Software model of the Monument a) line element b) solid element	
	c) shell element (c1 & c2)	89
Fig 5.3	Wind load for line modeling of the monument	90
Fig 5.4	Critical sections PP, KK and MM of the monument	91
Fig 5.5	Geometric dimensions at sections PP, KK and MM 1) actual dimensions	
	2) modified dimension	92
Fig 5.6	D-regions, disc and inclined column with protrusion	93
Fig 5.7	Stress at the boundary of D region replaced by an equivalent couple action.	95
Fig 5.8	Schematic representation of equivalent axial force	97
Fig 5.9	Section PP, KK and MM in the monument	99
Fig 5.10	Plan of the focus area, section X-X and Y-Y	99
Fig 5.11	Section Y-Y a) boundary actions b) Equivalent axial force and STM model	100
Fig 5.12	Two dimensional STM near column A, the boundary force and STM	101
Fig 5.13	Boundary forces and STM representation of compression section of node	102
Fig 5.14	Boundary forces on the tension side of disc near column A, a) & b) simple	
	truss c) & d) the refined STM with practical reinforcement layout	103
Fig. 5.15	Column type truss due o the adjoining simple truss in region near column 1	105
Fig 5.16	Reinforcement layout of region near column 1	106
Fig 5.17	Reinforcement layout of the Disk near Column A	107
Fig. 5.18	Boundary forces and STM model of region near column 4	107
Fig 5.19	Boundary forces and STM model of compression forces near column B	108
Fig 5.20	Boundary forces and STM model for tension forces (column B)	110
Fig 5.21	Boundary forces and refined STM model for tension forces	110
Fig 5.22	Boundary forces and STM representation of compression section of node	112
Fig 5.23	Reinforcement of Disc region near Column B	113

Fig 5.24 Reinforcement layout for the region near Column 1	114
Fig 5.25 The boundary force on the inclined Column 1 and Column 4.	115
Fig 5.26 Uniform column dimension for design of the truss model	115
Fig 5.27 Inclined columns with STM model	116
Fig 5.28 Reinforcement layout of inclined column.	118
Fig. A1. SAP 2000N – File Trus_thesis4 – Axial Force Diagram (Comb 1)	121
Fig. A2. SAP 2000N – File Trus_thesis4 - Moment 3-3 Diagram (Comb 1)	122
Fig. A3. SAP 2000N – File Trus_thesis4 - Moment 2-3 Diagram (Comb 1)	123
Fig. A4. SAP 2000N v7.21 – Restraint Reactions (COMB 1) [18].....	124
Fig. A4. SAP 2000N v7.21 – Moment 3-3 Diagram (COMB 1) [18]	125
Fig. A5. SAP 2000N v7.21 – Moment 2-2 Diagram (COMB 1) [18]	126

ABSTRACT

Through out history engineers have been looking for ways of designing structures that are simple and would accurately model real life objects. In order to achieve this, actual structures have to be modeled in such a way that they become amenable to analysis. This was mainly achieved by a mathematical modeling. Whilst many parts of structures can be modeled mathematically to relate accurately with the test results, some parts of a structure notably, where there are openings and discontinuities pose a problem. This is basically due to the inability to model them accurately, resulting in difficulty of obtaining reliable estimate of the stress values. On this line therefore various modeling approaches, for such regions of discontinuity have been proposed. These sections of “*discontinuity*” or in short “*D-regions*” include beam-column connections, areas of openings etc. These sections have been difficult to understand and analyze in the design of structures. Therefore, the question arises, how can all components of a structure be analyzed and hence understood and designed with equal accuracy? What alternative analysis approaches are possible?

In the past many structural analysis approaches have been developed to address the various problems faced in real life. Some of the advanced features include the *non-linear stress analysis*, *finite element method*, etc. further to this the strut-and-tie modeling has been developed as an alternative structural analysis method to address regions of discontinuity, whose analysis has so far been addressed through the conventional analysis approach.

The strut-and-tie model is a powerful tool for analyzing the structures in areas of disturbances or discontinuity in either geometry or statics. Hence, designing such special structures and

predicting their behavior will increase the possibility of using them in confidence, as well as making them safe.

The objective of this thesis is therefore to introduce a brief actual review of the theoretical background, definitions of the strut-and-tie model, its compliance to the real world, brief example of selected structures (as an application of the Strut-and-tie model to real structure) and designing of a special structure. The final result gives structural engineers options of analysis approaches capable of application to all types of systems. By considering an alternative approach to current design approaches this study will be applicable to the analysis and design of special structures such as beam-column connections, openings in the shear walls, deep beams above large opening of a building (for circulation), corbels, monuments etc.

The literature survey of the topic has encompassed review of landmark papers on this topic, textbooks, journals and available literature. Finally, two typical structures and one special structure, a monument, are designed in an attempt to visualize the Strut-and-tie model.

CHAPTER 1

1.1 Introduction to the Thesis

The design of structural members involves the analysis of the effects of loads or actions on the components and proportioning to resist them. Such an approach involves the determination of the internal forces distribution and their magnitude. Traditionally the forces are determined from assuming linear stress-strain distribution, as plane sections remain plane and the subsequent design is based on this linear assumption. In reality, however the stress distribution especially when it comes to structures such as deep beams is not linear, nor is the distribution known in the case of beam-column connections, etc. In order to take account of any uncertainties in this assumption, design approaches rely on the provision of detailing and other measures, implying that such structures may not be designed in a systematic and logical way.

In order to overcome such anomalies, there have been attempts of alternative analysis techniques designed to give a realistic estimate of stresses in regions of such discontinuity. The strut-and-tie model has been one of such attempts to propose a logical alternative analysis technique.

The strut-and-tie model is a powerful tool for analyzing the structures in areas of disturbances or discontinuity in either geometry or static cases. Designing the special structures and predicting their behavior will increase the possibility of using them in confidence, and it will also increase the performance of the structure as whole in safety and as well as economy.

1.2 The Study Issues

The issues considered in this study include the statement of the problem, the objectives of the study, the design and methodology and its application as well as the scope and limitations. All these are discussed in the following section in some detail.

1.2.1 Statement of the Problem

In the design of structures, the analysis of sections is carried out in order to give a realistic assessment of the stress distributions and hence the required strengths that are necessary to make the structure safe for use. In the history of structural design, great stride has been done in understanding the behavior of sections of structure under loading, and the associated stresses. Nevertheless, not all sections of a structure have been amenable to such analysis and understanding. For these sections, however, the final design has been based on what is called “rule of thumb” approach or the use of experience in determining possible responses and hence provision of the required material for its proper operation. This included careful detailing and provisions of protective measures to cater for possible demands of the structure under use. Such rule of thumb approach varies from place to place and no single approach can be recommended to be the best one.

The above discussion clearly show that the behavior of certain part of structure have been understood in better detail than others, although all sections of a structure are equally important in the safe service requirements. Some of the sections that have not been fully understood include what are called sections of “*discontinuity*” or in short “*D-regions*”, such as beam-column connections, areas of openings etc. These sections have been difficult to understand and

analyze in the design of structures. Therefore, the question arises, how can all components of a structure be understood equally and designed with equal accuracy? What alternative analysis approaches are possible?

The standard method of design cannot apply to the D-region (discussed later) because these regions are usually cracked sections and their behavior is non-linear. To achieve a design procedure that is consistent and applicable for every part of the member needs to be developed. At the same time, it needs to base on a realistic physical method. One such method, the Strut-and-Tie Model will be adapted to the structures as an appropriate solution.

1.2.2 Objectives of the Thesis

The objective of this thesis is therefore to introduce a theoretical background, definitions of the strut-and-tie model, its compliance to the real world, brief example of selected structures (as an application of the Strut-and-tie model to real structure). In doing so, the result gives structural engineers options of analysis approaches capable of application to all types of systems.

The objectives are therefore:

- To review literature on the strut-and-tie modeling approach
- To familiarize the strut-and-tie method of analysis
- To analyze a strut-and-tie model approach and compare with the elastic stress analysis
- To review an alternative approach to design based on strut-tie model of analysis
- To design special structures visualizing the response of the structure to the actions
- To solve numerical examples as applied to a particular special structure.

1.2.3 The Study Design and Methodology

The methodology for carrying out the research work has focused on the review of literature, journals and Internet resources. Particularly three landmark papers by Professor Schlaich [1, 2, 3] of the University of Stuttgart and his coworkers have been the bases for the recent development of the strut-and-tie modeling approach. Various data obtained from literatures are analyzed and interpreted. The result of structure using the non-linear analysis with the help of software vs. the Strut-and-Tie model is considered. Finally, based on these observations, conclusions and recommendations are formulated.

1.2.4 Application of the Study

By considering an alternative approach to current design approaches this study will be applicable to the analysis and design of special structures such as beam-column connections, openings in the shear wall, deep beams above large opening of a building (for circulation), corbels, monuments etc. These are few of the application area of the strut-and-tie model.

The strut-and-tie model is best used for the structure in the non-linear stress strain distribution even though it can be applied to linear section. It helps designers to visualize the effect of actions on every part of section. Once the designer is familiar with the method it will be easy to deal with special structures and come up with solution for those discontinues that may be difficult to analyze using current standard analysis approaches.

1.2.5 Scopes and Limitations of the Study

Due to the complexity of analysis of three-dimensional structures, the thesis content deals only with two-dimensional analysis of sections. However, if the structure's response in three-

dimensional plane is required, the rectangular plane may be looked at from differing orthogonal planes. Generally, modeling a structure in three-dimensional parameters tends to become cumbersome and complicates analysis; hence, the necessity to define it in two dimensions results in simplification of the analysis of the problem. Thought this was a limitation in modeling a structure, a 2-Dimensional STM approach yields rather a conservative result.

The focus of this thesis is limited to members with constant cross section. However, there is a possibility of treating some non-uniform cross sections by dividing them into uniform cross sections and adding up the results to obtain the stresses for the actual structure, as this procedure involves iteration it is best accomplished using a computer program.

The strut-and-tie model is different for differing load cases. Even for a particular loading, several models are constructed but obtaining the optimal model requires a lot of effort and the results of such modeling analysis may not give the final exact results. It is however, possible to obtain an optimal solution by refining the model to represent the actual internal flow of forces. On this line, the thesis gives guide for the selection of the best of the proposed models.

CHAPTER 2

2.1 Literature Review: Brief History of Design Development

Humankind has been constructing different structures for various objectives, and ever since the beginning of civilization, the need for a systematic analysis and design of structures has been pursued with vigor. This pursuit has had an objective of developing an analysis/design system that may be uniformly applied to all structure rendering safe and usable structures. Some of these approaches have obtained from experience or “rule of thumb” and confirmed by tests.

In the history of design of structures many systems of designing and proportioning structures were developed. Some of these analysis methods used for *simple determinate structure*: includes the geometric method, energy method, etc. Whereas for *simple* and *complex indeterminate structures* a more enhanced ones like force method, displacement method, matrix method, finite element method etc are adapted. All of these methods give safe and economical results for areas with linear stress-strain distribution range. The methods mentioned above, however do not show the flow of force and as a result give understanding of the behavior of the structures. Therefore, members that are different from the normally encountered standard type are designed based on the past experience.

2.2 Truss Analogy

One of the most common structures found in real life are trusses. Trusses have been in use in bridges roof structures, etc. In addition, their analysis has been well understood and standardized.

An Italian architect, Anddrea Palladio (1518-1580), is believed to have developed the first truss. His extensive work on the analysis and design of the trusses is in use until today. His concept of analysis is based on using axial forces i.e. tension and compression forces. This type of approach was exclusively used for the analysis of trusses and was not applied to other structural elements.

In 1899 a Swiss engineer named Ritter [4] and a German engineer named Morsch [5] (1902) proposed the use of the concepts of truss analysis for the understanding of forces in reinforced concrete beam and termed “truss analogy”. This concept of truss analogy, attempts to analyze the forces in members by converting the internal stresses to forces similar to those found in truss members namely compression and tension. For instance a simply supported reinforced concrete beam, shown in Fig. 2.1, is loaded with a uniform load. As can be observed the applied loading on the beam develops actions along inclined sections that resemble a truss with diagonal members.

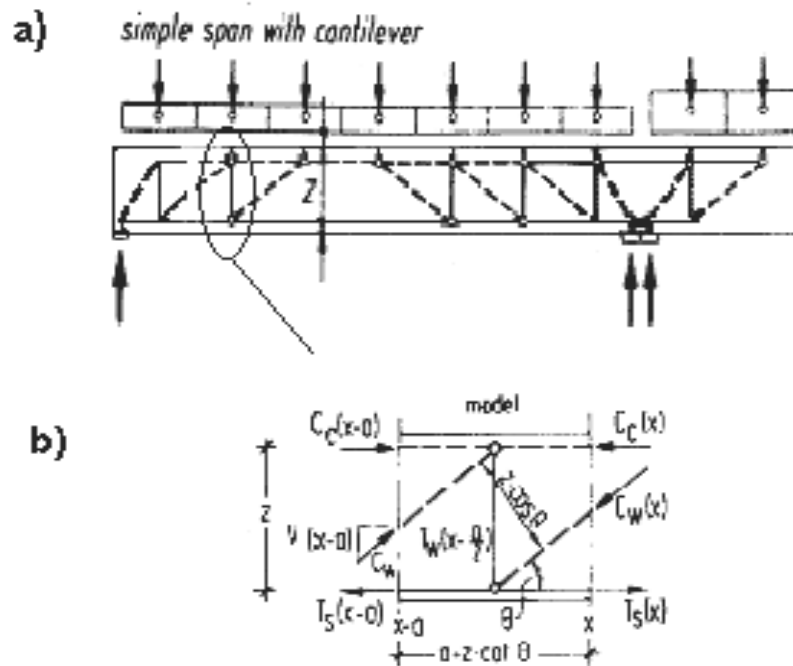
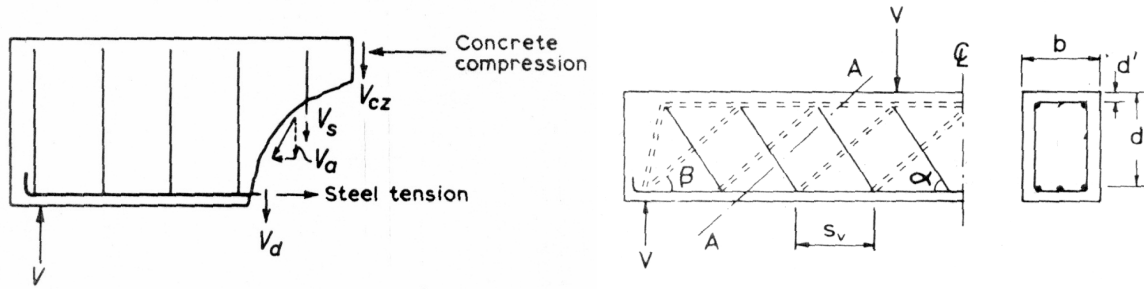


Fig 2.1 A simple beam with cantilever loaded at top with truss analogy model [2]

If we increase the applied loads on the beam, it fails due to diagonal cracking near the supports. The internal forces in the cracked section will form a pattern that is similar to truss system.



a) shear failure of beam

b) inclined stirrup to resist the shear

Fig 2.2 Internal forces of a cracked beam Shear transfer in beam [6]

The internal forces in the cracked section are resisted by the shear capacity, V_{sd} , of the beam and is estimated by the following expression:

$$V_{sd} = (V_{cz} + V_d + V_a) + V_s \quad \dots (1)$$

Where,

V_{cz} = shear strength of un-cracked concrete

V_d = shear strength of reinforcement

V_a = shear strength of inter locking due to crack section

V_s = shear strength of the stirrup

The main characteristic of failure in the above diagram is diagonal shear type of failure at the support section. These failure mechanisms may be mitigated by the provision of steel members to resist the diagonal failure or to interrupt the lines of cracks notably by providing stirrups. However, before any meaningful interpretation of the actions inside the cracked area can be made it needs to be defined mathematically. The most suitable modeling of this action may be done with resemblance to the actions inside members.

However, a beam with inclined cracks, as in Fig 2.2, develops compressive force C on the top “flanges”, tensile forces T in its bottom “flanges”, vertical tensions in the stirrups and inclined compressive forces in the concrete “diagonals” between the inclined cracks. An analogous truss replaces this highly indeterminate system and hence, we have the truss analogy type of analysis.

In general, the idea of a truss analogy for design of reinforced concrete beams for concrete has the conceptual scheme of showing the forces in the cracked beam section, which is highly indeterminate, by replacing it with an equivalent truss or “truss analogy”.

2.3 Development of the Strut-and-Tie Model

In the early days, engineers attempted different approaches to solve the common problem of structural engineering. Several papers were published and some have been further developed. In the same way, several publishers has been working in the line of “avoiding the use of rule of thumb” and to come up with a more rational design method.

Researchers such as Leonhardt [8], Rusch [9], and Kuper [10] have continued to explore the application of the truss method to analyze structures with a further application to determination of the shear capacity of members. However, it is only after the work of Thurlimann’s Zurich [11] School with Marti [7] and Mueller [12] that created the rational application in tracing it back to the theory of plasticity. After intensive laboratory tests and data correlation, Bay, Franz, Leonhardt and Thurlimann had shown various applications that strut-and-tie models could be applied to deep beams and corbels. In recent works, Cook/Michelle [13] uses the truss model to determine the forces in a structure. The approach of the various authors cited above differs in the treatment of the prediction of ultimate load and the satisfaction of serviceability requirements.

For such analysis to be practically relevant, the outputs obtained have to correlate with sufficient accuracy so that structures designed by such concepts are practical. These issues of finding results that are close to reality is an ongoing research and needs to be enhanced further.

CHAPTER 3

3.1 Design Of Structural Concrete Using Strut-and-Tie Model

Structural members transfer the applied load to their support through either direct axial force and/or flexural actions. From these actions, the internal forces at every point can be plotted to visualize the flow of forces in the structural members. These simplified plots of the stress trajectory resembles flow net type of diagram such as that shown below, Fig. 3.1.

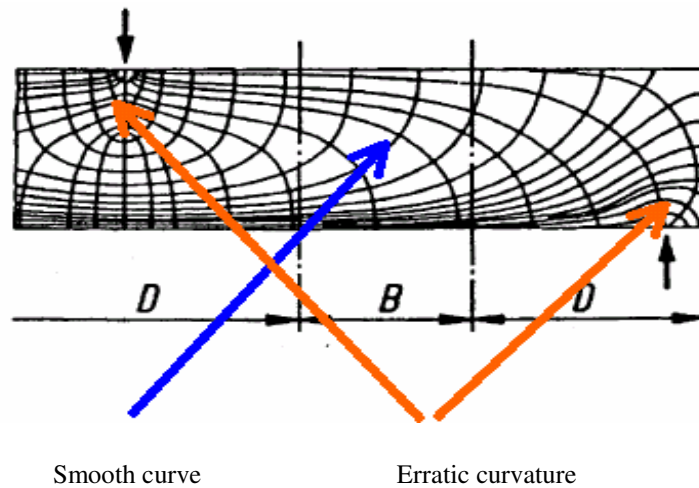


Fig. 3.1 Stress trajectory of half a deep beam for a point load and sub-division of the beam into B and D-region [1].

With the help of flow net diagram the effect of internal forces, either tension or compression, can be visualized easily. If an accurate understanding of the type/magnitude of the stresses in such a stress trajectory can be accurately understood, it may be possible to mitigate their actions so that the stressed member adequately copes with their effect.

If we attempt to further simplify the above structure and attempt to understand the stress trajectories we may obtain the following figure.

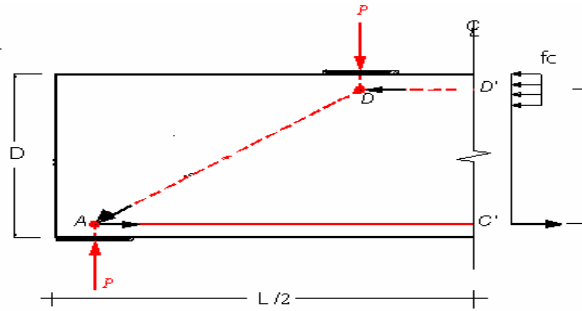


Fig. 3.2 A simplified stress direction for the half-deep beam

It has been observed from test and actual practice that a member loaded as per the above figure yields the indicated principal stress directions. This, it can easily be observed, resembles a diagonal member of truss. By analogy we may replace the stress trajectory by a simple truss. This analogy makes analysis conducive. Because the concept of truss analysis and design is well developed and understood its application by analogy to a reinforced concrete members makes analysis/design of such members easily applicable.

Therefore, in order to develop this analogy further, we need to define the truss analogy concept further. Any truss member is designed to carry either compression or tension forces. Members carrying compression are termed “struts” while those carrying tension are termed ties. Therefore, Strut-tie or compression-tension modeling of structural elements in order to make them easily analyzed.

3.2 Definition of Application of Strut-and-tie model

In standard structural analysis/design, members that are loaded with concentrated or distributed loads develop stress. The distribution of stresses is normally assumed to be linear or what is known as Bernoulli’s principle. However, in actual situation, the stresses at the point of

application of loads or the point of connection of members is significantly different from this assumption.

For instance, the variation of the stress distribution under a concentrated load over the depth of sections away from the point of application of the load is shown below.

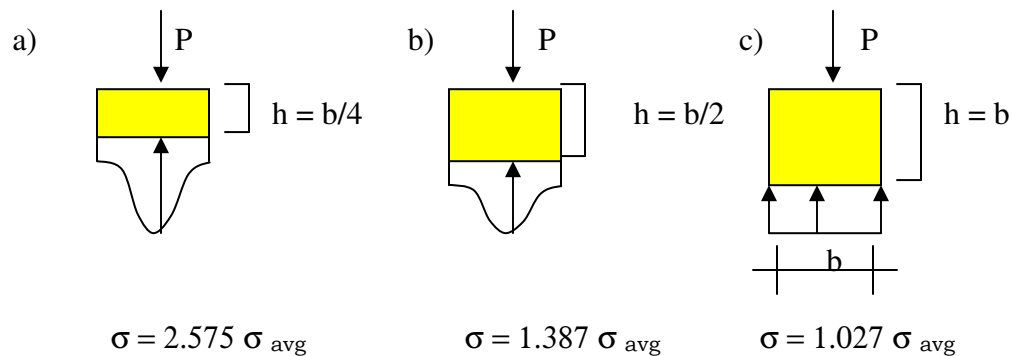


Fig. 3.3 Stress distribution for a point load on a section (a) at $\frac{1}{4}$ of the width of the section (b) at $\frac{1}{2} b$ depth and (c) at b depth [14].

Where, b = width of the structure

P = axial force on the structure

σ_{avg} = average stress P/A

σ = stress at a depth h

It can be seen that as the depth is increased the stress is decreased and becomes uniform. This is contrary to the usual assumption of a uniform stress distribution at all points of a structure, usually assumed in standard analysis.

Such instance occurs at supports of structures say beam to column connections or at the point of concentrated loads. We term such regions, regions of Discontinuity or D-regions. Any other

regions are termed as B-region or Bernoulli regions, where it is assumed that the stress distribution is linear.

The usual assumption that when an axial load applied on a member is distributed uniformly over the whole width will be reasonably accurate only after some depth from the loading point. The stress distribution beneath a concentrated load on a member varies with depth and width from the point of application, Fig 3.3. This shows that the stress distribution becomes more or less uniform in sections further from the application point and the stress distribution in transverse direction becomes approximately equal.

In summary, structural members are divided into two regions, *B-region* and *D-regions*. B stands for *Beam or Bernoulli* and represents those regions where beam theory or Bernoulli's hypothesis of plane strain distribution is applicable and assumed valid. The other portion, where the beam theory does not apply, is *D-regions or Discontinuous regions*.

3.2.1 B-regions

B-regions are found in beams and slabs with uniform load application where the section remains constant throughout and a linear stress distribution is assumed. The internal state of stress of such sections is derived by standard structural analysis methods, using the effects of the actions, such as bending moment, torsional moment, shear forces, etc.

In B-regions, loads are carried by the sectional resisting actions of the structural members. Most of the time, B-regions are un-cracked when the applied moment is less than the cracking moment ($M < M_{cr}$), and their internal state of stress is easily derived from the sectional property. The

sectional effects, the bending moment (M), Axial force (N), Shear force (V), Torsional moment (M_t) are determined using the elastic analysis- based on Hook's law and finite element method, using the sectional property such as area, second moment of inertia, etc.

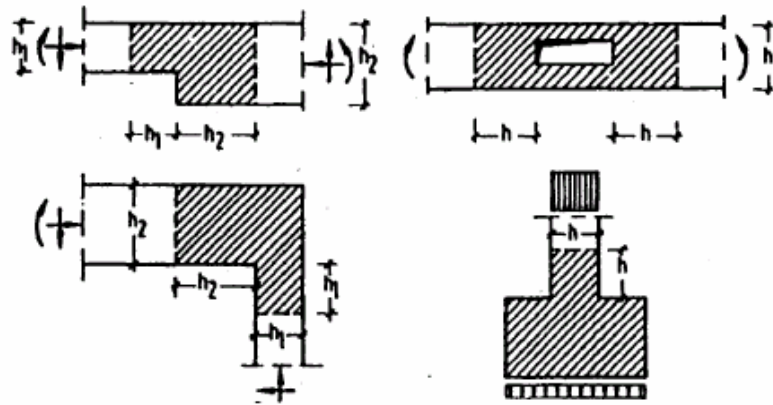
The formation of cracks, when the applied moment is greater than the moment carrying capacity of the section ($M_{cr} < M$), in the structure will disrupt the linear stress field and compels it to reorient the stress in a different manner. Then the structure starts to behave in a different way and the sectional property or rather the sectional capacity cannot be estimated easily as for un-cracked section.

Structures like slabs, which are predominantly linear, can be assumed as imaginary strip of linear members. As usual B-regions can be evaluated with the truss model, Fig 2.1, or using the standard method analysis. From this analysis, we get the boundary forces on B-regions that are applied in the D-regions. Then we can analyze the D-region alone as if the member is loaded with the boundary force or stresses.

3.2.2 D-regions

Regions, where the stress strain distribution is not linear, are called D-regions and are usually located near changes either in geometry (geometrical disturbances) or in location of concentrated forces (loading or supports). Some examples of the D-regions are deep beams, corbels, beams with, region near concentrated loadings, supports, connections, etc, as shown in Fig. 3.4.

a)



b)

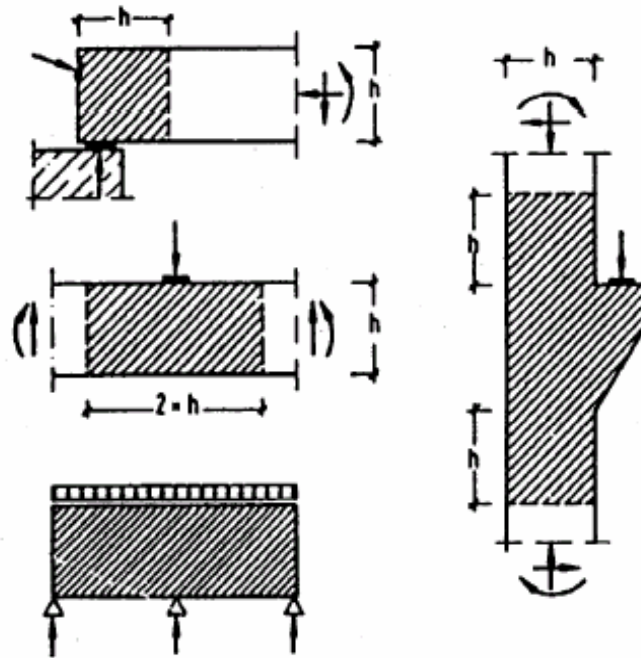


Fig 3.4 D-regions (shaded area) with nonlinear strain distribution due to (a) geometrical discontinuities (b) statical and/or geometrical discontinuities [1]

The stress distribution in D-region is not linear and the usual linear stress distribution is not applicable. Hence, the effects applied may be significantly affected by the magnitude and location of load application.

3.2.3 Steps in Identification and Analysis of B and D regions.

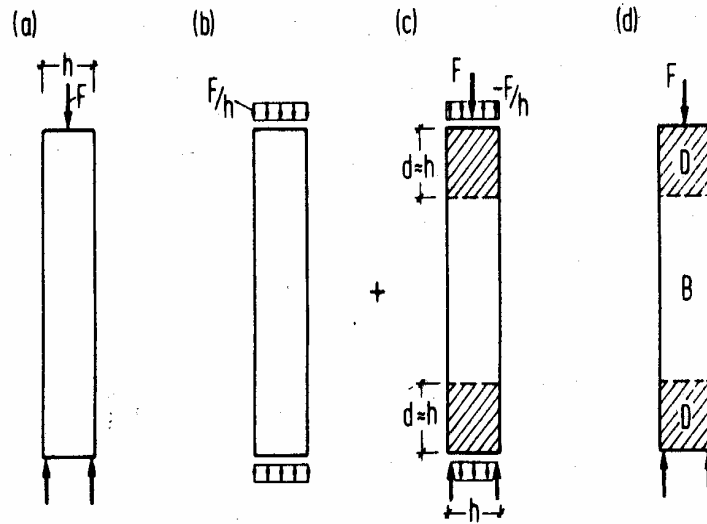
The first step in the stress analysis of a structure using the Strut-and-tie model is to define the respective B and D- regions, using both loading and geometry parameters. A further enhancement of this definition will focus on the concept of static discontinuities, where there is a sudden load change and geometric discontinuities where the structure changes suddenly. These are also forms of discontinuity.

There may also be the combination of the two discontinuities as in corbels or dapped-end beam with concentrated load closer to the support. Sometimes the regions are close that they overlap and will be considered as a single D-region.

As a general principle of defining B- and D-regions, Macgregor [6] suggests the following steps:

- Step 1. Replace the real structure Fig. 3.5a by fictitious one. Though the boundary equilibrium and the Bernoulli hypothesis should be satisfied at all times, Fig. 3.5b usually violates the actual boundary conditions.
- Step 2. Select a self-equilibrating state of stress as in Fig. 3.5c, which if superimposed on Fig. 3.5b satisfies the real boundary conditions of Fig. 3.5a.
- Step 3. Apply the Saint-Venants principle to Fig. 3.5c and determine the length over which the stress becomes negligible and, this depth is approximately equal to the width of the structure. This length ultimately distinguishes the D-region, Fig. 3.5d.

1)



2)

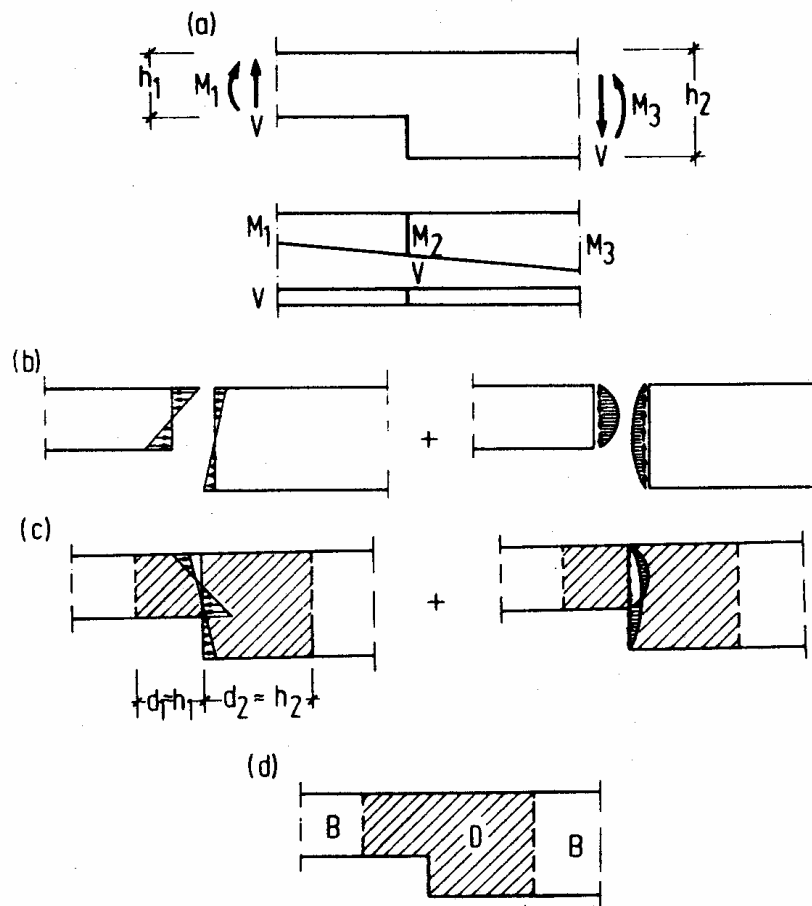


Fig 3.5. Detail showing different D-regions (1) identifying the D-region in deep beam, disturbance in statics only (2) identifying the D-region in dapped-end beam, disturbance in geometry [1]

3.3 General Analysis Procedure

It is usually difficult and cumbersome to start modeling a whole structure with strut-and-tie models. Dividing the structure into sub regions usually simplifies the overall analysis, for instance the following figure illustrated the approaches that may be used to model a structure into a Strut-and-tie modeling approach.

Steps in analysis

1. The first step in the analysis of structure that we would later desire to analyze as a Strut-and-tie model is to carry out an overall or global analysis using the standard analysis procedure. This may be a computer analysis or other standard methods. The output from such an overall analysis yields the boundary actions on the sub regions.
2. Subsequently the structure is categorized into B and D regions according to the procedure state in the previous section, fig. 3.6.

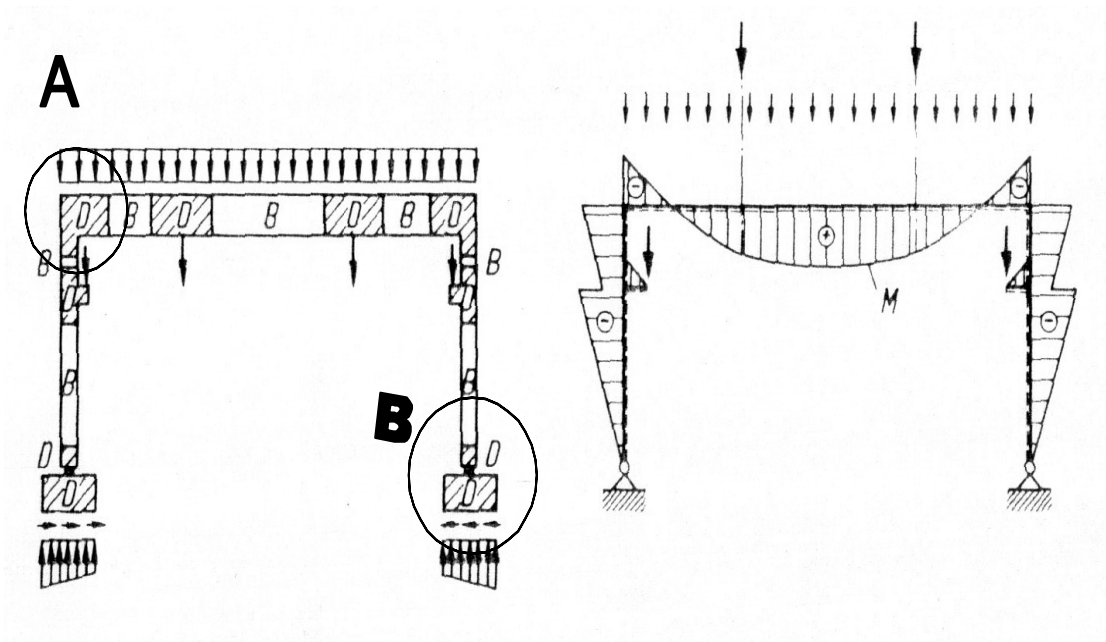


Fig. 3.6 A frame structure divided into B- and D-regions, statical system and its bending moments [2]

3. The boundary actions obtained from the global analysis are applied at the regions and the Strut-and-tie model approach is applied.
4. The stress at the ends of the B and D-regions is the same, that is linear, and the following expression is applied.

$$\sigma = My/I \pm P/A \quad \dots (2)$$

5. The boundary actions (axial forces, shear forces and bending moment), obtained from equilibrium are applied on the boundary of the D-regions and they are converted to equivalent axial forces in a systematic way to find their equivalents on the other boundary that used in Strut-and-tie model analysis, see the figure below.

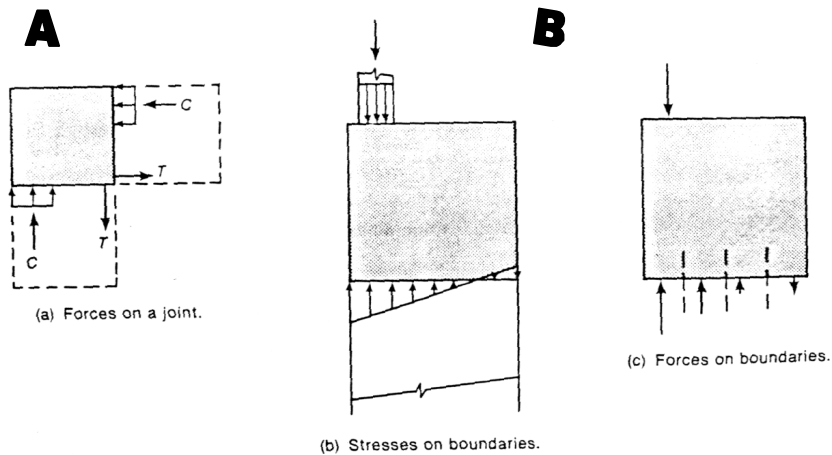


Fig 3.7 D-region with boundary stress distribution a) detail A- beam-column connection b) detail B- stress on the base of eccentrically loaded deep beam c) equivalent forces from the boundary stress of detail B.[6]

6. After the boundary internal actions are obtained the truss members are economically proportioned to resist these actions, with due consideration of to crack width, etc.

7. The final stage of this procedure is checking of the members dimension so that the dimensions provide correspond with the actual structural limitations. If this is not satisfied, the whole structure may have to be re-analyzed.

3.4 Stresses in Members (Stress Trajectories)

In design of reinforced concrete, we adapt two approaches;-

1. Un-cracked section: whereby the section is considered uncracked and linear stress distribution is assumed
2. Cracked sections, whereby the section is considered cracked and/or the stress distribution is non-linear.

Whilst it is a normal procedure to use both approaches for design, it is current practice to proportion members based on cracked sections or non-linear (parabolic) stress distribution in concrete.

In STM analysis it is assumed that the section being analyzed is cracked, hence a non-linear stress distribution governs. Members that are overstressed will usually fail in cracking, the crack path being a path of higher stress in the region. If we plot the stress trajectories of these high load distribution in a member, we may observe, the potential areas of failure or over stressing.

Therefore, by aligning our STM on the lines of high stress trajectories we may obtain a more realistic representation of the structure, stresses prior to failure or close to failure. This will give us the stresses at the lower bound plasticity.

One point to observe is that there is only one best STM model representation, in our attempt to align them with the trajectories of the stress, even though it might have several possible STM models constructed in the absence of the stress trajectory. From several possible trial models, it is possible to obtain the optimum alignment as per the recommendation of Schlaich [2]. As a general principle, the final STM model should coincide with the general inclination of the diagonal cracks, as in Fig 3.8.

The deep beam, for instance, with uniform load on top and supported at the ends is modeled as shown in the fig 3.8. The horizontal compression strut C and the tensile tie T are located at the statical center of the stress diagram. The length of the moment arm 'z' is developed from placing the couple axial forces on their center of application. 'z' affects the stresses developed in the tie. Larger arm means steeper inclination but lower stresses in the tie. The moment arm 'z' will be determined by applying mechanics of material at the point of maximum bending moment and at the same time where the shear is zero.

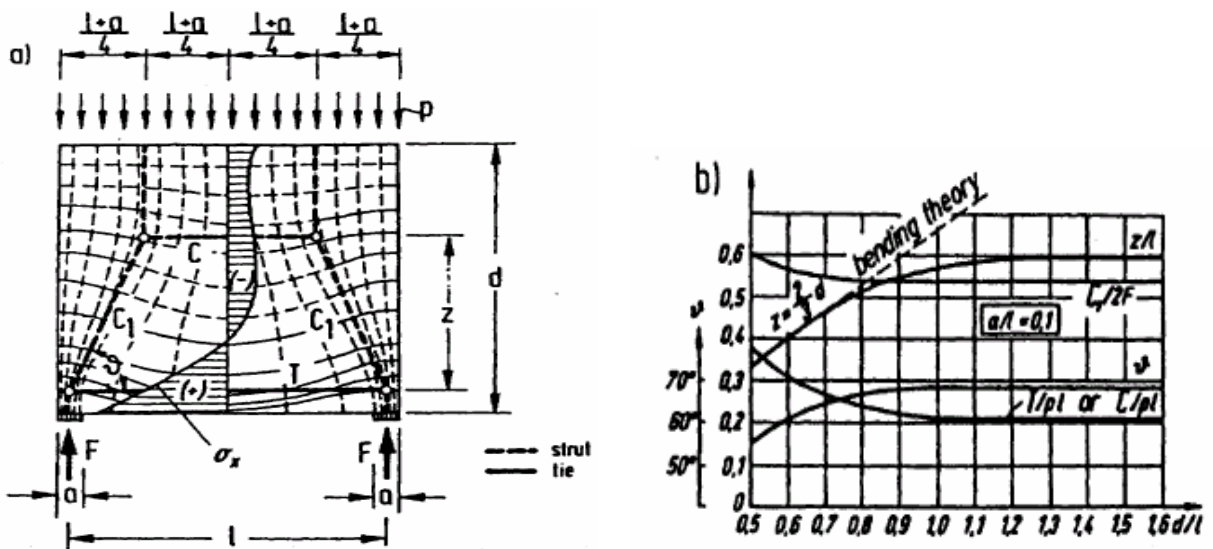


Fig 3.8 A typical D-region: a) elastic trajectories, elastic stresses and strut-and-tie model b) diagram of internal forces, internal lever arm z and strut angle θ . [2]

The depth 'z' is kept constant, for simplicity, between two adjacent points of zero moments. Fig 3.8b shows the variation of the moment arm 'z' between the bending theory and the strut-and-tie model for different span to depth ratio. The strut-and-tie model is superior in the region with a larger ratio of d/l i.e. in D-regions.

3.5 Constructing the Strut-and-Tie models using the Load Path method

In actual practice, it may be difficult to plot the stress trajectories without using specialized computer programs. This may therefore make the STM application rather difficult. As an alternative to the stress trajectory type of approach to STM a simplified *load path method* has been proposed.

This concept basically states that after obtaining the boundary forces an attempt is made to plot the path that these loads will follow from boundary to boundary. The load paths shall not cross each other. This can be seen in a simplified approach of the stress trajectory itself. Once we plot the load path, we may then reorient our STM along these paths. The following figure illustrates this approach.

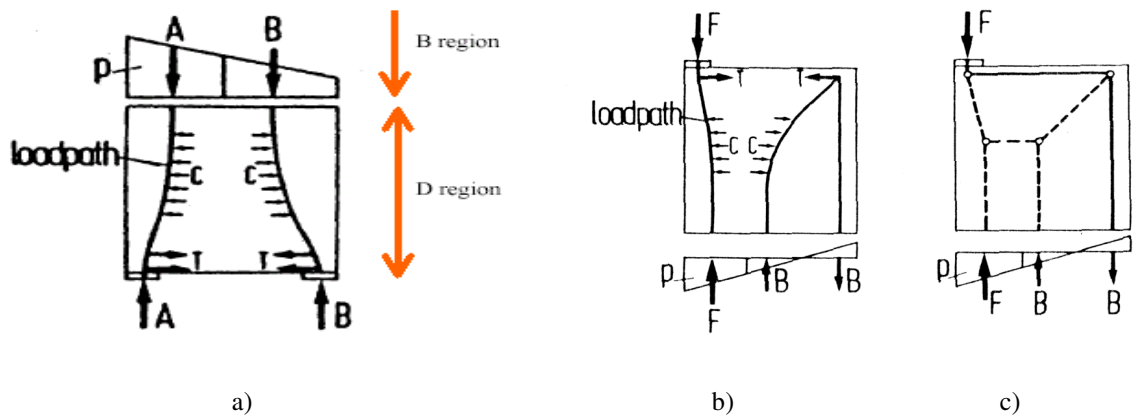


Fig 3.9 Load path and strut and tie model, the transverse compression and tension a) boundary pressure replaced by equivalent load b) single point force eccentrically loaded.[1]

The load path method is a powerful way to construct the strut-and-tie model. The figure above, fig 3.9, illustrate qualitatively for a structure with linearly varying stress distribution on the top and fully support from below. Each region's boundary equilibrium shall be satisfied. Then sub divide the boundary stress distribution of the region in such a way to find their equal counter part on the other end of boundary. The boundary forces obtained by subdividing the boundary stress are applied through the center of gravity of each subdivision and then connected with from boundary to boundary by a streamline.

Curvature of the streamline concentrate near nodes: supports, concentrated location of point load. In the vicinity of curvature, it requires gradual change in the force direction and there develops a transverse axial force; compressive C and tensile T in Fig 3.9a & b. C and T shall be equal to satisfy equilibrium. After establishing the load path, a straight-line shortest polygon replaces the streamline. A further illustration of this approach is shown below, Figure 3.10.

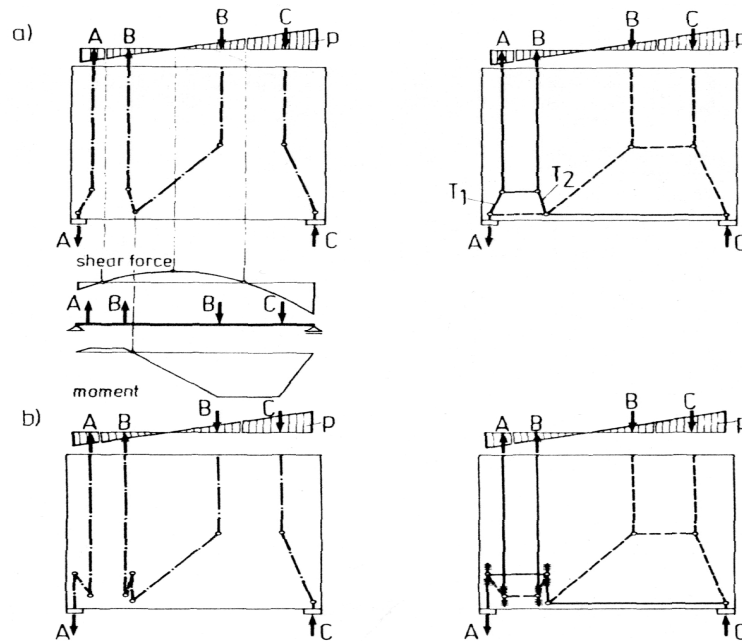


Fig 3.10 Two models for identical boundary load, internal stress and strut-and-tie model: (a) requiring oblique reinforcement (b) modified for orthogonal reinforcement [1]

When dividing the boundary forces some of the equilibrating forces found on the boundary i.e. their start and end is from the same boundary, Fig. 3.9 and Fig. 3.10. With the help of load path method, the strut-and-tie model will be easy to visualize and drawn that forms a U-turn path for the boundary force. One of the lines extending from the boundary forms a tie and the other strut. To satisfy the change in direction and equilibrium, an additional strut and tie have to be included. The internal forces introduced are then computed.

3.6 Selection of Optimal model

As can be seen in the above diagram, a number of possible STM models may be selected for the same loading. This then leaves us with the question, which is the most optimal and practical model that best resembles the actual stress distribution?

This approach of selecting the optimal models leads us to select an efficient one that requires minimum energy. The principle of minimum energy states that forces travel along the shortest path and with minimum deformation. The deformation in a member is from the contribution of both concrete and tie. In view of the fact that the strain in the concrete is small and negligible compared to the strain in the tie, it is safe to consider steel strain only. Therefore, a model with the minimum steel tie will be selected. Schlaich [1] summarizes this concept in the following expression:

$$\sum T_i l_i = \text{Minimum} \quad \dots (3a)$$

Where T_i = tensile force in the member

l_i = length of an element

For the exceptional case where the struts carry significant stress over considerable length and result in large strain in concrete, the above equation is modified to include this fact and the general form of the Eq. 3a to:

$$\sum F_i l_i \epsilon_{mi} = \text{Minimum} \quad \dots (3b)$$

Where: F_i = forces in strut or tie i

T_i = forces in tie i

l_i = length of member i

ϵ_{mi} = mean strain of member i

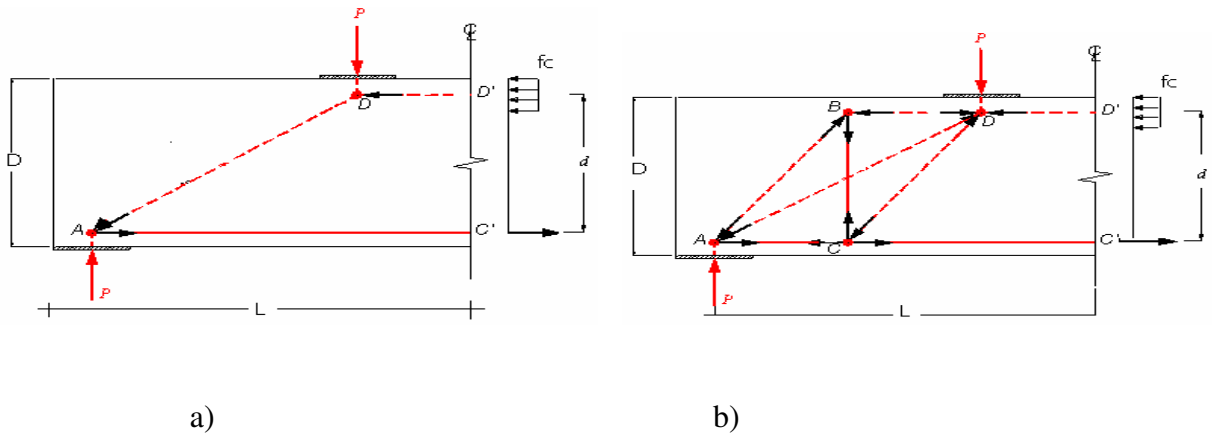


Fig. 3.11 half of deep beam loaded with point load a) simplified model b) refined model with better representation

The above formula, Eq.3, helps in eliminating the less suitable models but do not give the final solution. For example, both models in Fig 3.11 form a stable truss. Their member forces are determined in the usual way for both cases. Not only Fig. 3.11a uses less tie reinforcement but also reasonable orientation of the ties compared to model Fig. 3.11b. Moreover, applying the formula shows the same result in selecting a model, Fig. 3.11a. In special cases, models with higher steel are selected in order to have practical layout as in Fig. 3.12. The above criterion helps in eliminating less desirable models, figure below.

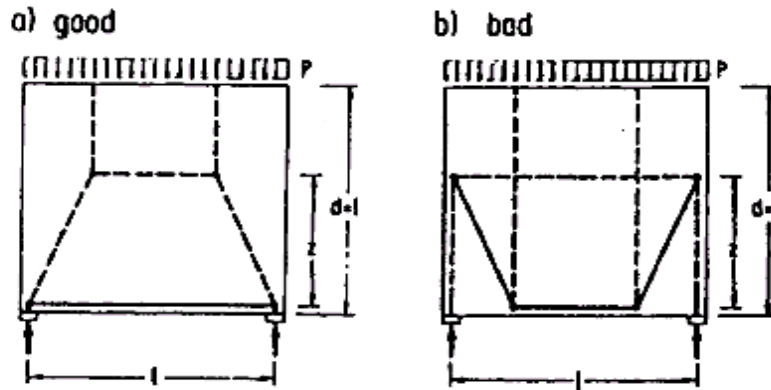


Fig 3.12 Trial model for deep beam supporting uniform load a) good model with minimum tie b) bad model with considerable tie [1]

3.7 Typical Representation of Strut-and-Tie Model of Regions

The following figures represent the different representation of the strut-and-tie model (STM) for B- and D-regions. As can be easily observed, the basic principles of the STM remain the same although it may be applied to various boundary conditions.

The application of the STM covers for both compressive and tension members as long as the boundary conditions are accurately identified. The diagram detailed below show the commonly encountered boundary conditions and their STM representation.

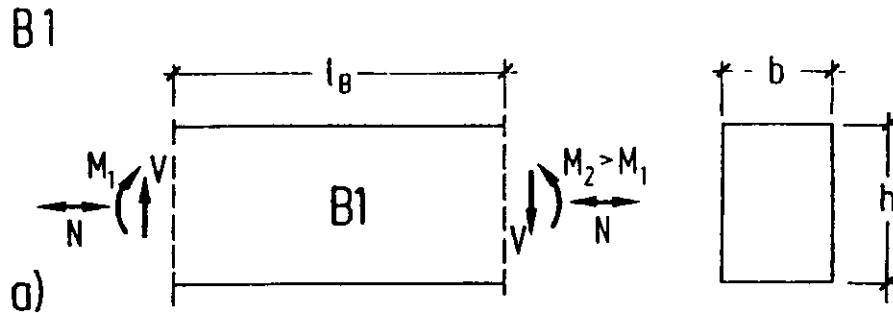
3.7.1 Typical B-regions

Typical B-regions have linear stress distribution and their representation may be defined basically in six ways which we may term as, B1-B6 type of truss. In some cases, it may be with some modification/combination of these representations.

Type B1

B1 type of STM modeling has at its boundaries moments, nominal axial forces/shears as shown in the figure below.

Boundary condition of type B1



STM representation of type B1 representation resembles the following diagram either with inclined or vertical stirrups.

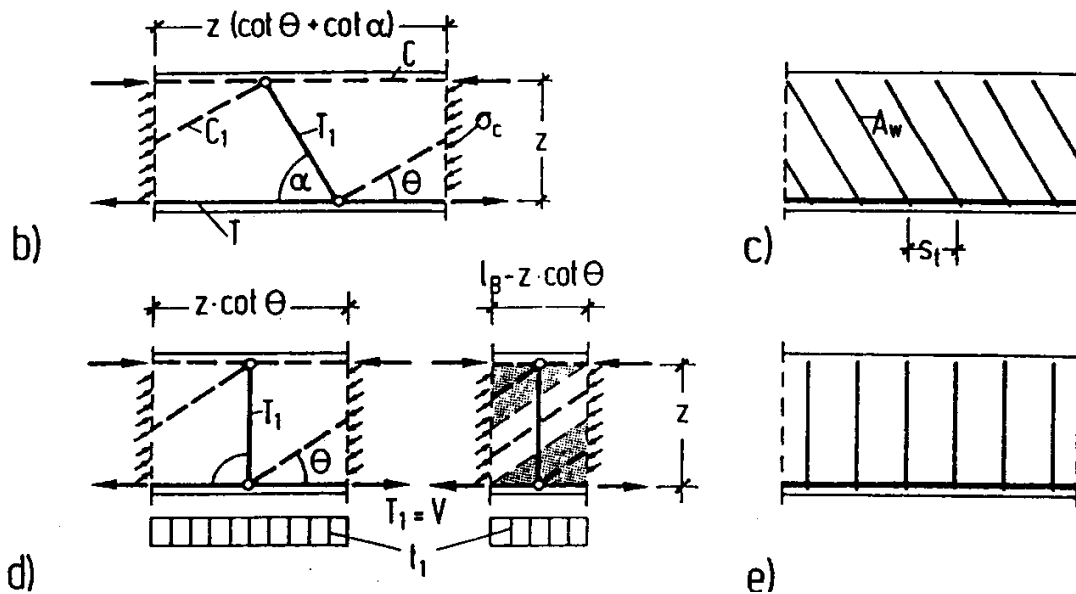


Fig. 3.13 Truss models of B1 region a) the boundary forces b) truss model with tie inclination α c) reinforcement layout d) truss model with vertical tie e) reinforcement layout [2]

Type B2

Type B2 has boundary conditions has on one side shear force and bending moment in combination whilst at the other end only shear force. Such regions represent a deep beam with continuously distributed edge loading, diaphragm wall of a box girder bridge and slabs carrying in-plane shear as horizontal stiffening member between the walls of the building. This model is obtained by assuming the resultant shear acting at the center of the vertical face or centroid of stress distribution.

Boundary condition of type B2

STM representation and reinforcement of type B2

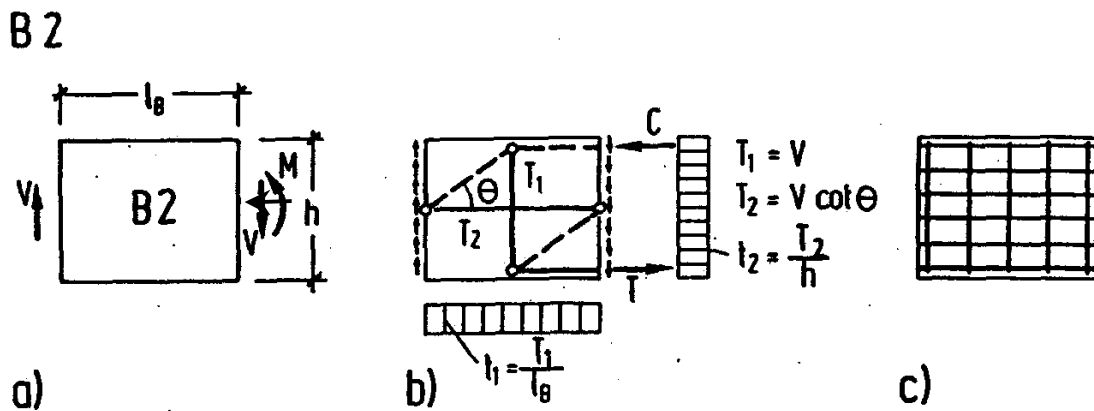


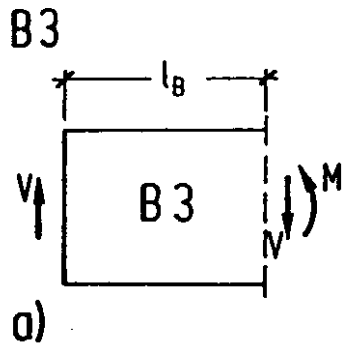
Fig. 3.14 Truss models of B2-region a) the boundary forces b) truss model with c) reinforcement layout [2]

Type B3

Type B3 has as its boundary condition a shear force on one side and an axial force, shear force and bending moment on the other. As one can observe, Type B3 resembles B2 with an addition of an axial force.

As this model is an indeterminate representation, we may break it down into two determinate parts to facilitate ease of analysis. Such regions represent the end of an indirect supported beam.

Boundary condition of type B3



STM representation and reinforcement layout of type B3

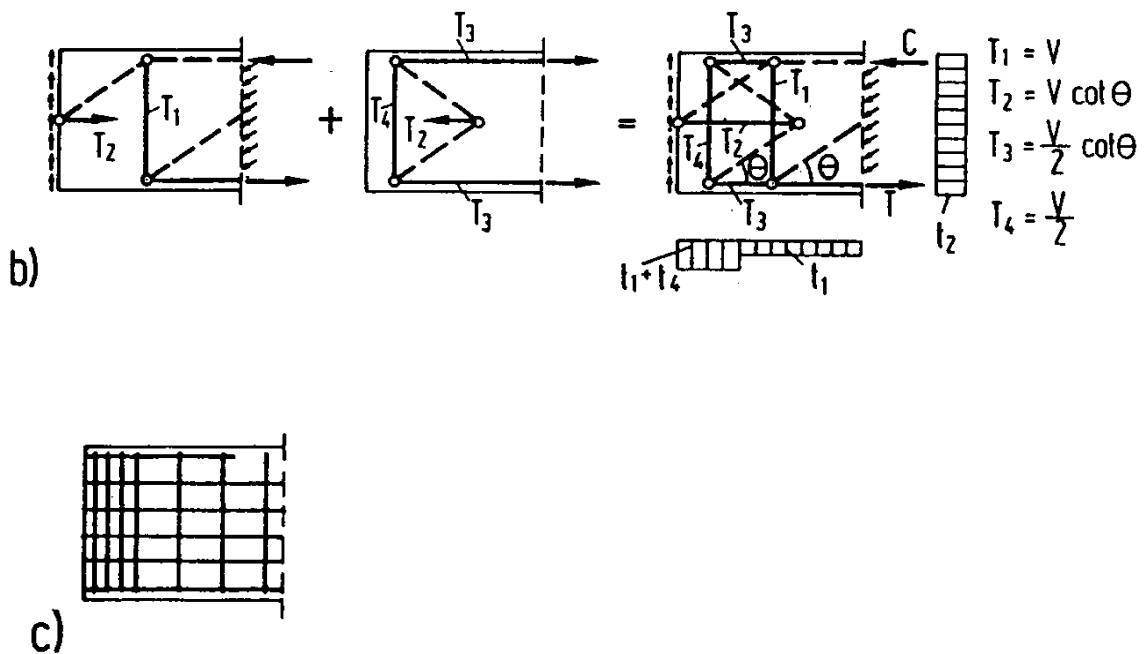


Fig. 3.15 Truss models of B3 region a) the boundary forces b) two determinate truss model and the sum c) reinforcement layout [2]

Type B4

This type basically resembles a type B1 representation but the axial force is significantly tensile resulting in tension in the STM chord members.

Boundary condition of type B4

STM representation and reinforcement of type B4

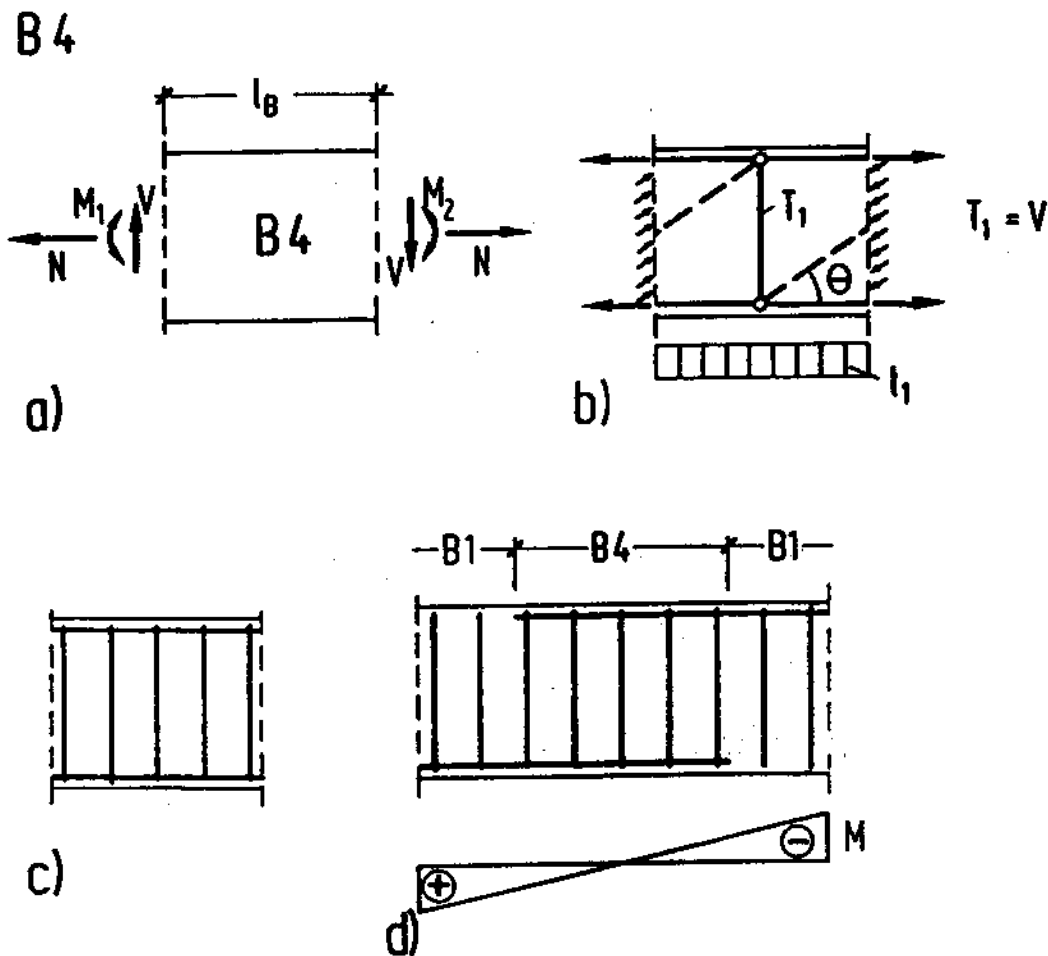
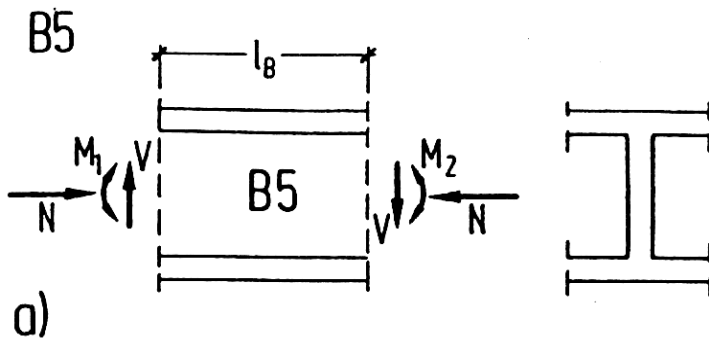


Fig. 3.16 Truss models of B4 region a) the boundary forces b) the truss model c) reinforcement layout d) B4 region with the adjoining B1 [2]

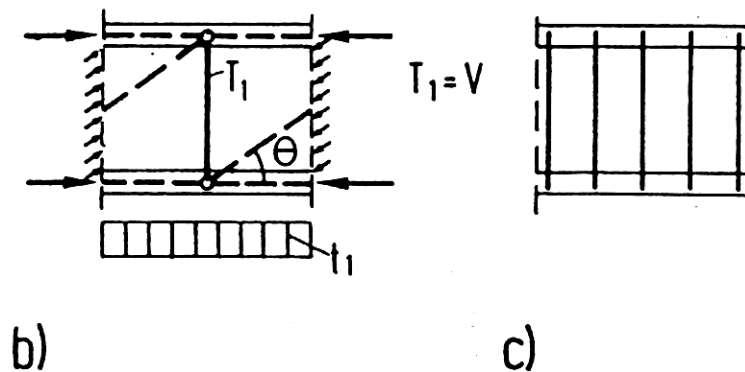
Type B5

Type B5 is a type of boundary region whereby the axial force is significantly compressive resulting in compression both top and bottom chord members. The compressive force is significantly as compared to the shear forces. Such boundary condition exists in compressive members such as columns and pre-stressed beams. Usually structural members that carry significant compressive axial force are 'I' sections as in the figure below.

Boundary condition of type B5



STM representation and reinforcement layout of type B5



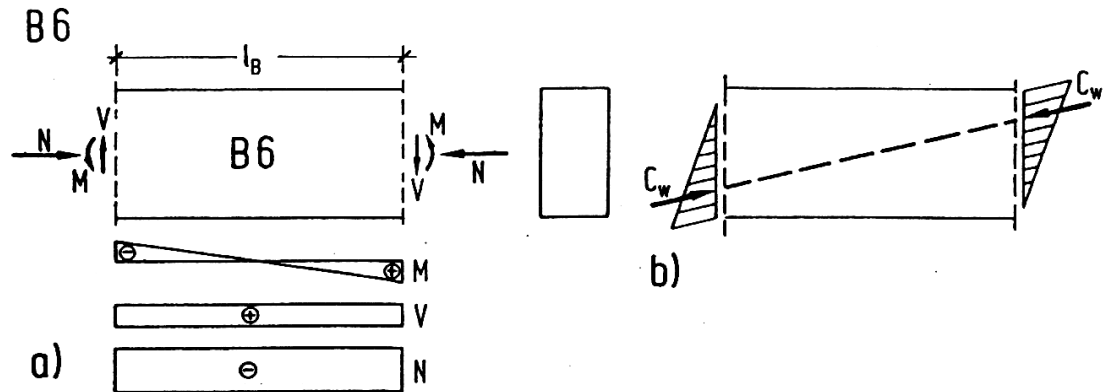
c)

Fig. 3.17 Truss models of B5 region a) the boundary forces b) the truss model c) reinforcement layout [2]

Type B6

Type B6 a type of boundary condition whereby the moment loads are so small that they do not develop any tension or compression stresses. However, it produces a diagonal compression.

Boundary condition and resultant force on the boundary of type B6



STM representation and reinforcement layout of type B6

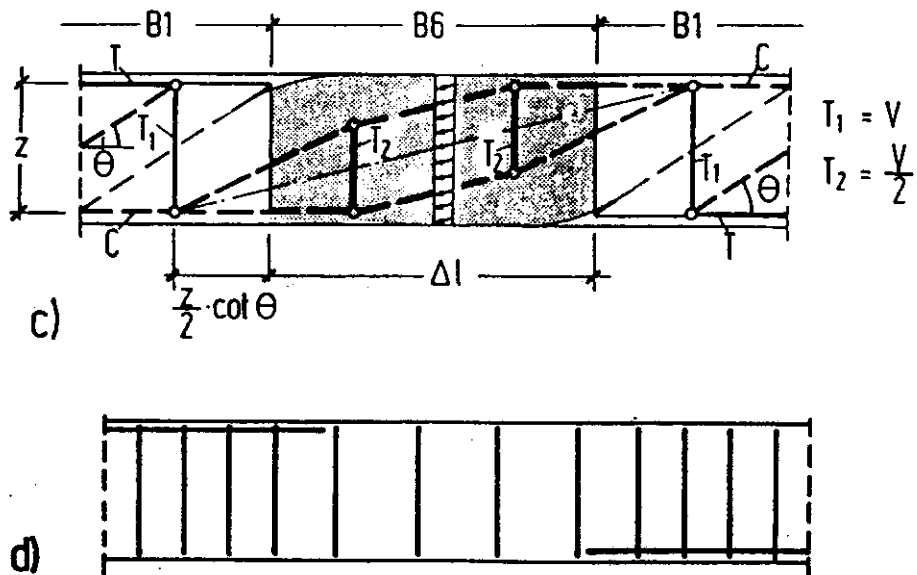


Fig. 3.18 Truss models of B6 region a) the boundary forces b) resultant compressive C_w c) the refined truss model and the T_2 d) reinforcement layout [2]

For such loading the boundary forces, compressive force, shear force and bending moment, are replaced by a single resultant force, fig 3.18. Hence, the internal force replaced by a single inclined compression forces.

The diagonal force, which is compressive over the depth, is confined in small width of the region and hence creating transverse tensile forces T_2 , fig 3.18c. As a result, stirrups are provided for the tension developed, quantified later.

3.7.2 Typical D-region Models

As mentioned earlier the stress distribution D-regions are regions where a non-linear stress distribution exists due to changes in either geometry or loading. Before proceeding to modeling the D-regions as STM the stress distribution of such regions may be obtained. Due to non-linearity of the stress distribution in such regions, typical stress distributions have been obtained from FEM methods coupled with expensive laboratory test. Once such stress distributions are understood it becomes simple to apply it to other D-regions with similar boundary conditions.

Similar to B-regions, D-regions also have varying boundary loading conditions. In the following section, we will show the various boundary conditions and their STM representation. D-regions vary from D1 to D12.

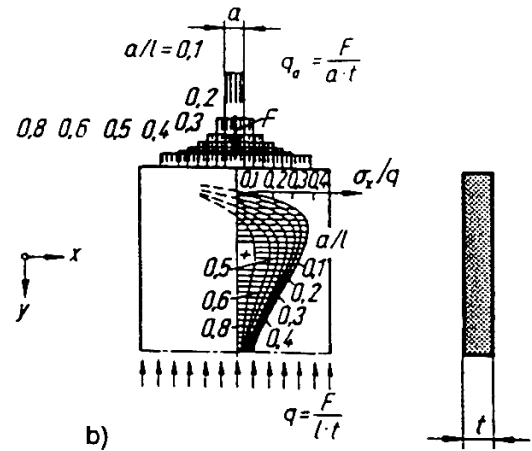
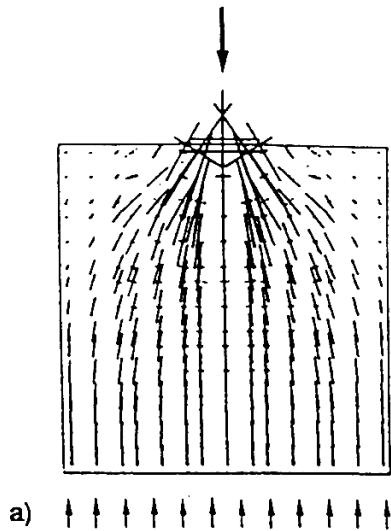
Type D1

It is a region with a point load on one boundary face while on the other boundary it is fully supported. A point load tends to distribute into the structure from the point of application, and becomes uniform at the other boundary of the D-region. This distribution results in transverse

tensile force at their interior sections. The tensile force intensity depends not only on the intensity of the applied load but also on the ratio of load application area to that of effective distribution area.

Boundary condition of type D1

Test result of stress distribution of application resembling Type D1



STM representation of type D1

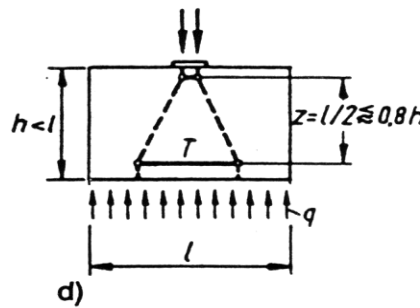
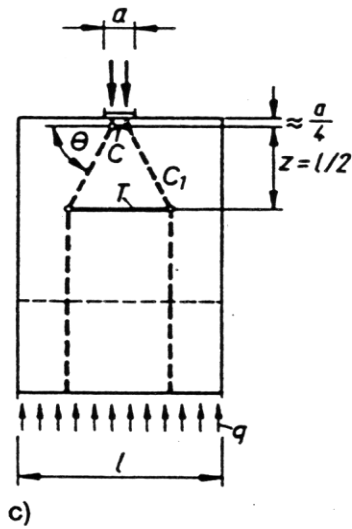


Fig. 3.19 Region D1 region a) the principal stress pattern b) transverse stress distribution for different a/l c) the strut and tie model for large depth d) for short depth [2]

Several authors have proposed an estimate of the transverse tension that is developed in such a D1 region. These are approximately equal and an integral T is determined [15], Eq. 4.

$$T = 0.25 F (1 - a / b_{\text{eff}}) \quad (\text{Eq 4})$$

Where: F = compressive force on top or on compressive member

a = width at the load point

b_{eff} = effective width of distribution

The above formula derived from the geometry of fig 3.19 and the inclination of the spreading of the force, ϑ . It also shows a compressive force equal to tensile force T develops below the load, near the surface. The depth h of the deep beam does not affect the transverse stress developed in the D-region as long as h is larger than the width. However, as the depth h decreases the D region blends with B-regions. Further reducing the depth will change the dimension of the D-region i.e. a new width of the D-region is equal to the depth h of the structure, fig 3.19c.

Type D2

In comparison to type D1, where the load is applied at the center, type D2's load is applied near edge rendering a different stress distribution, hence different STM. Such a stress distribution results in tension at the top and compression at the middle. The maximum tensile force developed at the top edge has a magnitude amounting to a third of the applied compressive load or $T_1 = F/3$ as obtained from test results and as shown in fig. 3.20.

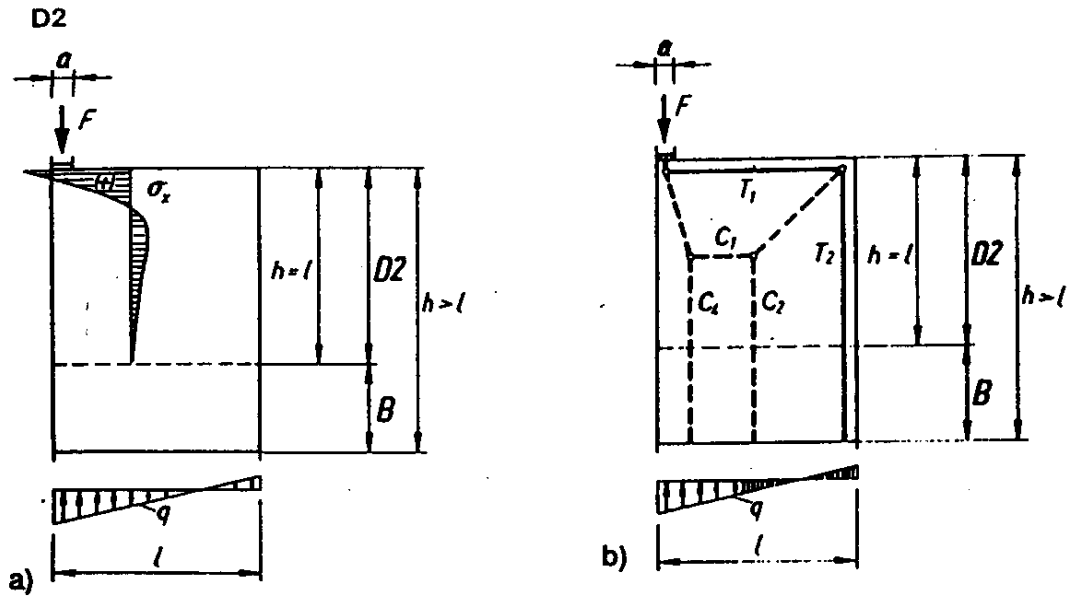


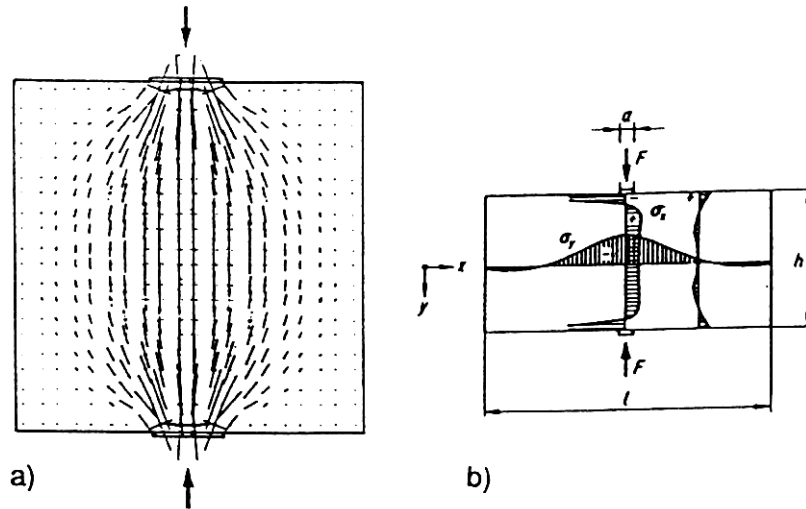
Fig. 3.20 Region D2 region a) the stresses diagram b) the strut and tie model [2]

Type D3

This type of region has a point load at one boundary and a point supported at the other. The stress pattern varies with depth and resembles that of type D1.

- (a) If $h/l = 2$ – it resembles two blended D1 regions.
- (b) If $h/l > 2$ – a B-region develops in the middle while the top and bottom resembles a D1.
- (c) If $h/l < 2$ – the region resembles two D1 with a reduce width i.e. $b = h$ and $b < l$.

Boundary condition and stress distribution of type D3



STM representation of type D3

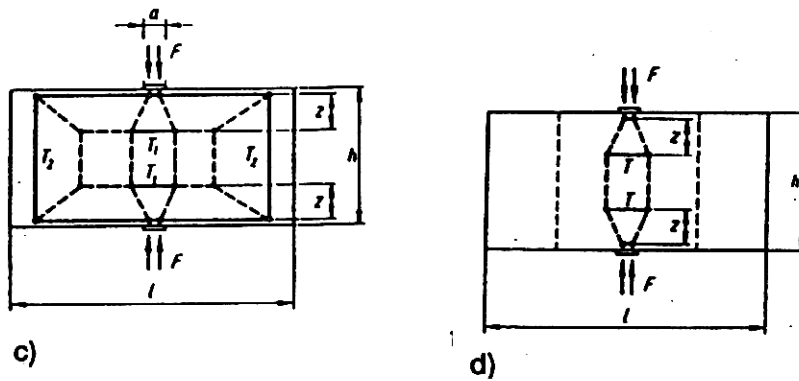


Fig. 3.21 Region D3 region a) the principal stress pattern b) stress distribution c) refined strut and tie model d) strut-and-tie [2]

Type D4

This type of regions is the same load as type D3 but at the edge. The stress distribution resembles to blends to two D2 type regions.

Boundary condition of type D4

STM representation of type D4

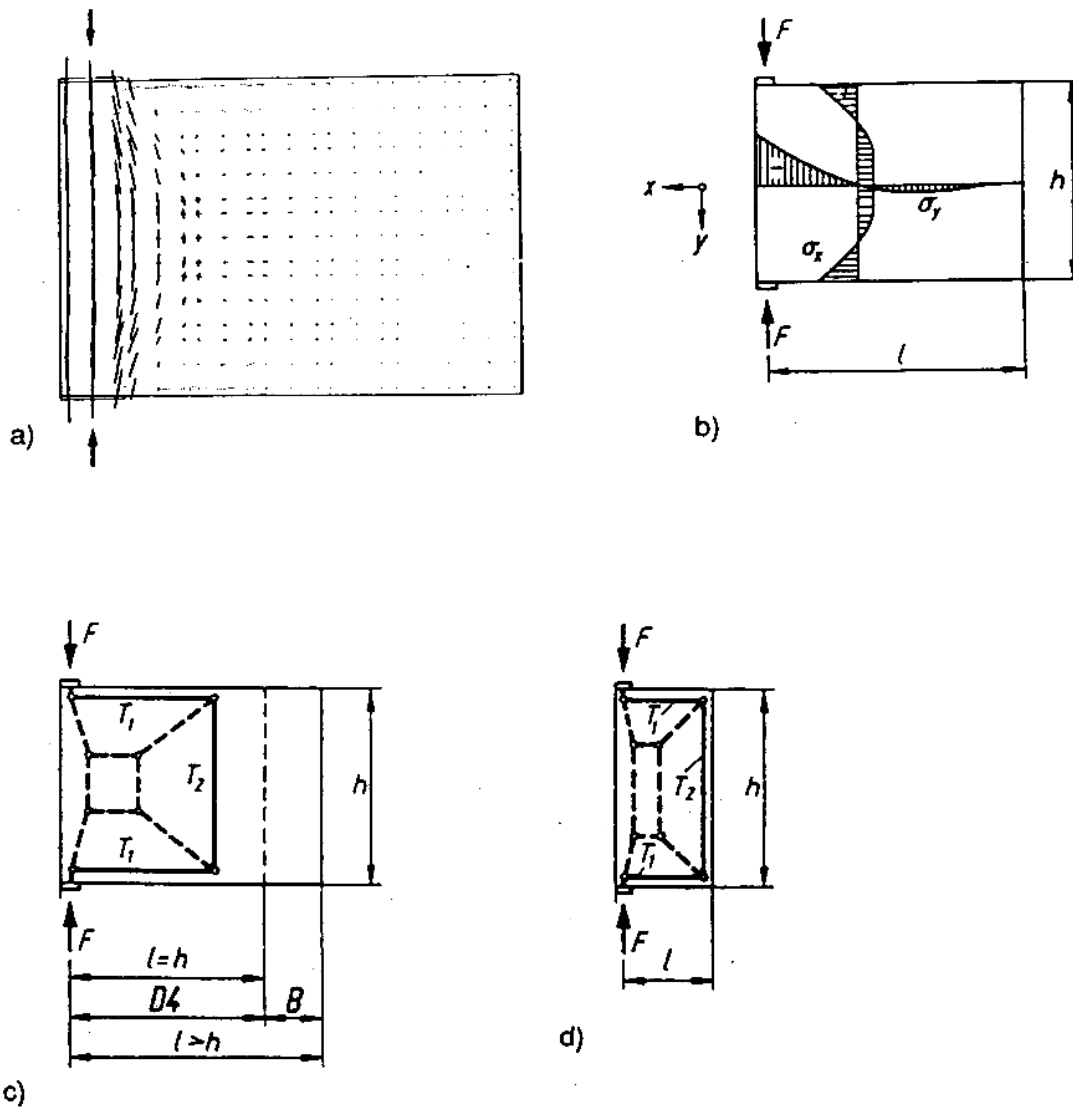
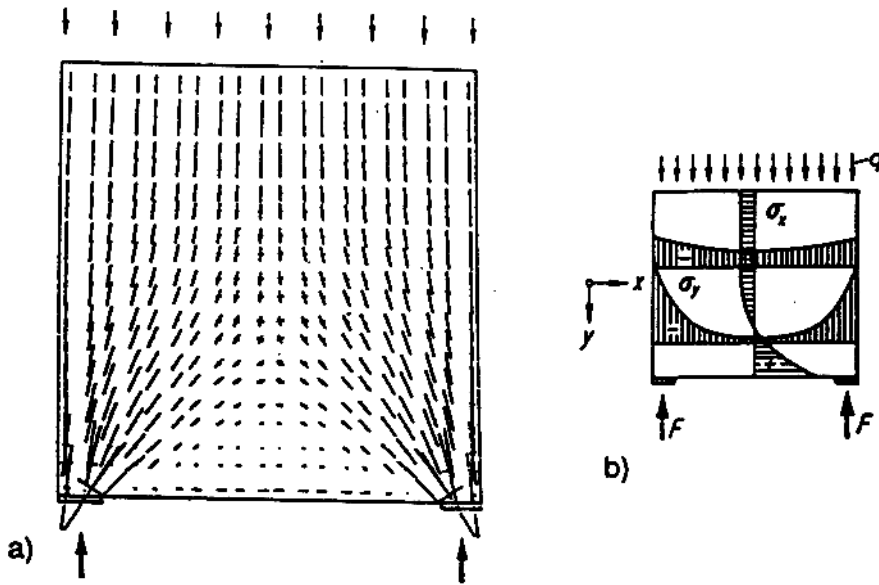


Fig. 3.22 Region D4 a) the principal stress trajectory b) stress distribution for different location in the region c) & d) the strut and tie model [2]

Type D5 and D6

Type D5 is with uniform load on the top and two supports from below (deep beam).

Boundary condition and stress distribution of type D5



STM representation of type D5

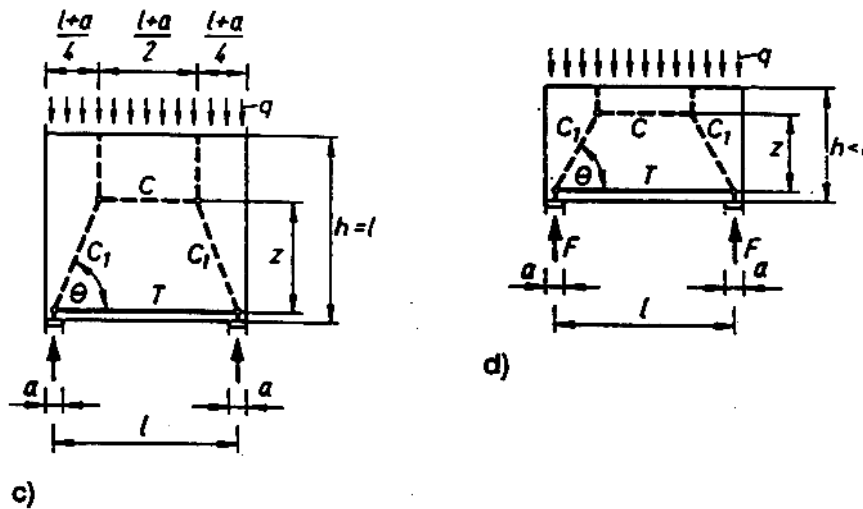
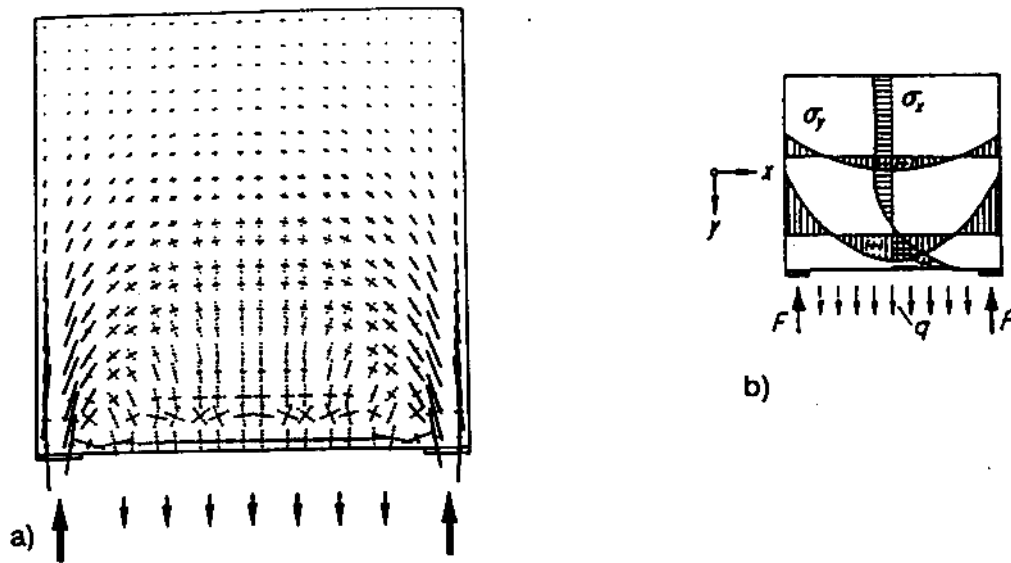


Fig. 3.23 Region D5 a) principal stress trajectory b) stress distribution in the region c) & d) strut and tie model [2]

Type D6 is with uniform load at the bottom and two supports are from below of the region (deep beam). The stress distribution resembles D5 but the reinforcements are modified to accommodate the point of application of the load.

Boundary condition and stress distribution of type D6



STM representation of type D6

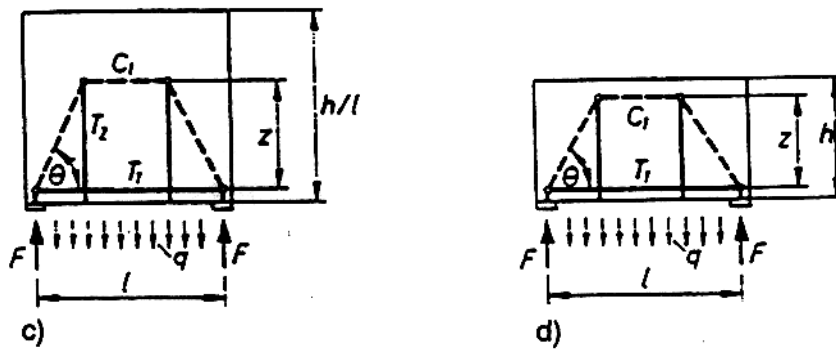
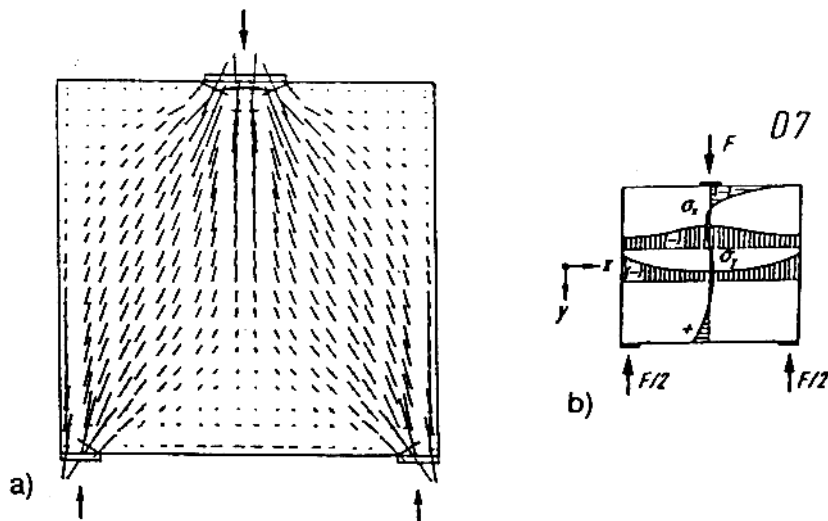


Fig. 3.24 Type D6 a) principal stress trajectory b) stress distribution in the region c) & d) the strut and tie model [2]

Type D7

This type of region is found in deep beam with a point load at the mid of top and two supports at the edges. The crude representation of such region is with a simple truss where the nodes are located near the load and the supports. A further refinement of the STM model, as in figure below, depicts actual stress distribution.

Boundary condition and stress distribution of type D7



STM representation of type D7

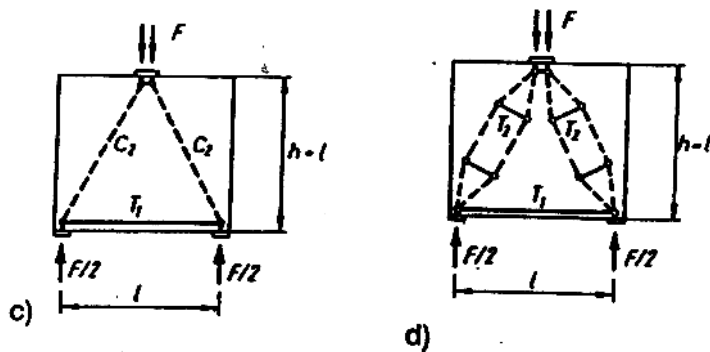


Fig. 3.25 Region D7 a) the principal stress trajectory b) stress distribution in the region c) simplified STM & d) the strut and tie model [2]

Type D8

This is a region with four loads/supports at the four edges of the region. It resembles a stress distribution of two blended type D5 regions.

Boundary condition of type D8

STM representation of type D8

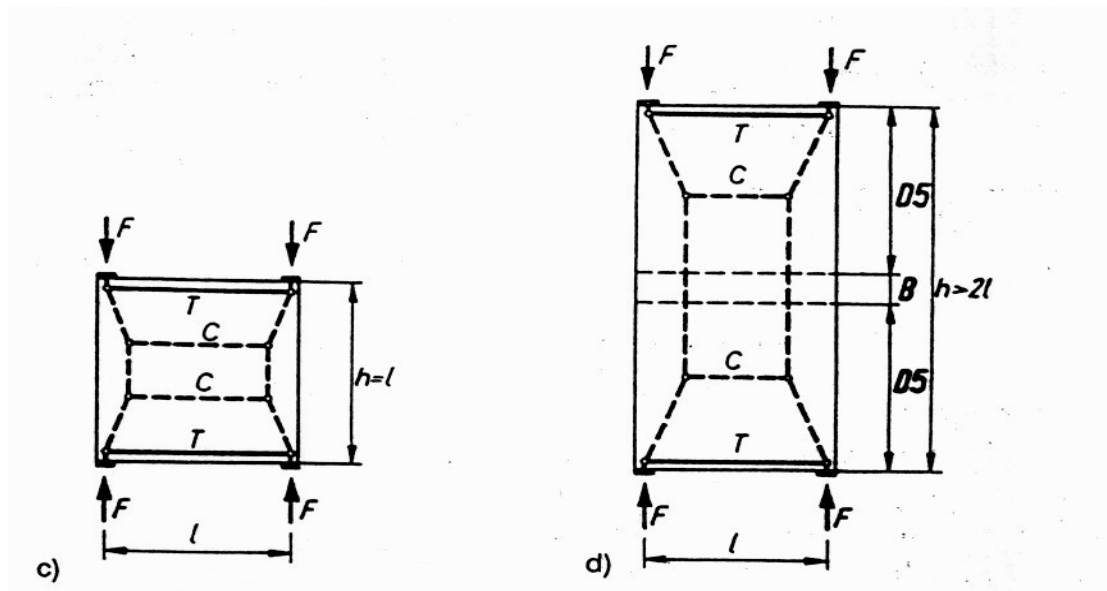
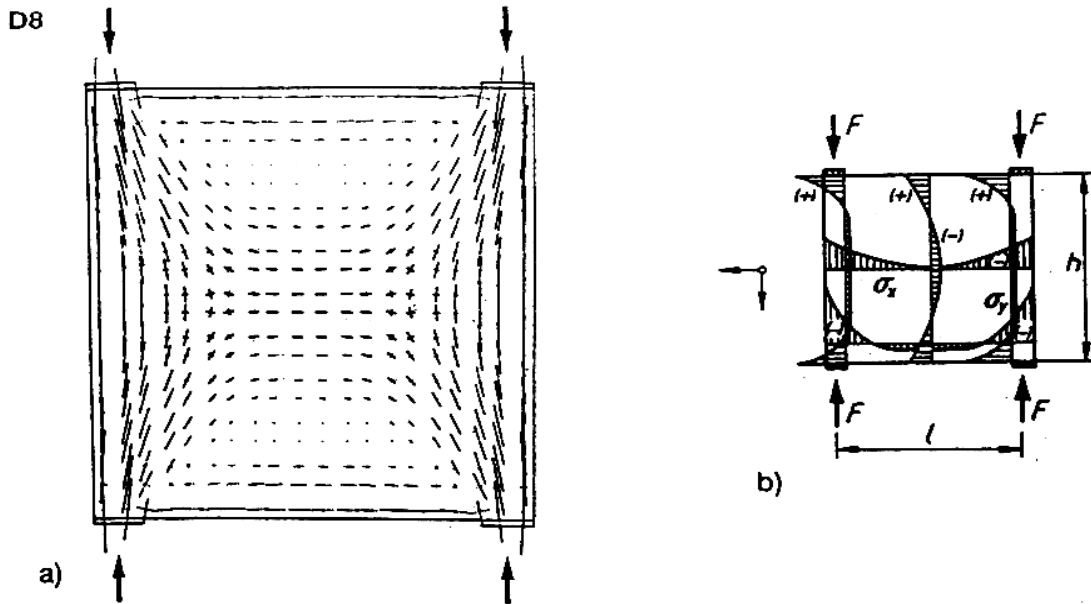


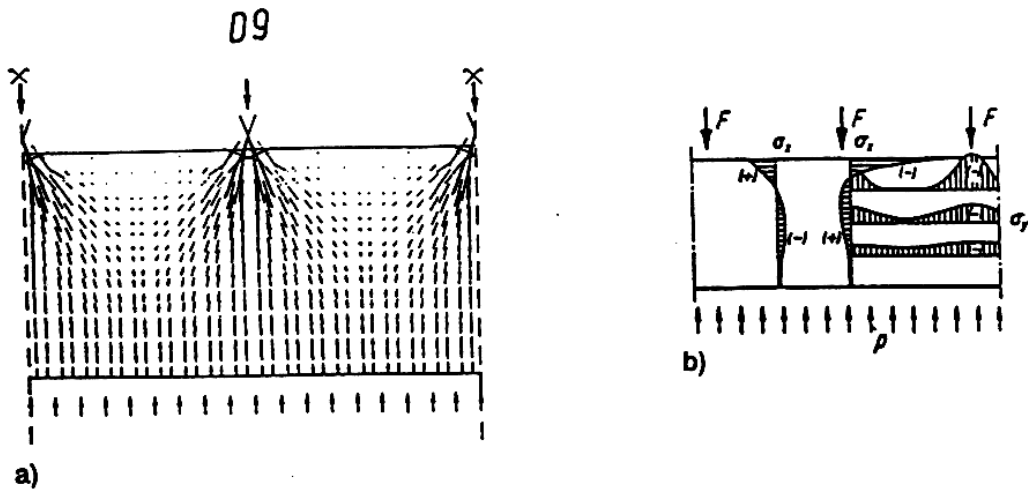
Fig. 3.26 Type D8 a) the principal stress pattern b) stress distribution in the region c) & d) strut and tie model [2]

Type D9 and D10

Type D9 is a region with more than one point load on the top and support on the other. The stress distribution is a mix of the type D1 and type D5.

Boundary condition of type D9

stress distribution of Type D 9



STM representation of type D9

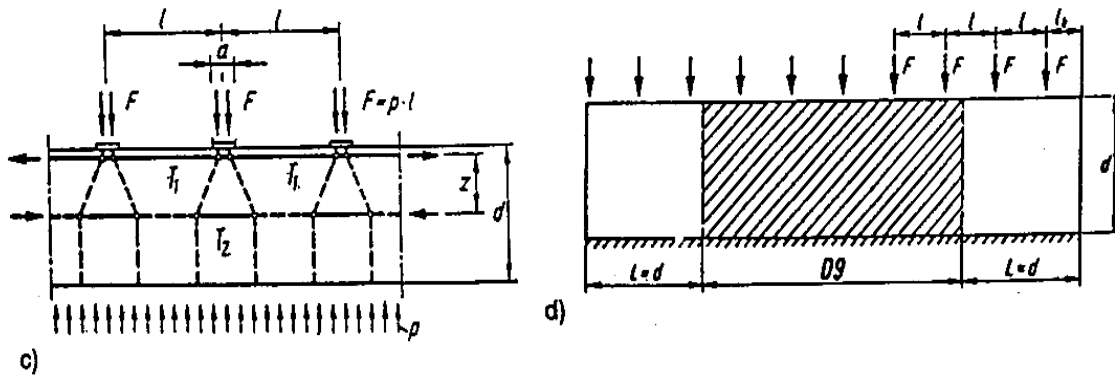
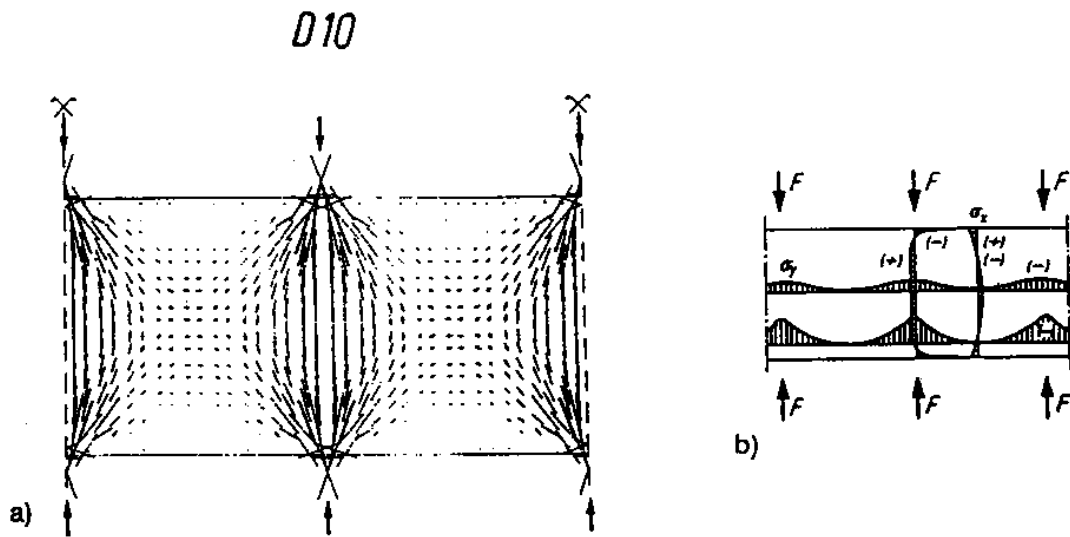


Fig. 3.27 Region D9 a) the principal stress trajectory b) stress distribution in the region c) the strut and tie model for d) location of D9 with adjacent regions [2]

Type D10

This type of region is with more than point loads and the supports. It resembles as the type several types D3 are placed side by side.

Boundary condition of type D10



STM representation of type D10

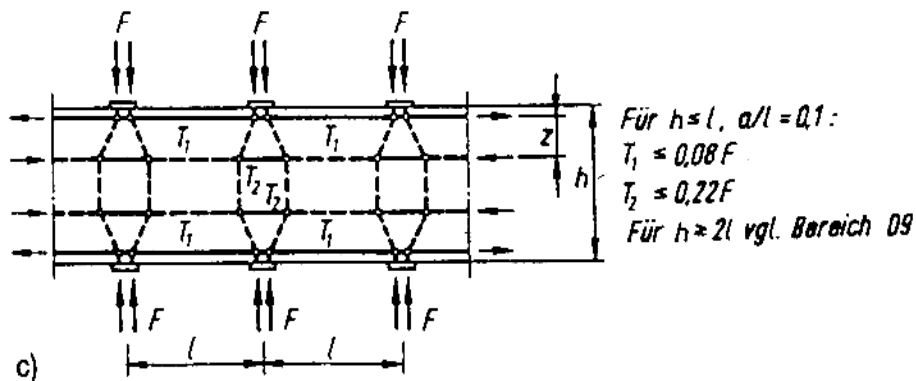
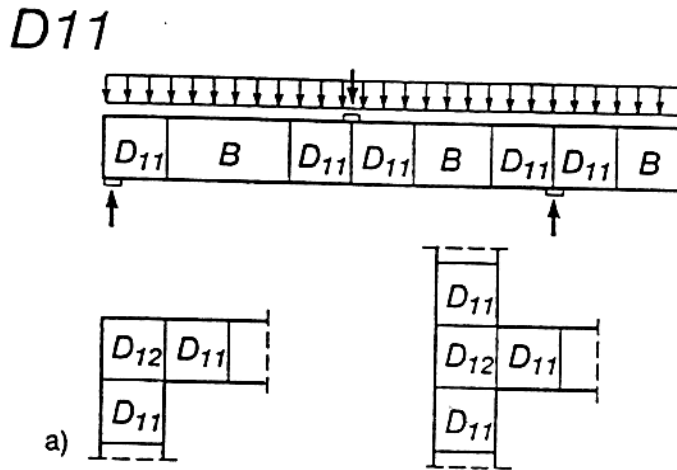


Fig. 3.28 Region D10 a) the principal stress pattern b) stress distribution in the region c) the strut and tie model [2]

Type D11 and D12

Boundary condition and location in actual structure of type D11



STM representation of type D11

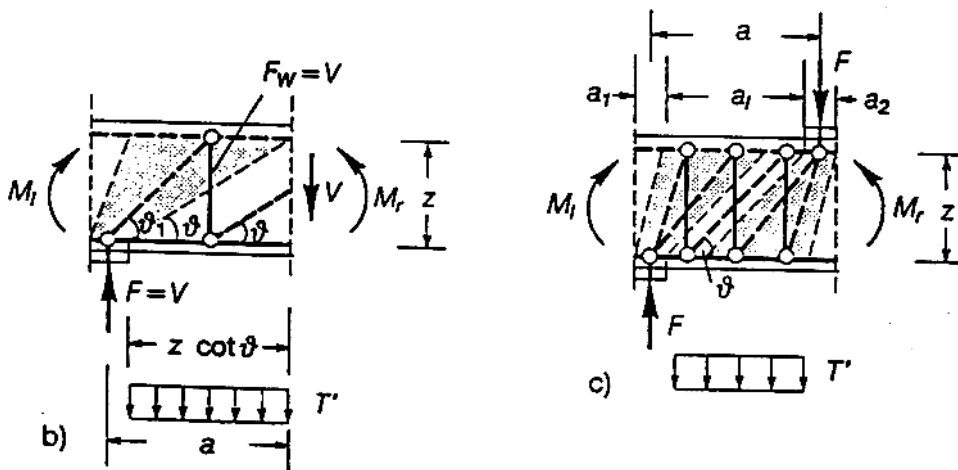
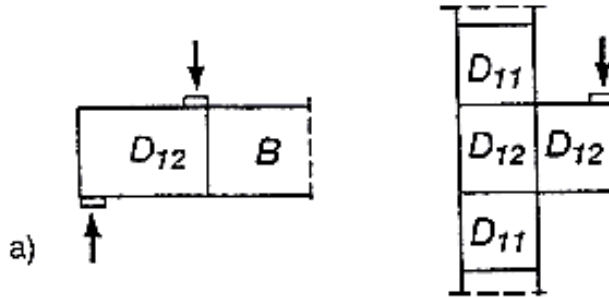


Fig. 3.29 a) location of D11 & D12 in the structure b) the strut-and-tie models of the two load paths c) the strut and tie model for refined model [2]

Type D11 Regions occur in the end supports of beams and plates. It provides transition from B and D12 regions. The parallel stress field represented by the continuation of strut C_{ϑ} and the angle of inclination ϑ is the same and continuation from the adjacent B1 region. This region is the same as the B1 region and dimensioned except support point.

Type D12

Boundary condition and location in actual structure of type D12



STM representation of type D12

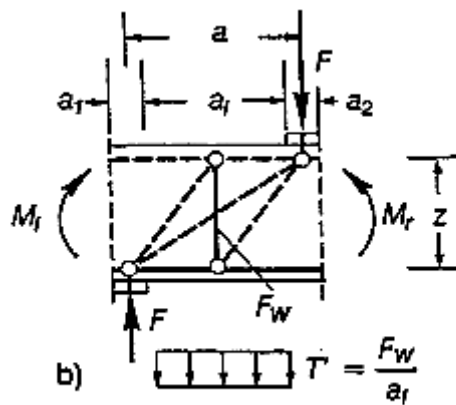


Fig. 3.30 Region D12 a) location in structure b) strut-and tie model [2]

It is a region where the concentrated load is near the support. Typically, it is near frame-corners, beam-connections, and corbels. Fig 3.30 shows two different force paths, a direct line connecting the load and the support and the load path with tensile force. The transfer of the load is a combination of direct shear and to some extent bending moment. It is the combination the two models that give an efficient STM model. The tensile force is estimated using Eq 5 suggested by Schlaich [2], as given below,

$$T_{\text{stirrup}} = F (2a / z - 1)/3 \quad \dots (5)$$

But, $0 \leq Fw \leq F$

F = the external load

a = distance between the axial forces

z = moment arm

As the distance between load point's increases, the bending moment becomes a dominant and the model with larger vertical tension force and reinforcement governs.

3.8 Design Criteria of Strut-and-Tie Model members

Once we finalized the modeling of the actual structure to an STM model, the next step prior to proportioning the members to resist the applied loads is to determine internal forces. We may achieve this by simple truss analysis, and once this is achieved we may proceed to the next step of designing the members. The strut-and-tie model consists of three members: the *concrete strut*, the *tensile members*, and the connection or *nodal zones* that is:

- (1) Tie or tension members
- (2) Strut or compression members and
- (3) Node or joint member

We will now attempt to discuss briefly the behavior of those elements.

3.8.1 Tie Members

Concrete structures consist of the reinforcement and concrete elements. When we model our structure as STM, we encounter both elements as a means of resisting tension or tie action. In most cases, the tension strength of concrete is too low to cater for the existing tension stress; therefore, reinforcement as stirrups is placed to resist diagonal cracking, especially in areas where progressive cracking may be a problem. However, in rare cases where it may not be possible to provide stirrups we may rely on the concrete tension strength. Since the tensile strength of concrete is not so easy to predict or assess. Schlaich [1] suggests that this strength element should only be used for equilibrium purposes in areas where no progressive failure is expected.

Once the tension forces are known, we may proceed to design of the ties as per Code requirements. That is the tension in the tie should be equal or less than the forces/stresses in the reinforcement.

$$T \leq A_s f_{yd} \quad \dots (6a)$$

$$f_{yd} = f_{yk} / \gamma_s \quad \dots (6b)$$

Where T – the net external tensile force acting on the tie, for steel or pre-stress

A_s – the total area of steel

f_{yd} – the design strength of steel

f_{yk} – the characteristic strength of steel, or pre-stressing steel

3.8.2 Struts or Compression Members

Struts are compressive members and in our STM modeling represent the compressive stress flow areas. As observed in numerous tests the compressive stress flows have differing shapes. The most common of them being

- Prismatic stress flow shape
- Fan shaped stress flow shape
- Bottle shaped stress flow shape, having
 - Vertical bottle shapes
 - Diagonal bottle shapes

In order to proceed to the design of struts we have to understand clearly these stress flow patterns in some detail.

a) Prismatic stress flow shape



Fig 3.31 prismatic strut stress distribution

The above figure illustrates a compressive member loaded at its ends by distributed forces. As can be seen, the stress distribution is uniform in the section and hence providing only minimum reinforcement in the section as per code requirement will suffice.

b) Fan shaped stress flow shape

In this case, the application of a load results in stress distribution that are fan shaped. Theoretically, minor tensile stress develops, but the tension force may be resisted by the

provision of minimum reinforcement as per code requirement.

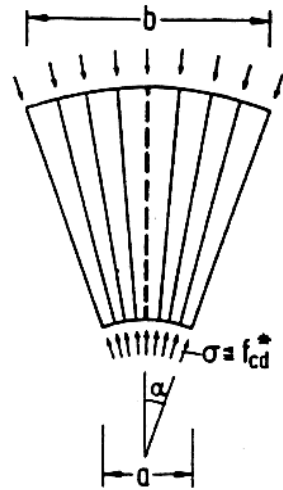


Fig 3.32 illustration of compressive stress field with their fan stress flow

c) Bottle-shape stress flow shape

This is a stress distribution in a member that resembles a bottle shaped figure. The most significant stress distribution is the development of transverse tension develops that aggravates the development of cracks due to significant boundary forces. These cracks may enhance the premature failure of the section. Normally there are two types of bottle shaped stress distribution representations.

Type A – Vertical Bottle shaped

When the section is loaded as in figure below with the geometry of the shape, a bottle shaped stress distribution develops. The stress distribution in a region depends not only on the intensity of the applied but also on the geometry of the region. In the event that the depth of a section is large when compared to the width of the region, the transverse tensile stress developed is not the same, that is when the stress is confined in the structure's width as when compared to unconfined

one (the stress is allowed to fully distribute in the region), as shown in Fig 3.33. For such loading and orientation of the strut, Schlaich [2] reports from test results, confirming this truth and estimates the tensile force developed for the confined region ($b/L \leq 2$) by equation Eq. 7a and for unconfined one by Eq. 7b.

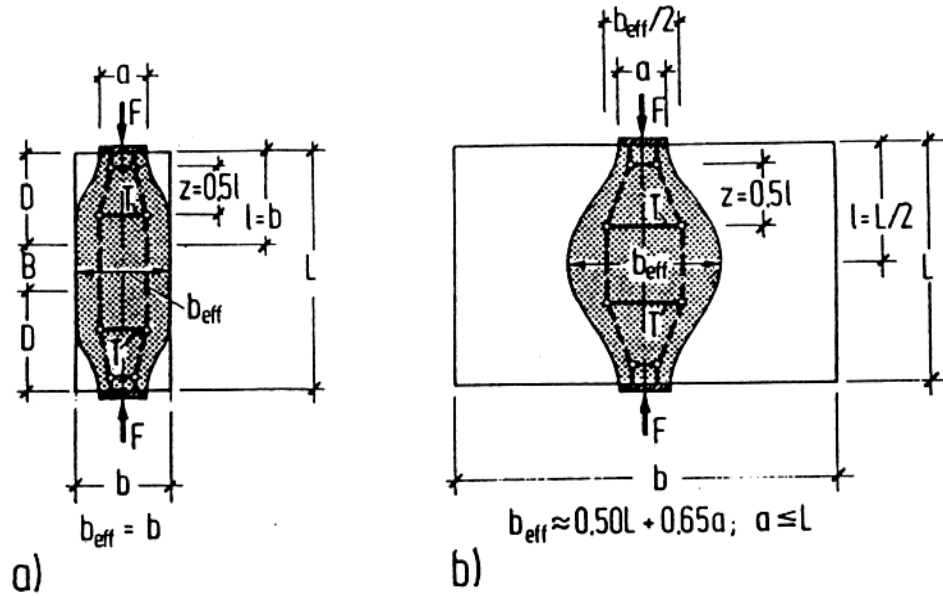


Fig 3.33 Bottle shaped strut a) confined to the width b) unconfined section [2]

$$T = 0.25 * F (1 - a / b_{eff}) \quad (\text{Eq. 6a})$$

$$T = 0.25 * F (1 - 0.7 * a / L) \quad (\text{Eq. 6b})$$

Where, F = compressive stress on the strut

T = tensile force

a = width of the node at one end

b_{eff} = effective width of bottle-shaped, as in Fig 3.33

Type B- Diagonal bottle-shaped strut

When the strut or stress distribution is diagonal in relation to the boundary of the region; the pattern in the figure below is observed. The tensile width is obtained from the Eq. 7b and the effective width of the bottle region as Macgregor [6] suggests is estimated from the following expression.

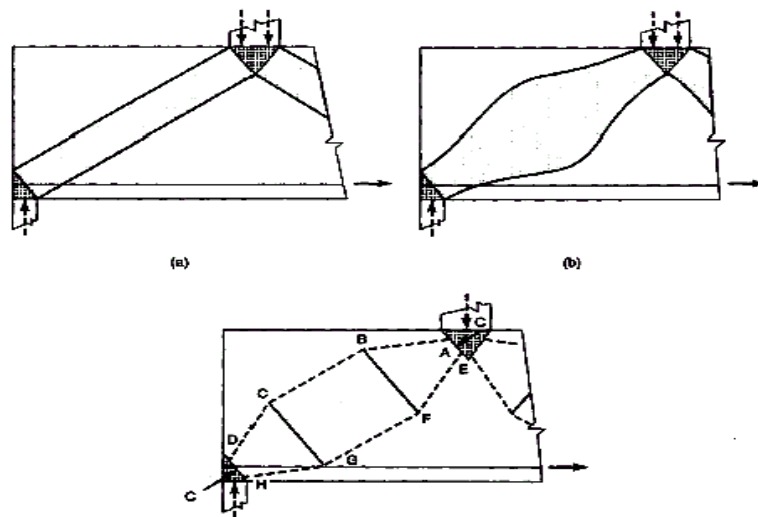


Fig 3.34. Compression member a) prismatic strut b) bottle shaped model c) strut-and-tie model of the “bottom-shaped” strut. [6]

Macgregor [6] proposes an effective width over which the transverse stress distributes for diagonal compressive struts given by:

$$b_{\text{eff}} = a + l/6 \quad (\text{Eq. 7})$$

\leq but less than the available width

Where, l is the length from face to face of the node.

The bottle stress distribution extends in to the region to a depth of one and half the width of the bottle stress distribution, $1.5b_{\text{eff}}$. The tensile force is estimated using the same Eq 7b. The above model is for 2-dimensional plane or state of stress distribution. Similarly, for the 3-Dimensional

models it follows the same consideration as for 2-dimensional but with triaxial concrete strength. The concrete strength, for 2-Dimensional STM model for design purposes is determined as:

- a) $f_{cd}^* = 1.0 f_{cd1} = 0.85 f_{cdk}$: for undisturbed and uniaxial state of compressive stress ;
- b) $f_{cd}^* = 0.8 f_{cd1} = 0.7 f_{cdk}$: if tensile strain in the transverse direction is large or the crack is parallel to the compressive strut;
- c) $f_{cd}^* = 0.6 f_{cd1} = v f_{cdk}$: as above but for skew cracking or skew reinforcement and angular cracking anticipated, for skew cracks with extraordinary crack width. Occurs if the model is not consistent to the elastic stress analysis e.g. to obtain the ultimate capacity in redistribution of internal forces.

Note that the f_{cd1} is the design value of the uniaxial compressive design strength of the concrete divided by partial safety factor (f_{cd} as in EBCS-2) and that v is defined as Eurocode 2 [17] of an allowance for sustained loads is included in v but not in f_{cd} .

$$f_{cd1} = 0.85 f_{cdk} = 0.85 (f_{ck} / \gamma_c) \quad \dots (9a)$$

$$f_{cd} = 0.85 f_{ck} / \gamma_c \quad \dots (9b)$$

$$v = (0.7 - f_{ck} / 200) \geq 0.5 \quad [\text{in N/mm}^2] \quad \dots (9c)$$

The concrete strength increases in two and three dimension state of compression or when confined in the transverse direction. Moreover, this may be considered if the confinement actions are reliable, by bulk concrete or stirrups. In the event of uncertainty the most critical concrete strength (c), in the above expression shall be used for design.

Prof. Schlaich [1], from laboratory test, suggests the tensile strength of concrete can be used as to avoid tension reinforcement. In the following diagram, the bold line shows the mechanical reinforcement ratio, $\omega = 0.06$, where $\omega = A_s f_{yd} / (t \cdot f_{cd})$, that give us tension force equal to the concrete tensile force. Beyond this point, provision of reinforcement is a necessity for the transverse tension developed, as in Fig 3.35.

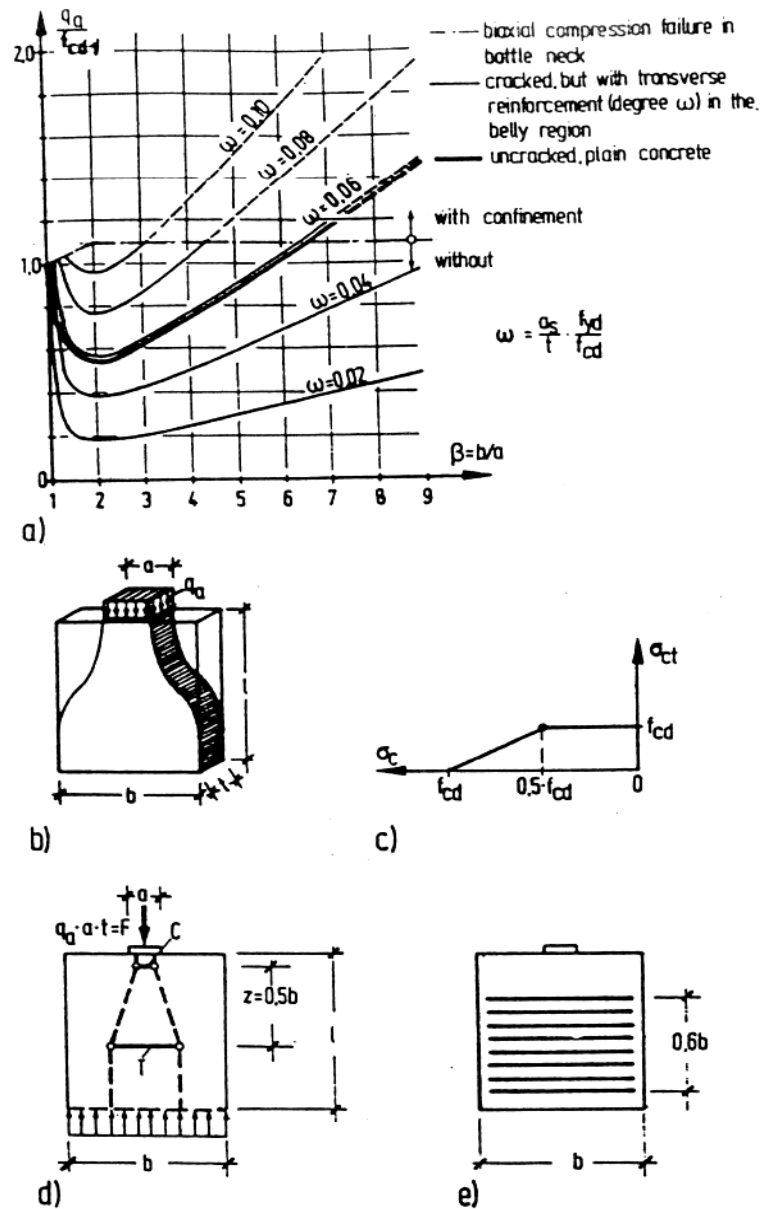


Fig 3.35 Bold curve in showing the plain concrete a) confined to the width b) bottle shaped stress distribution c) two phases of concrete strength d) STM model e) reinforcement layout [1]

3.8.3 Nodes

The third component of the STM modeling is the connection for the struts and Tie or the nodes. In terms of the streamline stress distributions the changes in the direction of the stress are considered as nodes. In areas where the stresses end in one point we have singular nodes where as the stress flow line spread out we have what we call a *smeared nodes*. This is shown in the figure below.

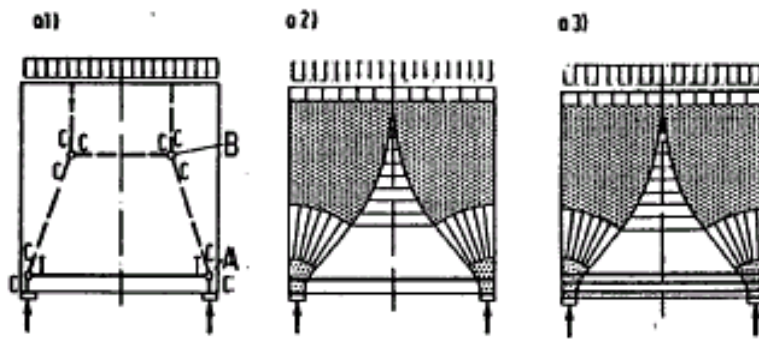


Fig 3.36 Simply supported deep beam with uniform load a1) STM model a2) stress distribution a3) refined reinforcement layout [1]

The forces at the nodal points have always to satisfy the equilibrium requirements and since the critical node is a singular one and design of such a node normally satisfy all requirements. In the design process, the concrete strength of the nodes may be expressed by the following expression.

$$f_{cd}^* = 1.1 f_{cd1} = f_{cdk} \quad : \text{ for true compression node without significant transverse tensile force;}$$

$$f_{cd}^* = 0.8 f_{cd1} = 0.7 f_{cdk} \quad : \text{ for compression-tension nodes.}$$

Typical Nodes regions could be either compression or compression tension with or without reduced area of application. The geometry of the nodes is partially known at the initial stage like support width, direction of struts and ties. The other sides are determined from the strength

criteria. The nodes can have a straight line or serrated borderlines. It is always [18] advisable to use straight boundaries perpendicular to axis for all types of nodes, Fig 3.37.

Based on the geometry of the nodes we may have several types of nodes. There are basically two types of node depending on the boundary loads.

- (1) Pure compression node: This is a case where the forces actions on the nodes are purely compressive and where there are no significant tensile forces on the plane in consideration. The following diagram illustrates the basic feature of the compressive nodes. Such nodes are located at the edge and middle supports of deep beams, corbel at the face of column, etc.

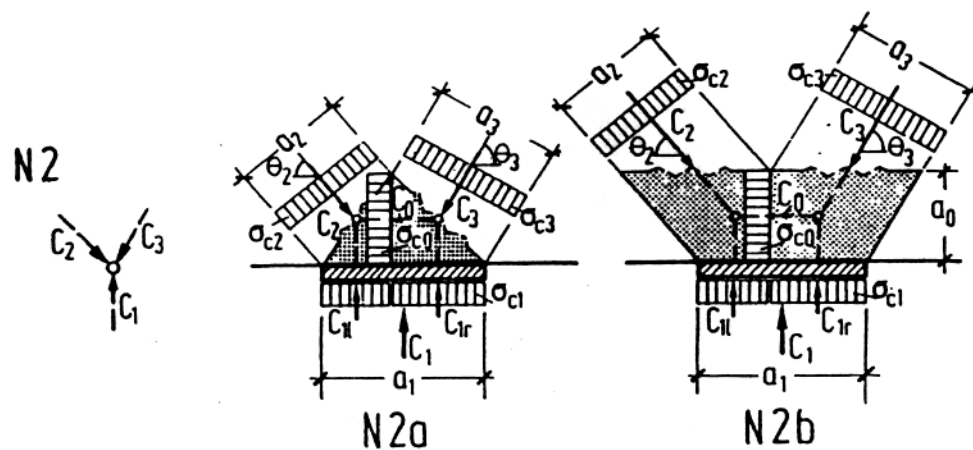


Fig 3.37 Node N2 with two different idealizations, detail as N2a and N2b. [2]

Schlaich [2] suggest, for such nodes checking of only two perpendicular section of the node, side a_1 and a_0 , will be sufficient for strength requirement of the node using the follow expression.

$$\sigma_{c1} = C_1 / (a_1 b) \leq 1.1 f_{cd1} \quad \dots (11a)$$

$$\sigma_{co} = C_o / (a_o b) \leq 1.1 f_{cd1} \quad (\text{only if } a_o < a^*_o) \quad \dots (11b)$$

$$a_o = a^*_o = a_1 / (\tan \vartheta_2 + \tan \vartheta_3) \quad \dots (11c)$$

Where σ_{c1}, σ_{co} = the compressive stress at the respective node face

C_1, C_o = the compressive force at the respective node face

a_1, a_o = the width of the respective side of the node

a^*_o = the vertical width of the node by considering equal stress on the node face

f_{cd1} = the uniaxial concrete strength

(2) Tension-compression: this is a case where there is both compressive and tension force acting on the node. The following diagram illustrates the basic feature of a tension-compression node.

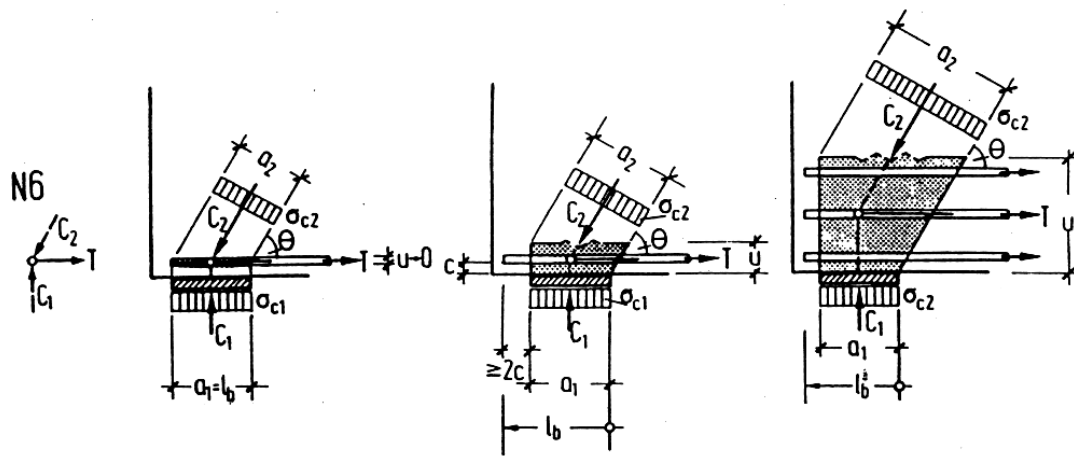


Fig 3.38 Node N6 a) single layer tie with anchorage at the mid of the node b) single layer tie with full node anchorages c) multiple layer of ties with full anchorage. [2]

For such nodes, both compressive nodes shall be checked for the concrete strength using the following expression.

$$\sigma_{c1} = C_1 / (a_1 b) \leq 0.8f_{cd1} \text{ (or } 0.7f_{cd} \text{)} \quad \dots (11a)$$

$$\sigma_{c2} = C_2 / (a_2 b) \leq 0.8f_{cd1} \text{ (or } 0.7f_{cd} \text{)} \quad \dots (11b)$$

Where, a_2 = node width in side 2

$$= (1 + u \cot \vartheta / a_1) \sin^2 \vartheta$$

σ_{c1}, σ_{c2} = the compressive stress at the respective node face

$C1, C2$ = the compressive force at the respective node face

a_1, a_0 = the width of the respective side of the node

b = the width of the structure

u = the depth of reinforcement layer in the node

f_{cd1} = the uniaxial concrete strength

Due to the presence of tensile forces, there is a tendency to form cracks, which result in the reduction of the concrete Schlaich [2] suggests a strength reduction factor of 0.8 of that of pure compressive node concrete strength.

Depending on the amount and orientation of the reinforcement, a complex stress distribution develops. The presence of such reinforcements therefore affects the determination of the node dimensions at the faces. As shown above, the width of a side of the node perpendicular the reinforcement may be defined as follows, depending on the number of layer, diameter and placement of reinforcements.

$U = 0$ for single layer reinforcement not reaching the deviation compression field

$U = d_s + 2c$ for single layer reinforcement with a minimum length in excess of compression field

$U = d_s + 2c + n*s$ for n layers of reinforcement and an excess length $\geq s/2$.

Where, c = concrete cover,

n = number of bar layers

s = spacing between the layers

In structures that carry high tensile forces result in multi layer of reinforcements and the effective depth of placing these reinforcements, as suggested by Schlaich [2], shall be as given below.

$$u = \leq 0.20h \quad \dots (12)$$

$$\leq 0.20 l$$

Where h = height of the D-region and

l = span of the deep beam

In cases where the width of load/support application is small compared to the thickness/width of the structure, the stress distribution will resemble the bottle-shape and develops a transverse tension. Stirrup or loop type reinforcement shall be provided in the region.

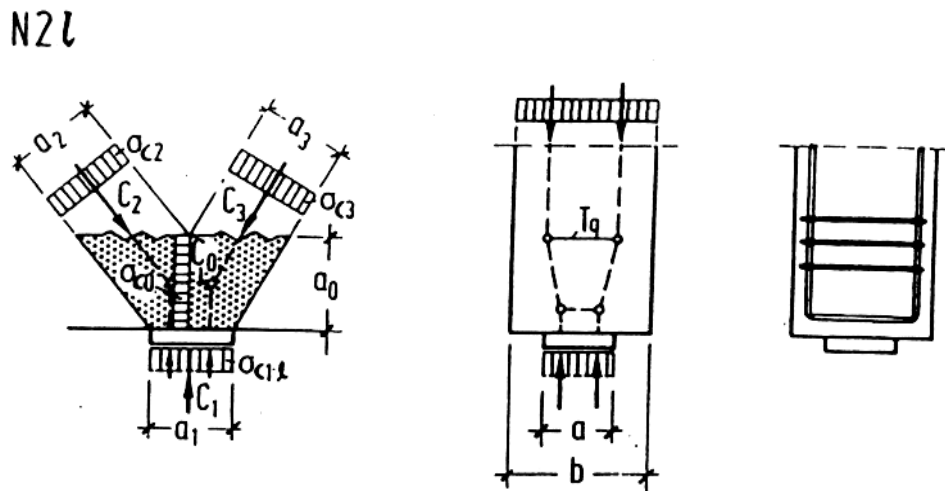


Fig 3.39 Node N2l with narrower load area of N2, strut-and-tie model and reinforcement layout. [2]

The transverse force in such region is estimated using the same expression for bottle shaped strut but by replacing the effective width of distribution by the narrower width of the structures. As

the application width of the load is smaller than the width of the section, the stress at the boundary obtained using the previous expression shall be modified to include the reduction of the width and hence is given as follows.

$$\sigma_{c1 \ell} = C_1 / (a_1 a) \leq f_{cd}^* \quad \dots (13)$$

Where, C_1 = load applied on the node

a = width of application of the force

a_1 = width shorter than the thickness of node region.

In such a case, the structure is highly stressed in a different manner and one needs to consider the strength variation. From tests of the concrete in such regions, the Eurocode 2 [17] allows a provision of a triaxial compressive strength of concrete for local pressure in the design of such regions as used in the equation above. This strength is given by the following expression:

$$f_{cd}^* = A_{c1} f_{cd} / A_{c0} = b f_{cd} / a_1 \leq 3.3 f_{cd} \quad \dots (14)$$

f_{cd}^* = Triaxial compressive strength for local pressure

A_{c1} = larger area of bearing /node

A_{c0} = narrowed area of concrete

b = width of larger

a_1 = narrower width

The above analyses focus on the compressive type of nodes and enumerate the technique for analysis and design of such systems. On the same line, a tension-compression node is analyzed similarly as shown below.

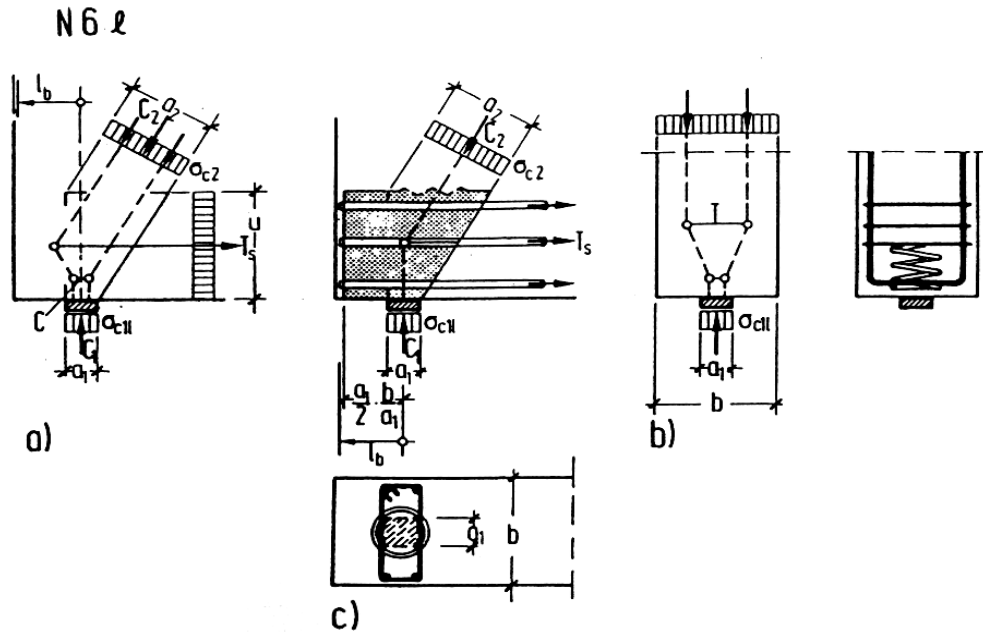


Fig 3.40 Node N6l a) STM with moved node b) section with narrower width c) transverse force reinforcement [2].

We may have a complex node pattern other than mentioned above as for ‘folded plate edge’ or beams with torsion, the node forces are as shown in the figure below.

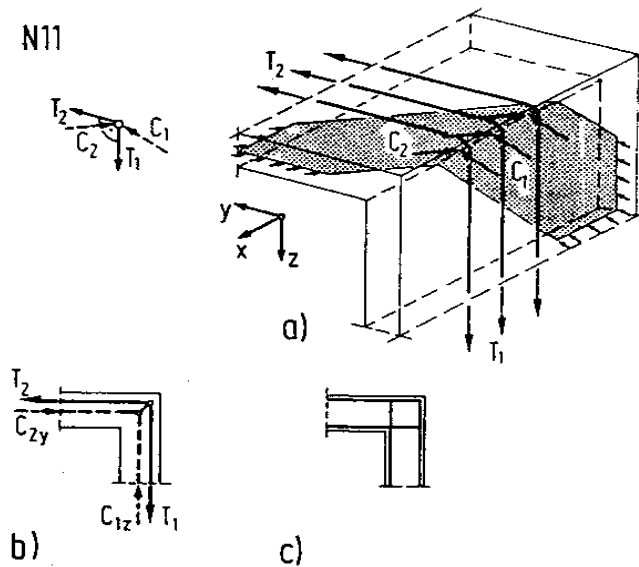


Fig 3.41 Node N11, the beam-column connection in 3-D b) strut model of the node c) reinforcement layout [2]

In such event, Leonhardt [8] recommends placing of closely spaced reinforcement to overcome crack problems.

CHAPTER 4

4.1 Application of Strut-and-Tie Model – Example 1

Having reviewed the theoretical background of the STM, we will now design a simply supported deep beam to illustrate the approaches discussed in the previous section.

4.2 Data of the deep beam

Design of a Deep Beam using STM approaches

A deep beam, shown below, is required to resist factored loads of 1250 KN. The material property for the design is C-25 and Fe400. Supports/loading is bearing plates with dimension of 450x500x10 mm and assumed to be safe in bending. Design the beam using the STM.

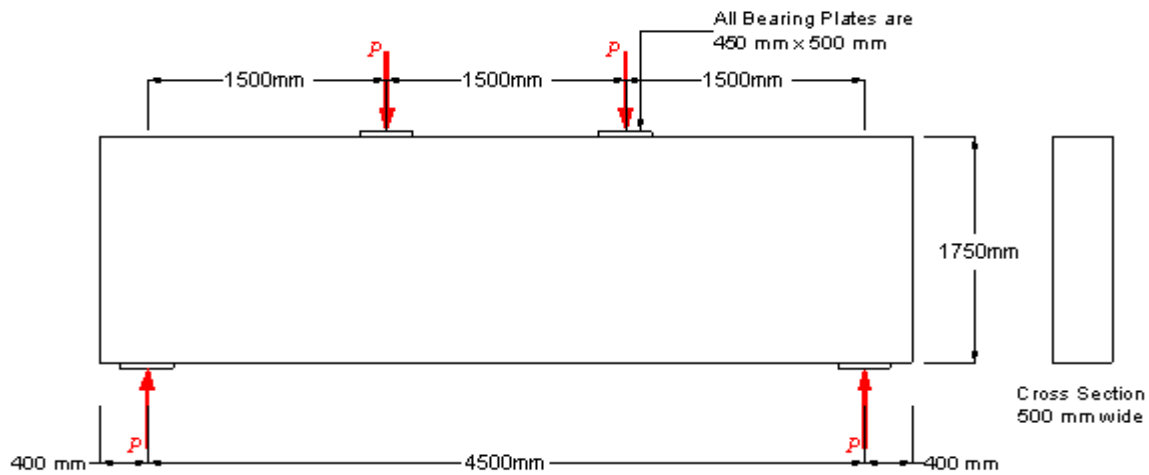


Fig 4.1 simply supported deep beam, dimensions and loading

4.2.1 Design procedure

Step 1: Define material/loading data

Material Data

Design concrete strength, $f_{cd} = 0.85 f_c' / \gamma_c$

$$f_{cd} = 0.85 * (0.8 * 25) / 1.5 = 11.33 \text{ MPa}$$

Design steel strength, $f_{sd} = f_{yk} / \gamma_s$

$$f_{sd} = 400 / 1.15 = 347.8 \text{ MPa}$$

Loading, Two equal loads are placed at one third of the top span

$$P = 1250 \text{ KN}$$

Step 2: Obtain boundary forces through the Overall/Global analysis of the structure.

Considering the sum of moment at the one of the support and due to symmetry gives:

$$\sum F_V = 0, \sum F_H = 0 \text{ and } \sum M = 0$$

$$R = P = 1250 \text{ KN}$$

$$\sigma_{BP} = R / A_{BP} = 1250 \cdot 10^3 / (0.45 \cdot 0.5) = 5.56 \text{ MPa} < f_{cd} = 11.33 \text{ MPa (OK!)}$$

Step 3: divide the structure in to B- and D-regions

The structure will be divided into B- and D-regions by defining the limit of the regions.

- define the D-regions by a vertical section at a distance D from the edge of beam, D1.
- define the D-regions by a vertical section at a distance D/2 for each side of the span loads, D2 as shown in figure below.

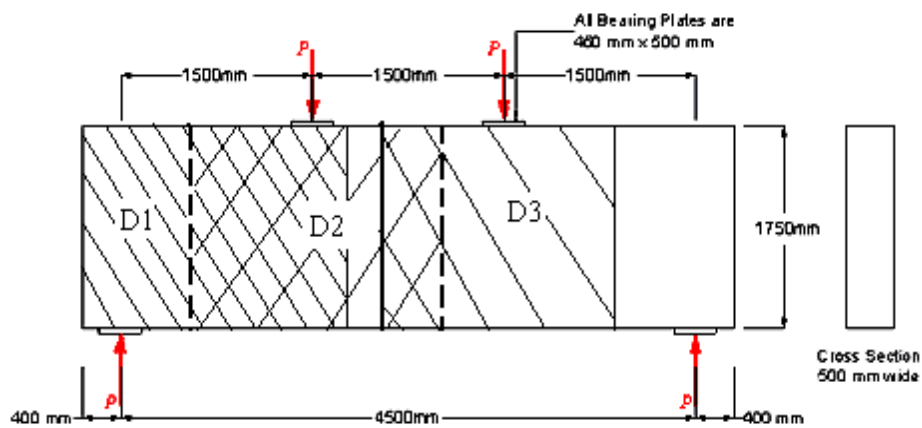


Fig 4.2 deep beam, division of the section into D-regions

Trial model 1

$$\text{Members AD, } C_{AD} = P / \sin \theta = 1250 \text{ KN} / \sin 45.8^\circ = 1743.6 \text{ KN}$$

$$T_{AC'} = P / \tan \theta = 1250 \text{ KN} / \tan 45.8^\circ = 1215.6 \text{ KN}$$

Trial Model 2

This model is indeterminate to the first degree. Therefore, by assuming one of the member forces, the other is analyzed. In the model the assumption is vertical stirrup supports half of the vertical load and then considering node equilibrium to obtain the truss forces.

$$T_{BC} = 0.5P = 0.5 * 1250 \text{ KN} = 625 \text{ KN}$$

Node B

$$C_{AB} = T_{BC} / \sin \theta_1 = 625 / \sin 64^\circ = 695.4 \text{ KN}$$

$$C_{BD} = C_{AB} \cos \theta_1 = 695.4 \cos 64^\circ = 304.8 \text{ KN}$$

Node A

$$P = C_{AD} \sin \theta + C_{AB} \sin \theta_1$$

Rearranging

$$C_{AD} = (P - C_{AB} \sin \theta_1) / \sin \theta = (1250 - 695.4 \sin 64^\circ) / \sin 45.8^\circ = 871.8 \text{ KN}$$

$$T_{AC} = C_{AB} \cos \theta_1 + C_{AD} \cos \theta = 695.4 * \cos 64^\circ + 871.8 * \cos 45.8^\circ = 912.5 \text{ KN}$$

Node C

$$C_{CD} = T_{BC} / \sin \theta_1 = 625 / \sin 64^\circ = 695.4 \text{ KN}$$

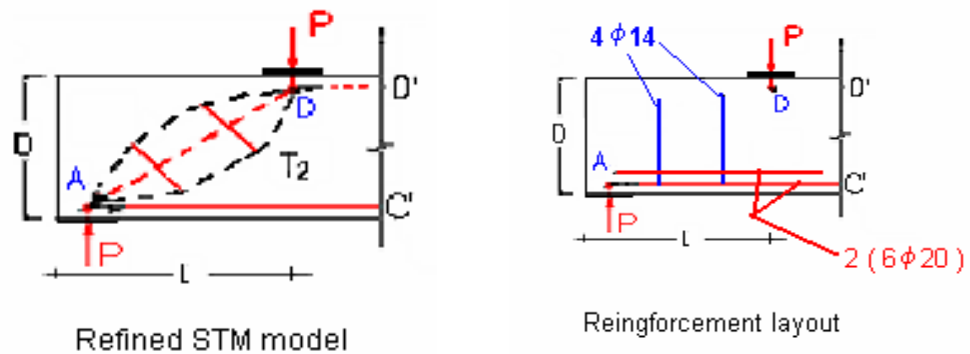
$$T_{CC'} = T_{AC} + C_{CD} \cos \theta_1 = 912.5 + 695.4 \cos 64^\circ = 1215.6 \text{ KN}$$

Step 7: Design the members

Now that we have determined the member force, we will proportion the members to carry the loads safely.

Trial Model 1

The strut AD is inside the concrete and will be safe since the critical strut is strut DD'. The strut DD' is safe since it is obtained from equilibrium at the boundary. However, strut AD develops a transverse tension and shall be provided with the tensile reinforcement using the expression suggested by Macgregor [6].



4.5 Half of Deep Beam a) refined STM model b) Reinforcement layout for main and Transverse tension force

$$T = 0.25 C (1 - a / b_{\text{eff}})$$

a = width of the strut at the node

$$b_{\text{eff}} = a + l / 6$$

C = compressive force on the node

$$\text{Length of the strut, } l = \sqrt{(1.54^2 + 1.5^2)} = 2.14\text{m}$$

$$a = C_{AD} / (0.8f_{cd} * b) = 1743.6 / (0.8 * 11.33 * 500) = 385 \text{ mm,}$$

$$b_{\text{eff}} = a + l/6 = 0.385 + 2.14/6 = 1.10 \text{ m}$$

$$T = C (1 - a/b_e) / 4 = 283.3 \text{ KN}$$

$$A_s = T / f_{yd} = 283.3 \text{ KN} / 347.8 \text{ MPa} = 815 \text{ mm}^2$$

Since the orientation is not practical and are replaced by vertical reinforcement,

$$A_{SV} = A_S / \cos 45.8^\circ = 1170 \text{ mm}^2$$

Using $\phi 14$ $A_b = 153 \text{ mm}^2$ required # of bars is 7.6

Use Two 4 $\phi 14$ closed stirrup for each transverse tension (two 4 $\phi 14$ stirrups = 1224 mm^2 , Fig 4.5b)

The tensile member is provided with reinforcements, Let us calculate the tension reinforcement and the depth placed.

$$A_s = T_{AC} / f_{yd} = 1215.6 * 10^3 / 347.8 = 3495 \text{ mm}^2$$

Using $\phi 20$ $A_b = 314 \text{ mm}^2$ required # of bars is 11.2

Use 2 Layers of 6 $\phi 20$ with a total $A_s = 3768 \text{ mm}^2$

Depth of placing the tie is $d' = 3\phi/20 + \phi_s + \text{cover} = 3*20/2 + 12 + 25 = 67 < d'$ provided =100 mm (OK!!!).

Trial Model 2

The critical width of the strut for STM model is usually at the boundary and hence strut DD', which is automatically safe from moment calculation. All other members of the STM are considered to be safe. However, the struts shall be checked for the transverse tensile force and provide the corresponding reinforcements.

$$\text{Width of } C_{AB} = 695.4 \text{ KN} / (0.8*11.33*0.5) = 154 \text{ mm}$$

$$\text{Width of } C_{BD} = 304.8 \text{ KN} / (0.8*11.33*0.5) = 67 \text{ mm}$$

$$\text{Width of } C_{AD} = 871.8 \text{ KN} / (0.8*11.33*0.5) = 193 \text{ mm}$$

Transverse Tie of the strut

$$\text{For } C_{AB} \quad l_{AB} = \sqrt{(0.75^2 + 1.54^2)} = 1.71 \text{ m}$$

$$b_{\text{eff}} = 0.154 + 1.71 / 6 = 0.439 \text{ m}$$

$$A_{SAB} = \{695.4 * (1 - 0.154/0.439) / 4\} / 347.8 = 326 \text{ mm}^2$$

Using $\phi 12$ $A_b = 113 \text{ mm}^2$ required # of bars is 2.8

Use two stirrup loop 2 $\phi 12$ with a total $A_s = 2 \times 452 = 904 \text{ mm}^2$

For C_{AD} $l_{AD} = \sqrt{(1.5^2 + 1.54^2)} = 2.14 \text{ m}$

$b_e = 0.193 + 2.14 / 6 = 0.550 \text{ m}$

$A_{SAB} = \{871.8 * (1 - 0.193 / 0.550) / 4\} / 347.8 = 407 \text{ mm}^2$

Using $\phi 12$ $A_b = 113 \text{ mm}^2$ required # of bars is 3.6

Use two stirrup loops 2 $\phi 12$ with a total $A_s = 2 \times 452 = 904 \text{ mm}^2$

Longitudinal main reinforcement

$T_{CC'} = T_{AC}$ of model 1. Hence the reinforcement is the same i.e. use 2 layers of 6 $\phi 20$ with a total

$$A_s = 3768 \text{ mm}^2$$

However, for the tie $T_{AC} = 912.5 \text{ KN}$

$$A_s = T_{AC} / f_{yd} = 912.5 / 347.8 = 2624 \text{ mm}^2$$

Using $\phi 20$ $A_b = 314 \text{ mm}^2$ required # of bars 8.4

Use 9 $\phi 20$ extension from the tie member CC' a total $A_s = 2826 \text{ mm}^2$

Note that the area of reinforcement near for support for trial model 2 is lower than for model 1.

For this reason model 2 is easier to anchor than model 1.

4.3 Application of STM – Example 2

4.3.1 Corbels

In this example, the STM-design-example will be addressed to a corbel to illustrate the approaches. Corbels are structural member that extends out from a column or wall. Their shear span to depth ratio shall be less than or equal to unity. They are constructed monolithically with

the support. The initial depth of corbel is determined from the shear capacity of concrete (EBCS- [16] pp 43).

$$V_{Rd} = 0.25 f_{cd} b_w d \quad \dots (15)$$

The failure mode of corbels is either concrete crushing or steel yielding but there are several variety of failure modes. The steel failure could be yielding of end anchorage at the column or at the loading and concrete crushing; compressive crushing or shearing of the concrete, and bearing failure under the loading. If the reinforcement anchorage is with hook rather than welding plate, it shall be secure enough for the concrete not to spill off at beyond the loading point.

Design Example of Corbel

Design a corbel given to resist a factored load 400KN. The point of application of the load is specified from the mechanical requirements i.e. 200 mm from the face of the column and the corbel protrudes 400mm with the point of application of the vertical load is. The column size 500x500, architectural requirement; the material property is C-30 and Fe400, fig 4.6.

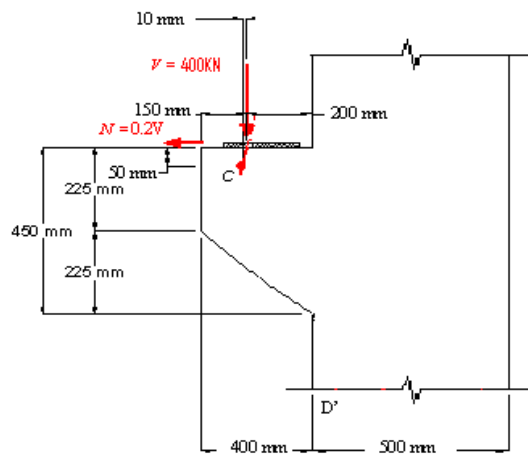


Fig. 4.6 Corbel, dimensions and loadings

4.3.2 Design procedure

Step 1: Determine the material/loading data

The design strength concrete is, $f_{cd} = 0.85 f_c' / \sigma_c$
 $f_{cd} = 0.85 * (0.8 * 30) / 1.5 = 13.6 \text{ MPa}$

The design strength steel is, $f_{sd} = f_{yk} / \sigma_s$
 $f_{sd} = 400 / 1.15 = 347.8 \text{ Mpa}$

Step 2: Propose section dimensions

Check for the section strength below the bearing plates for the assumed section.

Preliminary bearing plate size: 400*200*15 mm

Bearing beneath plate: $\sigma_{bp} = V / A_{bp} = 400 * 10^3 / (400 * 200) = 5.0 \text{ MPa} < f_{cd}$

The initial depth is assumed by the concrete shear capacity given in section above from EBCS.

$$d = V_{Rd} / 0.25 f_{cd} b_w$$

$$d = (400 * 10^3) / 0.25 * (13.6 * 10^6) * 0.4 = 0.294 \text{ m}$$

$$D = d + \text{cover} + \phi/2 = 294 + 25 + 20/2 = 329 \text{ mm}$$

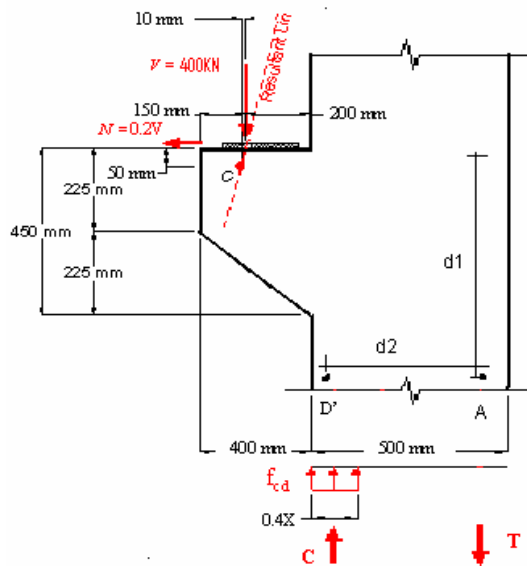


Fig. 4.7 Corbel with preliminary dimensions

The assumed overall depth of corbel near the face of the column is 450 mm and the shorter depth shall be at least half of the face depth (code requirement) i.e. 225mm. The dimensions are proportioned as in Fig. 4.7a. The center of tension region is 30mm from the face while the compressive region is 0.4x from the left face of the column. A horizontal force of 0.2V is applied at the surface and in the STM model the solid line is for tension forces.

Step 3: Obtain boundary forces through the overall/global analysis

The concrete resisting force is:

$$C = 0.8x * b * f_{cd}$$

$$= 0.8x * 0.5 * 13.6 = 5440x \text{ KN}$$

From force equilibrium:

$$C - T - 400 = 0$$

Taking moment at A the moment arm d1 & d2 for vertical and horizontal force is:

$$d1 = 0.50 + 0.20 - 0.03 + 0.01 = 0.68 \text{ m}$$

$$d2 = 0.45 - 0.05 = 0.40 \text{ m}$$

The moment arm for concrete compressive force

$$d = D - 0.03 - 0.4x$$

$$= 0.50 - 0.03 - 0.4x = 0.47 - 0.4x$$

From the moment equilibrium

$$V * d1 + H * d2 - C * d = 0$$

$$(400 * 0.68) + (80 * 0.4) - (5440x) * (0.47 - 0.4x) = 0$$

$$304 - 2556.8x + 2176x^2 = 0 \text{ or } x^2 - 1.175x + 0.140 = 0$$

$$x = 0.135 \text{ m}$$

The depth $d = 0.47 - 0.4(0.135) = 0.416 \text{ m}$

And the compressive force is, $C = 5440 (0.135) = 734.4 \text{ KN}$

Hence, $T = 734.4 - 400 = 334.4 \text{ KN}$

Step 4: Determine B and D-region

Corbels as discussed previously are as usually D-regions.

Step 5: Define an STM model

The STM model of the corbel region is as shown in the figure below.

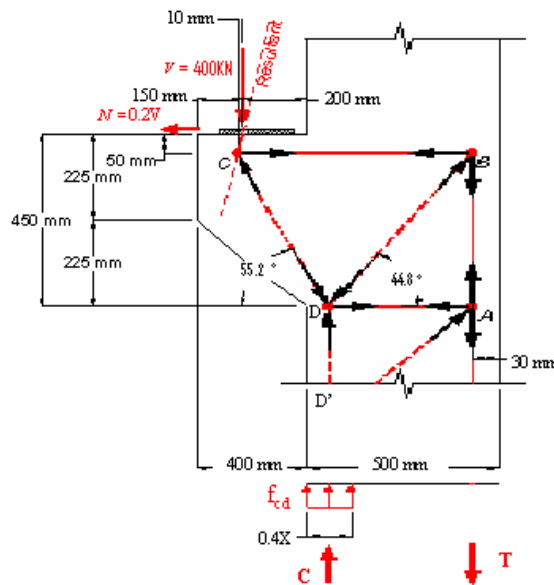


Fig 4.8 Strut-and-tie model of a corbel for the loading and dimensions

Step 6: Determine the member forces

The STM model is determinate where the member force are determined by nodal equilibrium

Node C: node C is located initially before calculating for the compressive C and tensile T. It shall have a depth of 50 mm from the surface and 10 mm left of load application.

Node B: it is 30 mm from the end of column and 680 mm left horizontally from node C.

Node D: is located $0.5x = 0.068 \text{ m}$ from the left end and 450mm from top edge of corbel.

Node A: is located 402mm horizontally from D.

$$\angle BCD = \arctan (400 / 278) = 55.2^\circ$$

$$\angle BDA = \arctan (400 / 402) = 44.8^\circ$$

Member force

Equilibrium of the node C:

$$C_{CD} = V / \sin 55.2^\circ = 400 / \sin 55.2^\circ = 487.1 \text{ KN}$$

$$T_{CB} = C_{CD} * \cos 55.2^\circ + H = 487.1 * \cos 55.2^\circ + 80 = 358.0 \text{ KN}$$

Equilibrium at the node B:

$$C_{BD} = T_{CB} / \cos 44.8^\circ = 358 / \cos 44.8^\circ = 504.5 \text{ KN}$$

$$T_{BA} = C_{BD} * \sin 44.8^\circ = 504.5 * \sin 44.8^\circ = 355.5 \text{ KN}$$

Equilibrium at the node D:

$$C_{DD'} = C_{CD} * \sin 55.2^\circ + C_{BD} * \sin 44.8^\circ = 487.2 * \sin 55.2^\circ + 504.5 * \sin 44.8^\circ = 755.5 \text{ KN}$$

$$T_{DA} = C_{BD} * \cos 44.8^\circ - C_{CD} * \cos 55.2^\circ = 504.5 * \cos 44.8^\circ - 487.2 * \cos 55.2^\circ = 79.93 \text{ KN}$$

The discrepancy in the result of $C_{DD'}$ is due to the selection of node D to be 0.5x instead of 0.4x from the face of the wall.

Checking the available width concrete area

The strut $C_{DD'}$ as seen in step 3 from the moment calculation, it is within the acceptable limit, fig 4.9. The other struts are inside the column and are accommodated safely. The strut OD need transverse tie to resist the concrete cracking.

To determine the effective width of the strut, the effect of tension force is considered, Fig 4.9.

Node C: for a single layer of steel and the diagonal strut is obtained from the expression

$$\sigma_1 = \sigma_2 \cos^2 \varphi$$

Rearranging,

$$\sigma_2 = \sigma_1 / \cos^2 \varphi = 5 / \cos^2 34.8^\circ = 7.36 \text{ MPa} < f_{cd} = 13.6 \text{ MPa}$$

$$a_2 = C_{CD} / b f_{cd} = 7.36 / (0.4 * 13.6) = 165 \text{ mm (Ok !!)}$$

$$\text{Length of the strut is: } \sqrt{(278^2 + 400^2)} = 487 \text{ mm}$$

$$\text{Effective width } b_{\text{eff}} = a + l / 6 = 165 + 487 / 6 = 246 \text{ mm}$$

$$\text{Transverse force, } T = C \{ 2 (1 - a / b_{\text{eff}}) \} / 4 = 487.1 \{ 2 * (1 - 165 / 246) / 4 \} = 80 \text{ KN}$$

$$A_s = T / f_{yd} = 80 * 10^3 / 347.8 = 230 \text{ mm}^2$$

$$A_s = 230 / \cos 55.2 = 403 \text{ mm}^2$$

$$\text{Using } \phi 12 \text{ } A_b = 153 \text{ mm}^2 \text{ required \# of bars } 2.65$$

$$\text{Use 2 layers of } 2 \phi 12 \text{ with a total } A_s = 452 \text{ mm}^2$$

For the tie members the area of reinforcement is determined.

$$A_{CB} = T_{CB} / f_{yd} = 487.1 * 10^3 / 347.8 = 1400 \text{ mm}^2$$

$$\text{Using } \phi 16 \text{ } A_b = 200 \text{ mm}^2 \text{ required \# of bars } 7$$

$$\text{Use 1 layers of } 7 \phi 16 \text{ with a total } A_s = 1400 \text{ mm}^2$$

$$\text{And placing width of the bars is } = n\phi + (n-1) * 20 + 2 * \text{cover} = 7 * 16 + 6 * 20 + 2 * 25 = 282 \text{ mm}$$

(OK!)

$$T_{BA} = 355.5 \text{ KN} < T_{CB}$$

Hence $A_{BA} < A_{CB}$ and extension of the ties beyond this region will be sufficient.

$$T_{DA} = 79.9 \text{ KN}$$

$$A_{DA} = T_{DA} / f_{yd} = 79.9 * 10^3 / 347.8 = 229 \text{ mm}^2$$

$$\text{Using } \phi 10 \text{ } A_b = 78 \text{ mm}^2 \text{ required \# of bars } 2.9$$

$$\text{Use 2 layers of } \phi 10 \text{ loop with a total } A_s = 308 \text{ mm}^2$$

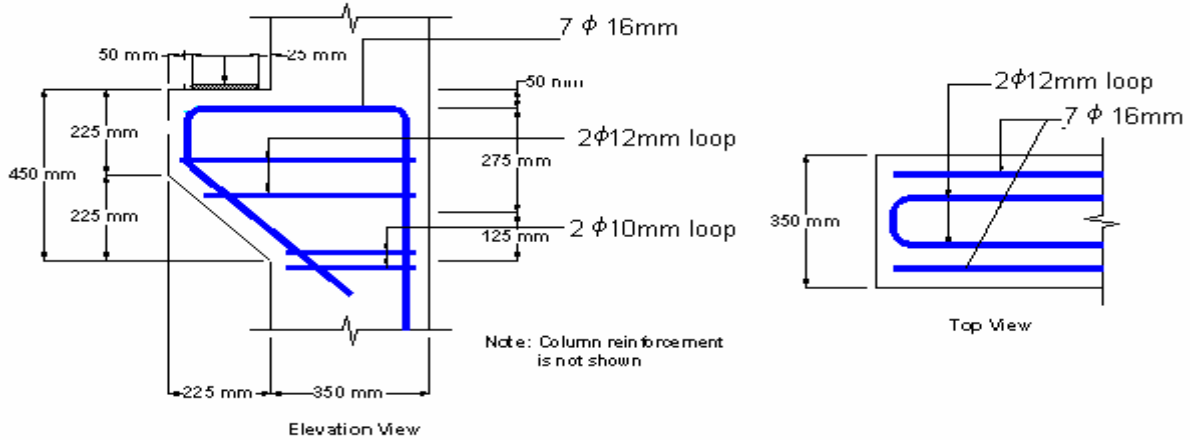


Fig 4.9. Corbel with the width of the struts and tie reinforcement layout.

Step 7: Checking Code requirement

The EBCS-2 recommends for the loading placed in the range of $0.4 d_c$ to d_c , the design is using simple strut-and-tie model. But loading placed at a distance from the face of the column d_c , where d_c is the depth of concrete, it can be designed as cantilever. However for deeper corbels other adequate models may be considered.

Corbels shall be designed for a horizontal force not less than 20% of the vertical load that act on the corbel unless other justification lead to given lower result. However the depth of concrete d_c assumed from shear consideration. In corbels with the $d_c \geq 300\text{mm}$ and the primary reinforcement $A_s \geq 0.4A_C f_{cd}/f_{yd}$, then closed stirrup of not less than $0.4A_s$ should be distributed over the effective depth d_c to resist concrete spill off and even helps in redistribution of forces.

But in the above particular example,

$$h_c = 400\text{mm} > 300\text{mm} \text{ and } A_s = 1400\text{mm}^2 < 0.4 (416 \cdot 400 \cdot 13.6 / 347.8) = 2603\text{mm}^2$$

Hence, according to EBCS-2[16] it does not need to place stirrup to protect concrete spill off.

However the strut-and-tie model will recommend a distribution of bars perpendicular to strut OD

and DB of 230mm^2 or equivalent reinforcement to accommodate practical layout of 403mm^2 shall be placed parallel to the bearing plate.

4.3.3 Some Typical Corbel STM models

Three typical corbels loading and their strut-and-tie model are given below help to visualize the stress flow. It is apparent that for different load condition the load path is different and shows areas where tension tie have to be considered.

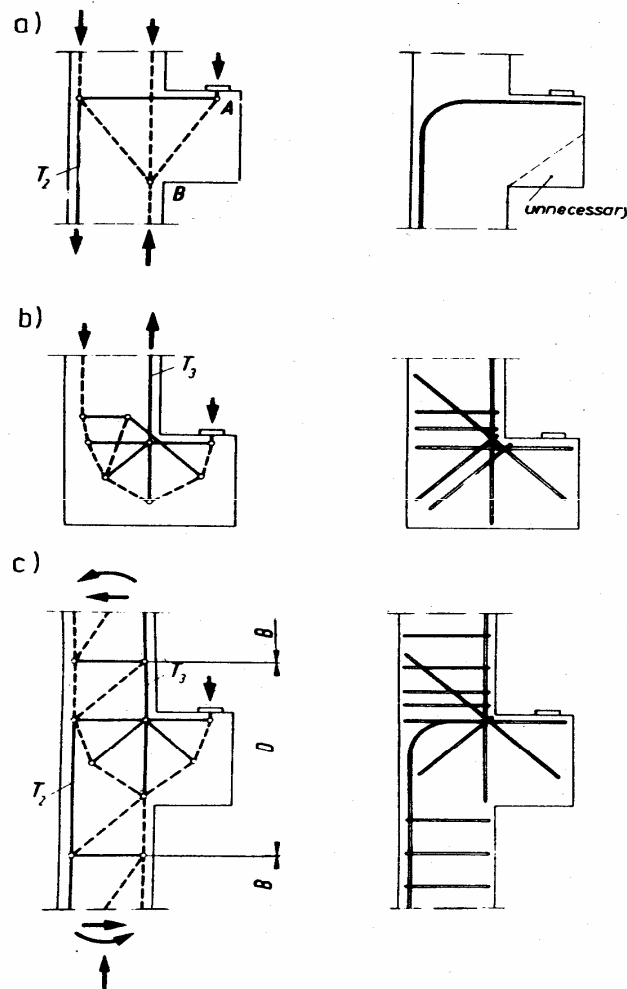


Fig. 4.10 Three typical corbels with different loading, strut-and-tie model and possible structural reinforcement. [1]

CHAPTER 5

5.1 Design of Special Structures Using Strut-and-Tie Model

A monument at Bahir Dar

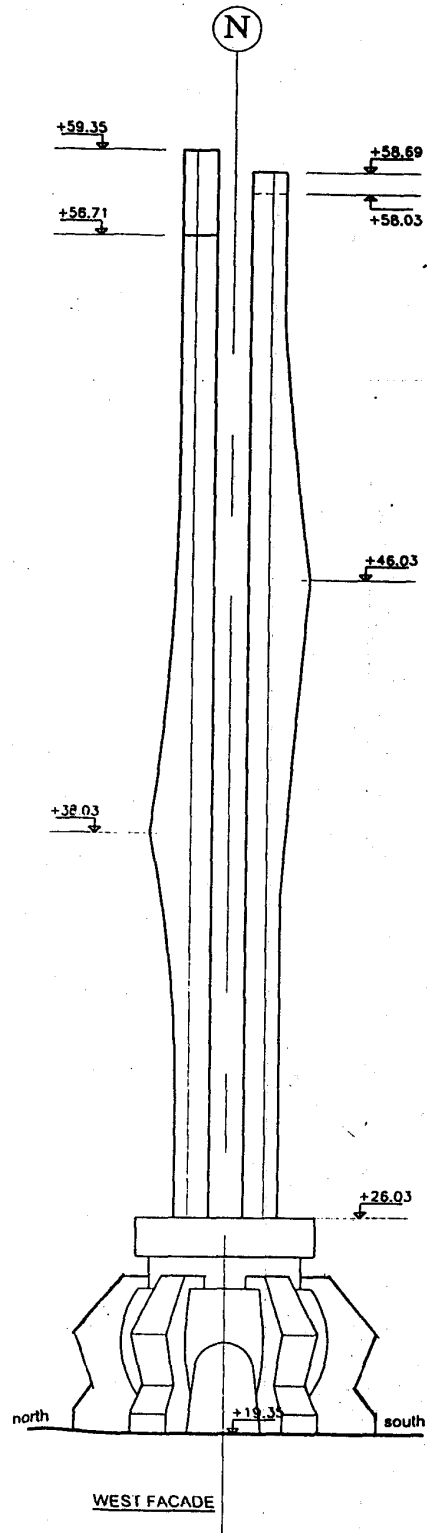
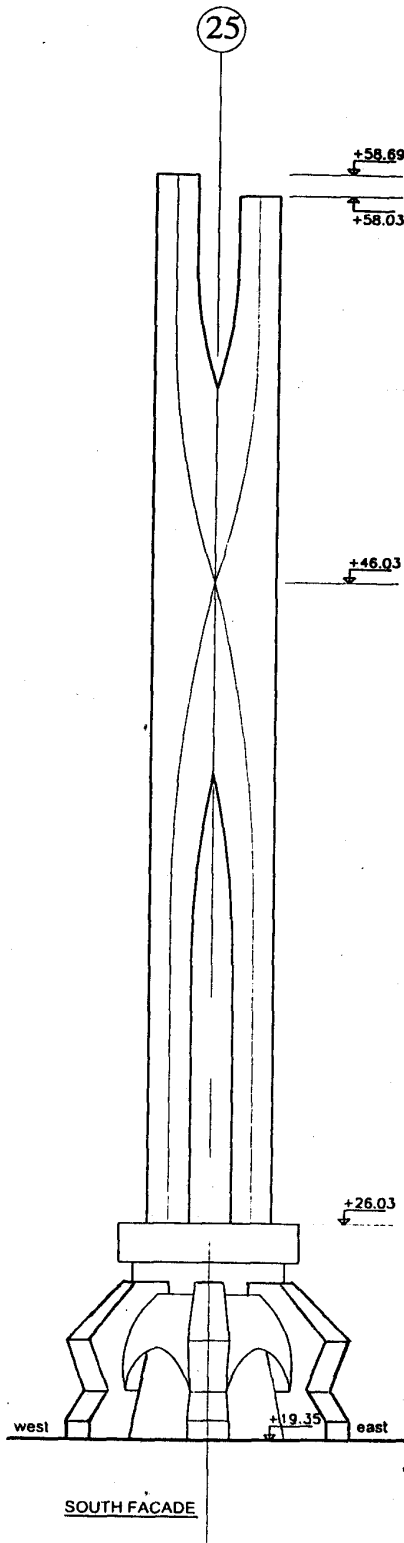
As an attempt to demonstrate the application of the principles of the strut-and-tie model to a special structure, a modeling and analysis of an obelisk will be done. This obelisk, *Martyr's Monument*, is an actual structure that was under construction in Bahir Dar, fig 5.1.

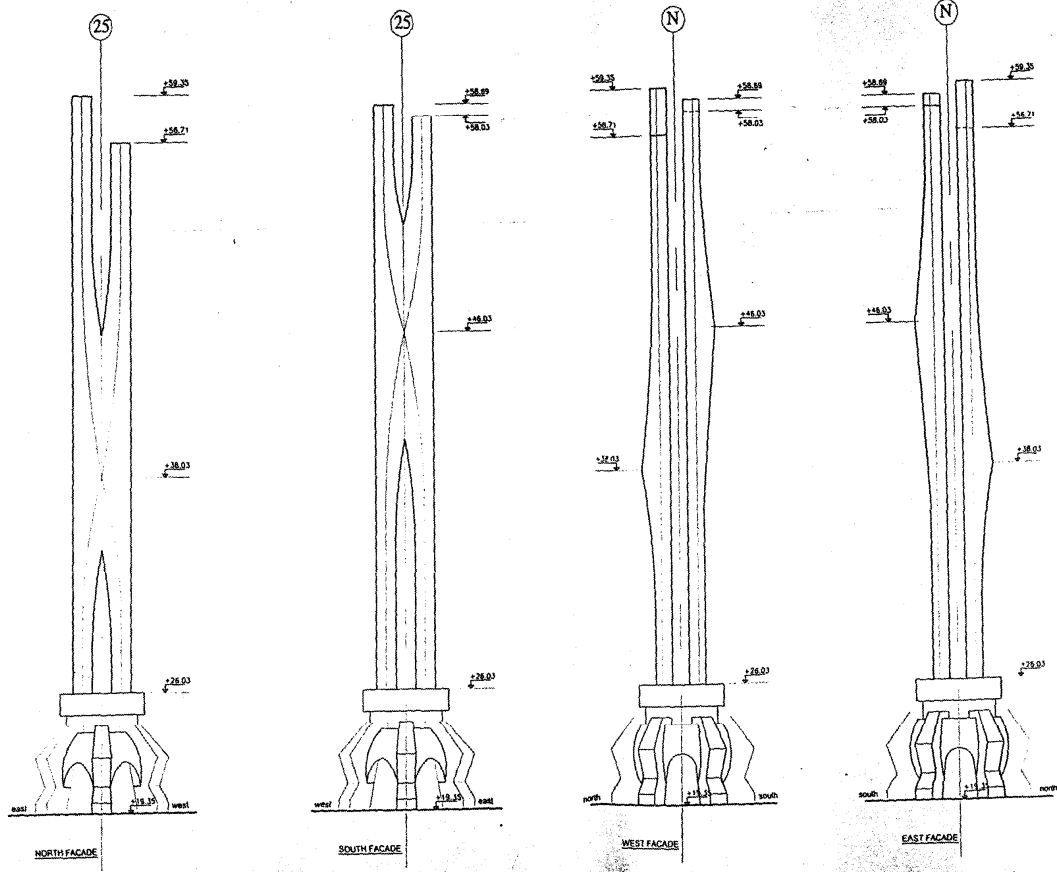
5.2 System Description

The monument is a freestanding reinforced concrete structure founded on a circular mat of diameter 12.16 m at level + 14.10. Six foundation columns with trapezoidal cross sections originate from the circular mat at an inclination angle of 75° and continue with constant cross sections to level + 18.50, where they are tied together with a grade beam.

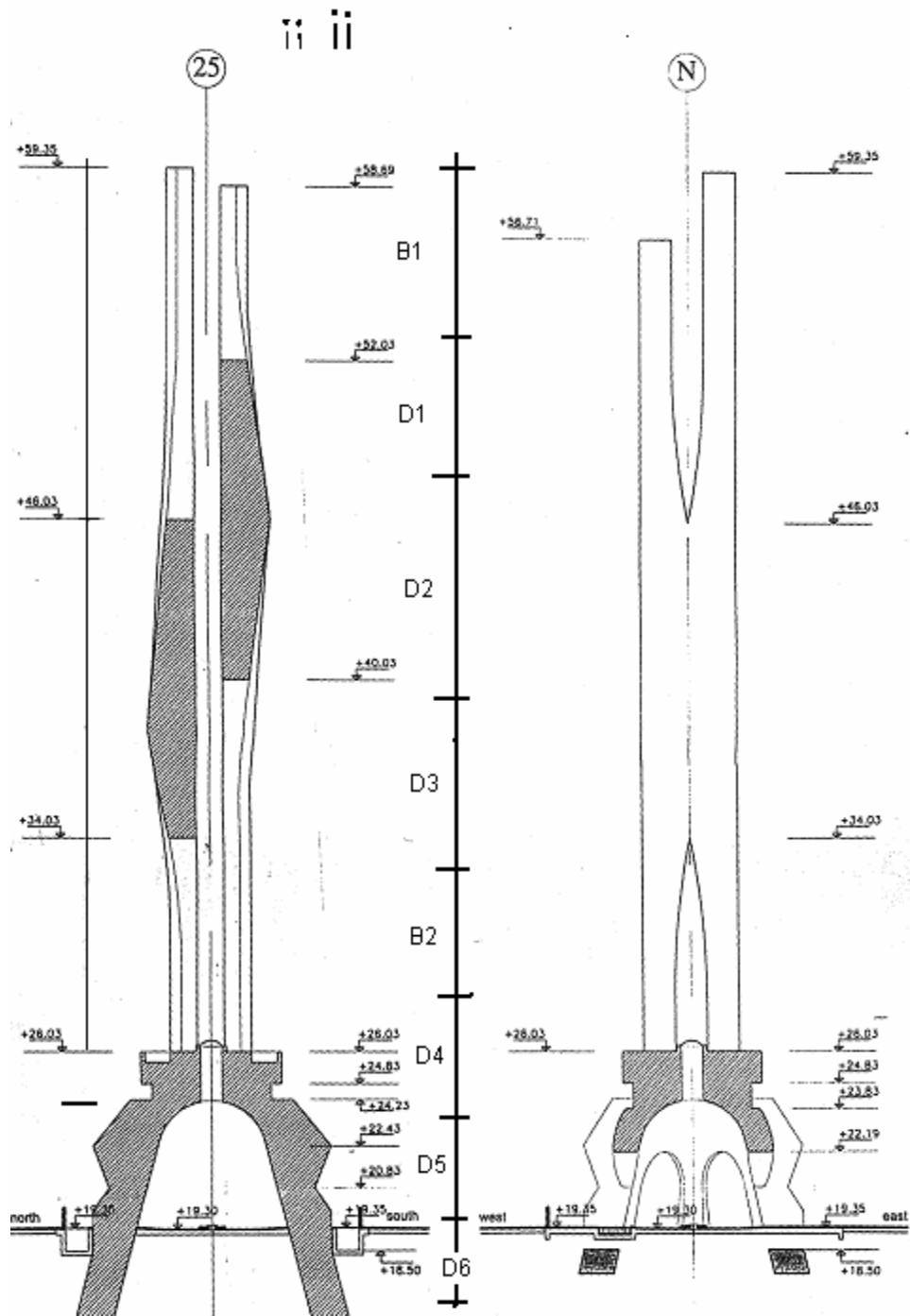
The extensions of the inclined columns above the grade beam are rather irregular in shape consisting of column zones at their interior defined as such for the structural scheme. They continue to the top of the disc to level +26.03 with their cross sections gently tapering from $b_1/b_2/h = 1200/824/1383$ mm at the top of the grade beam to 605/350/900 mm at the top of the disc [18].

Two pairs of vertical columns cantilever from the circular disc, each pair merging into a single column at levels + 38.03 and + 46.03. The highest point on one of the columns reaches an elevation of + 59.35. The figure below shows the overall dimensions of the monument.





b) Elevation of the monument



c) Section of the monument and B and D-regions

Fig 5.1 Architectural features of the monument

5.3 Design and Analysis Assumptions

Material data

- Unit weight of reinforced concrete 25 KN/m³
- Concrete grade C30
- Steel grade S-400

Loading Assumptions

Wind load magnification is considered but for brevity and clarity, detailed calculation is omitted.

Wind load coefficients and loads applied are indicated in Table 5.1,

- Due to geometry and the wind direction, wind action on the wider surface (N-S facades) governs.
- With the separation distance of only 1000 mm, each leg on the leeward side is completely shielded by the windward legs for wind actions in N-s direction.
- Each sub regions is replaced with uniform section
- For the wind calculation, the basic reference wind velocity, $V_{ref,o} = 22.0\text{m/s}$

Reference wind pressure

$$\begin{aligned}q_{ref} &= 0.5 \rho V_{ref}^2 \\ &= 0.5 * (1.0) * (22)^2 \\ &= 242.0\text{N} / \text{m}^2\end{aligned}$$

5.4 Loading on the structure

Two types of loading conditions will be considered in the analysis of the structure, with the following combinations:

- i) Self weight of the structure
- ii) Wind loads

As per the recommendation of EBCS [16], Section 1.9.4.5, a structure may be designed for wind loads in lieu of Earth Quake loads when such loads are deemed to be critical. Bahir Dar is located in Earth Quake free zone. Therefore, only wind loads have been considered [18]. On this line, the following load combination is considered:

- i) Combination 1 **1.35G + 1.5W**
- ii) Combination 2 **1.0G + 1.5W**

With this combination, we will now attempt to provide the data for the wind loading of the structure. The wind coefficients obtained by calculation are tabulated below, and these will be used to obtain the forces that will act on the structure.

Table 5.1 Coefficient of wind load, magnification factor and wind loads at different height

Factor ()		factor		coef(+ve)	coef (-ve)	Factor			
Z _o	Z _{min}	K _r	C _t	C _{pe}	C _{pe}	Φ _B			
0.01	2	0.17	1.5	0.8	-0.5	1.37			
V _{ref,0} =		22	(m/s)	Width of monument		3.6			
V _{dir} = C _{tem} = C _{alt} =		1		q _{ref} (KN/m ²) =		0.242			
V _{ref} (m/s)=		22							
Z _e	Cr	C _e	We	We (Suction)	Magn +ve We	Magn -ve We	Wind load +ve	Wind load -ve	
1.2	0.901	3.433	0.665	-0.415	0.911	-0.569	3.280	-2.047	
2.2	0.917	3.528	0.683	-0.427	0.936	-0.585	3.369	-2.106	
3.2	0.981	3.914	0.758	-0.474	1.038	-0.649	3.738	-2.338	
4.2	1.027	4.205	0.814	-0.509	1.115	-0.697	4.015	-2.510	
5.2	1.063	4.441	0.86	-0.537	1.178	-0.736	4.242	-2.648	
6.2	1.093	4.639	0.898	-0.561	1.230	-0.769	4.429	-2.767	
6.68	1.106	4.725	0.915	-0.572	1.254	-0.784	4.513	-2.821	
7.68	1.129	4.886	0.946	-0.591	1.296	-0.810	4.666	-2.915	
8.68	1.15	5.03	0.974	-0.609	1.334	-0.834	4.804	-3.004	
9.68	1.169	5.16	0.999	-0.624	1.369	-0.855	4.927	-3.078	
10.68	1.186	5.278	1.022	-0.639	1.400	-0.875	5.041	-3.152	
11.68	1.201	5.387	1.043	-0.652	1.429	-0.893	5.144	-3.216	
12.68	1.215	5.488	1.062	-0.664	1.455	-0.910	5.238	-3.275	
13.69	1.228	5.582	1.081	-0.675	1.481	-0.925	5.331	-3.329	
14.68	1.24	5.67	1.098	-0.686	1.504	-0.940	5.415	-3.383	
15.68	1.251	5.753	1.114	-0.696	1.526	-0.954	5.494	-3.433	
16.68	1.261	5.831	1.129	-0.706	1.547	-0.967	5.568	-3.482	
17.68	1.271	5.905	1.143	-0.714	1.566	-0.978	5.637	-3.521	
18.68	1.281	5.975	1.159	-0.723	1.588	-0.991	5.716	-3.566	
19.68	1.289	6.042	1.17	-0.731	1.603	-1.001	5.770	-3.605	
20.68	1.298	6.106	1.182	-0.739	1.619	-1.012	5.830	-3.645	
21.68	1.306	6.168	1.194	-0.746	1.636	-1.022	5.889	-3.679	
22.68	1.314	6.227	1.205	-0.753	1.651	-1.032	5.943	-3.714	
23.68	1.321	6.283	1.216	-0.76	1.666	-1.041	5.997	-3.748	
24.68	1.328	6.338	1.227	-0.767	1.681	-1.051	6.052	-3.783	
25.68	1.335	6.39	1.237	-0.773	1.695	-1.059	6.101	-3.812	
26.68	1.341	6.441	1.247	-0.779	1.708	-1.067	6.150	-3.842	
27.68	1.347	6.49	1.256	-0.785	1.721	-1.075	6.195	-3.872	
28.68	1.353	6.537	1.266	-0.791	1.734	-1.084	6.244	-3.901	
29.68	1.359	6.583	1.275	-0.797	1.747	-1.092	6.288	-3.931	
30.68	1.365	6.628	1.283	-0.802	1.758	-1.099	6.328	-3.955	
31.68	1.37	6.671	1.292	-0.807	1.770	-1.106	6.372	-3.980	
32.68	1.376	6.713	1.3	-0.812	1.781	-1.112	6.412	-4.005	
33.68	1.381	6.754	1.308	-0.817	1.792	-1.119	6.451	-4.029	
34.68	1.386	6.794	1.315	-0.822	1.802	-1.126	6.486	-4.054	
35.68	1.391	6.833	1.323	-0.827	1.813	-1.133	6.525	-4.079	
36.68	1.395	6.871	1.33	-0.831	1.822	-1.138	6.560	-4.098	
37.68	1.398	6.896	1.335	-0.834	1.829	-1.143	6.584	-4.113	
38.68	1.403	6.932	1.342	-0.839	1.839	-1.149	6.619	-4.138	
39.68	1.407	6.968	1.349	-0.843	1.848	-1.155	6.653	-4.158	
40	1.41	6.99	1.353	-0.846	1.854	-1.159	6.673	-4.172	

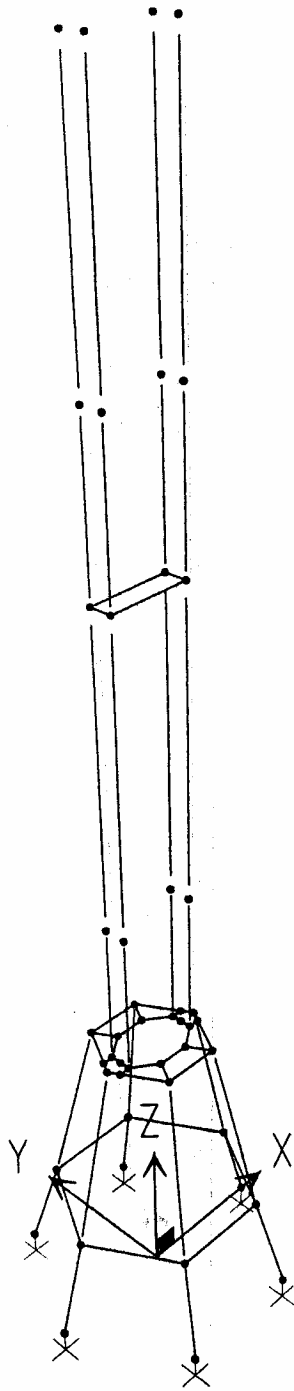
5.5 Structural Modeling and Applied Loading

In an attempt to idealize the structure so that it is suitable for computer software modeling and analysis, line elements were selected to represent the basic characteristics of the geometry of the of the structure. The two types of models used were

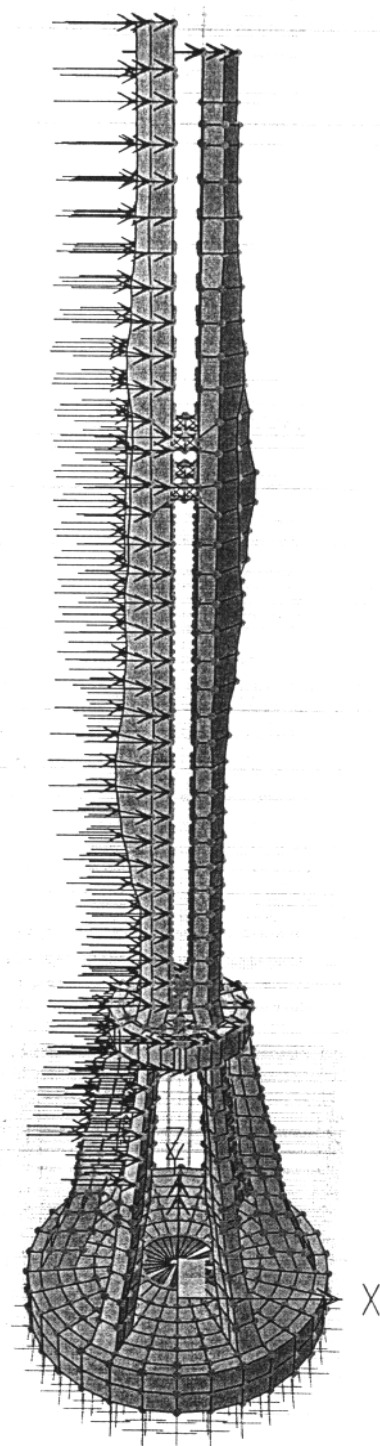
- Line modeling run using SAP 2000N, fig 5.2a
- Solid and shell elements, with non-regular cross sections, run with SAP 2000N (fig 5.2b & c)

As indicated in the drawings of the model, the main difficulty in analyzing the structures, modeling the areas where the geometry of the monument changes in plan/elevation, namely the disc region and the inclined column with protrusions, sections PP & KK. Therefore, the application of the Strut-and-tie modeling has focused on these critical areas.

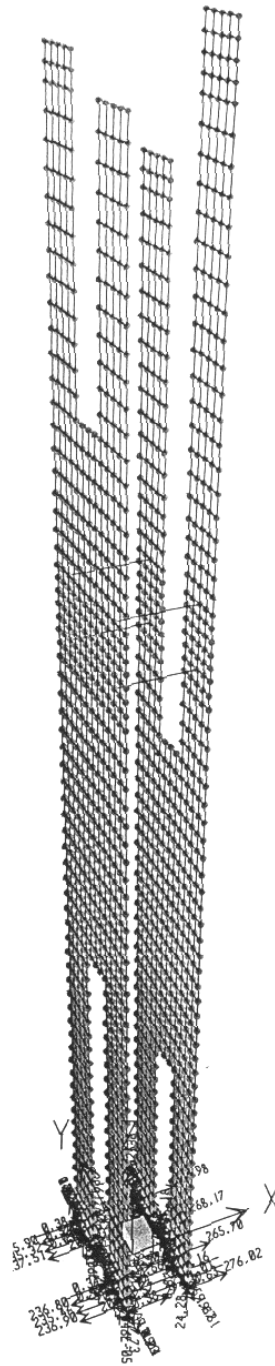
As mentioned above a solid/shell alternative-modeling approach was utilized for software analysis using SAP 2000N. The actual structure was divided into the B- and D- regions prior to inputting the data for the software analysis (see fig. 5.1). This subdivision is based on the statically/geometrical discontinuities. Since the monument is uniformly loaded, the division is based on the geometrical consideration. The results of this approach and the alternative solid/shell models are attached in annex 1.



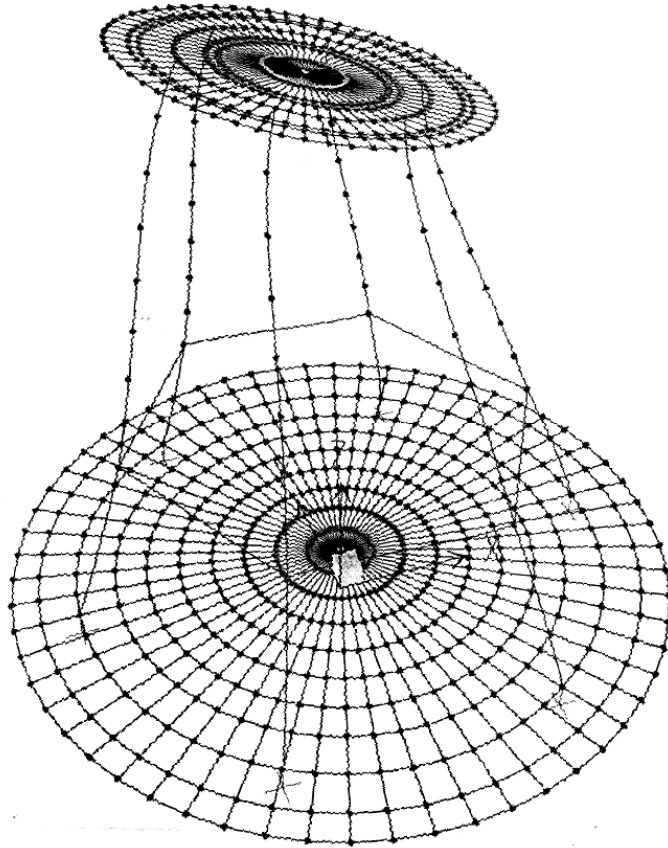
a) Line element modeling of the Monument



b) Solid element modeling of the Monument, with wind loading [18]



c1) Shell element modeling of the Monument, as Cantilever column [18]



c2) Shell modeling of the Monument, bottom part (deformed) [18]

Fig 5.2 Software model of the Monument a) line element b) solid element c) shell element (c1 & c2)

5.6 Input data

5.6.1 Loading

The loading applied as mentioned earlier comprises of the structure's own weight and wind loads, appropriate for the chosen locality Bahir Dar, in the indicated combination, figure below.

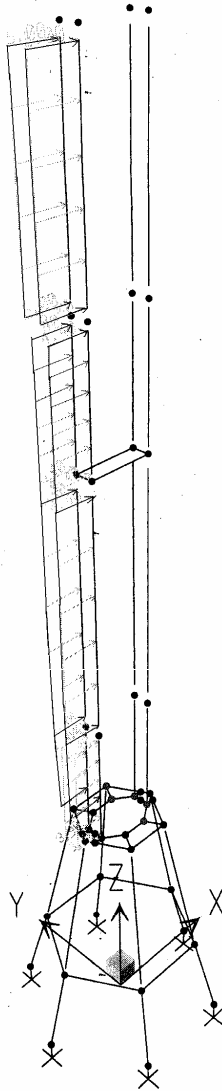


Fig 5.3 Wind load for line modeling of the monument

The basic assumption of the loading data has focused on the approaches whereby parts of the structures are assumed to carry their own weight only even though they contribute to structural support to element above them, the dome near the circular section and the protrusion of the inclined column.

5.6.2 Geometry

The irregular sections of the inclined columns and the vertical cantilever columns are approximately replaced by rectangular sections, as shown below.

$$d_{avg\ 1} = d_{VAR} / 3 + h = 0.4/3 + 0.6 = 0.73\ m \quad \text{section PP}$$

$$d_{avg\ 2} = d_{VAR} / 3 + h = (0.6 - 0.3) / 3 + 0.3 = 0.4\ m \quad \text{section KK}$$

$$d_{avg\ 3} = d_{VAR} / 3 + h = (1.2 - 0.82) / 3 + 0.82 = 0.94\ m \quad \text{take } 0.82m \quad \text{section MM}$$

Where d_{VAR} = depth of the net difference

d_{avg} = average depth of the region

h = height of the cross section

Section ii = the location of the irregular section in the structure

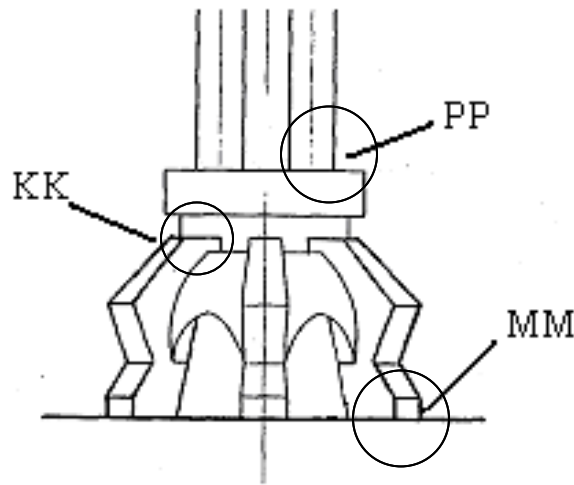


Fig 5.4 Critical sections PP, KK and MM of the monument [18]

The sectional properties are shown below.

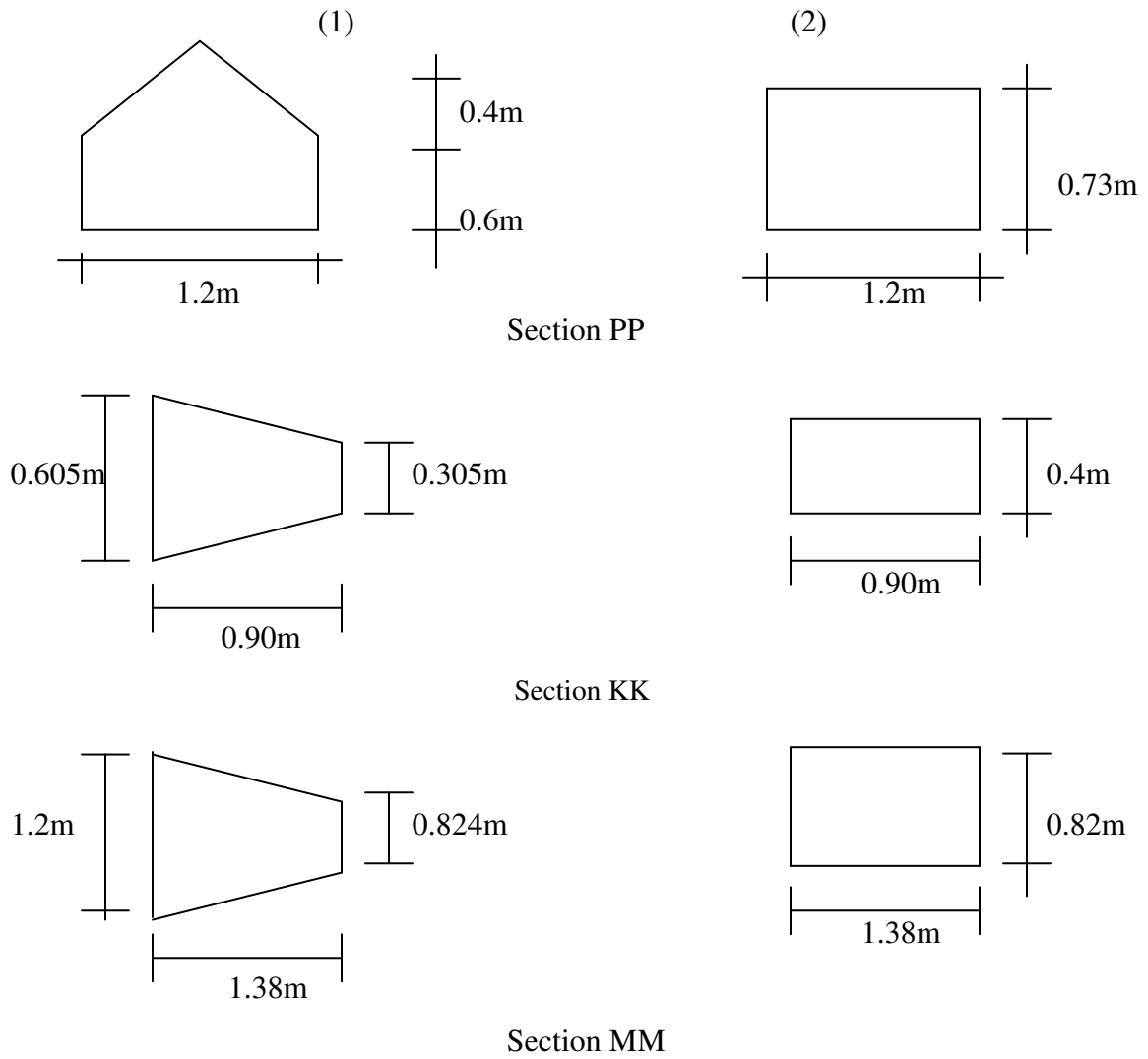


Fig 5.5 Geometric dimensions at sections PP, KK and MM 1) actual dimensions 2) modified dimension

5.7 Overall Analysis of the Monument

The model was run with the SAP 2000N– structural analysis software. [the results is attached in the annex 1].

Comments/observations

- The structure was modeled using line/shell elements as an alternative approaches for comparison purposes

- The output of the two modeling (shell/solid and line element) approaches are different
- The significant difference in the output data relate to the areas indicated as KK, PP and MM in fig. 5.4.
- These regions are basically the D-regions in the modeling.

5.8 Analysis and Design using the Strut-and-Tie model

The structure is made of reinforced concrete grade C-30 steel and grade S-400. As indicated above, the disc region and the inclined columns with protrusions were identified since the more complex regions of the structure and therefore chosen for the application of the Strut-and-tie modeling.

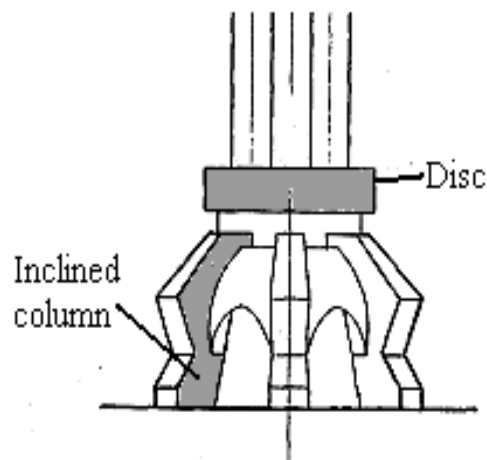


Fig 5.6 D-regions, disc and inclined column with protrusion [18]

Note that the disc is subtended between the sections PP and KK whereas the inclined column is subtended between KK and MM.

5.8.1 Boundary forces determined as Initial step

The results of the software analysis, namely axial force, shear force and bending moment, are replaced by their Strut-and-tie modeling to an equivalent axial force, which are tension/compression axial forces. These actions were obtained from previous analysis given in reference [18].

The stresses at the boundary of B and D-regions are equal and for such conditions to obtain the boundary force the usual assumption that stresses are linear can be assumed. However for our case, the equivalent axial force replaces the boundary action (moment). Therefore, force couple-approach was utilized in lieu of the moment action. One point that needs to be observed here is the fact that the particular section will be acted upon by two boundary actions, the axial force and the bending moment. The shear force is neglected in analysis since its effect relatively small when compared to the other two actions is.

As mentioned above, the Strut-and-tie modeling approach is based on axial forces and therefore to convert the actual boundary actions to Strut-and-Tie Model assumptions, the effect of moment has to be converted to an equivalent static action. To this end, the following expression using the force-couple approach will yield the desired result.

The alternative assumption may include

$$\text{i) } C = M / z, \quad \text{where, } z \approx 0.9d \text{ or} \quad \dots (16a)$$

$$\text{ii) } C = M / z, \quad \text{where, } z = d - 0.4 * x$$
$$\text{and } M = 0.8 * x * f_{cd} * b * (d - 0.4x) \quad \dots (16b)$$

Where, f_{cd} = design compressive strength of concrete

x = the depth of compressive concrete

z = moment arm

b = width of the section

d = effective depth of the section

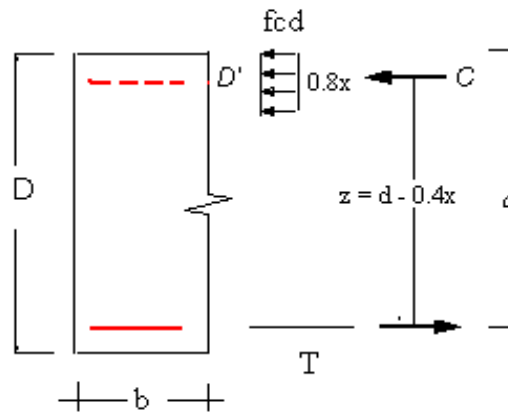


Fig 5.7 Stress at the boundary of D region replaced by an equivalent couple action.

The above equation contains expressions for the cross sectional dimensions namely b and d . However, since we are attempting to analyze two regions, circular and inclined trapezoidal section, we will obtain two differing load application points with varying dimensions.

This means that there will be two differing dimension at the top and bottom of the location. For analysis purpose, we will formulate an equivalent section by converting the initial section dimension to the desired result.

After obtaining the equivalent area, we will now proceed to obtain the converted axial actions from the initial boundary actions. The conversion process is based on the following expression.

$$F = M / z$$

But $M = 0.8 * x * f_{cd} * b * (d - 0.4x)$

Where $f_{cd} = 30 * 0.85 * 0.8 / 1.5 = 13.6 \text{ MPa}$ for pure compression section

$f_{cd} = 0.8 * f_{cd} \text{ (pure compression)} = 13.6 * 0.8 = 10.9 \text{ MPa}$ for tension-compression

$f_{yd} = 400 / 1.15 = 348 \text{ MPa}$ for steel design

In the final stage, the axial forces obtained from the above expression will be combined with the effects of the direct axial effects. This combination will be carried out as follows yielding a total axial force, C_{tot} .

$$C_{tot} = C_M + N / 2$$

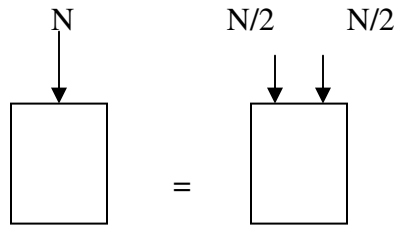
Where, C_{tot} = the combined axial effect

C_M = compressive axial force due to the moment, Eq 16

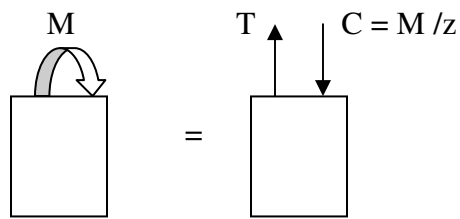
N = the axial force (obtained directly from the analysis)

The couple action of the moment effect has differing direction, which in one end will increase the axial effect while in another it will reduce the axial effect, as shown in the following diagram.

1) Effect due to the axial load only

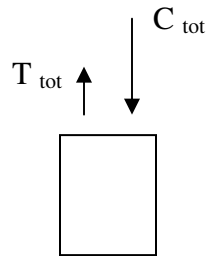


2) Effect due to the moment and their equivalent axial force



Where, $C_M = T_M$

3) Effect due to couple action replacing the moment action



$$C_{\text{tot}} = C_M + N / 2$$

$$T_{\text{tot}} = T_M + N / 2 = N / 2 - C_M$$

Fig 5.8 Schematic representation of the combination effect of axial force and bending moment (at the boundary), equivalent couple and the final axial force on the boundary

Using the above expressions, the conversion of the boundary actions into equivalent Strut-and-Tie Model forces is carried for the section of the structure, which we design. These forces are tabulated below for ease of reference.

Table 5.2 Forces acting on the PP section, forces acting at top of disk

Disc top	N [KN]	M [KN-m]	V [KN]	Compressi on depth x [m]	C_M moment) [KN]	C_{tot} $C_M + N/2$ [KN]	T_{tot} $T_M - N/2$ [KN]
Pair A	1219	1348.5	120.1	0.18	2350(-)	2959.5(-)	1740(+)
Pair B	1920	1197.7	71	0.16	1958.4(-)	2918.4(-)	998.4(+)

Table 5.3 Forces acting on the section KK, forces at the bottom of disk

Disc bottom	N [KN]	M_{3-3} [KN-m]	M_{2-2} [KN-m]	C_{M33}^* [KN]	C_{M22}^* [KN]	X [m]	C_{tot} [KN]	T_{tot} [KN]
1	521.2	445.9	0	376(-)	0	0.05	608.6(-)	87.4(+)
2	1,139.8	242.8	130.6	204.4(-)	358	0.05	786.9(-)	352.9(-)
3	2,082.3	131.3	125.9	110.5(-)	194	0.05	1171.1(-)	911.15(-)
4	2,543.9	313.5	0	264(-)	0	0.05	1533.9(-)	1011(-)

*- C_{ii} is the effect moment in the axis ii on the section

Table 5.4 Forces acting on section MM, or the bottom section of the inclined column

Inclined Column bottom	N [KN]	M_{3-3} [KN-m]	M_{2-2} [KN-m]	C_{M33}^* [KN]	C_{M22}^* [KN]	X [m]	C_{tot} [KN]	T_{tot} [KN]
1	732.5	233.3	0	199.0(-)	0	0.05	565.2(-)	167.0(+)
2	1339.0	1,209.0	110.0	103.0(-)	114	0.05	790.4(-)	548.6(-)
3	2,302.4	745.0	108.0	63.7(-)	150	0.05	1226.2 (-)	1,077.0(-)
4	2,767.0	201.0	0	171.8(-)	0	0.05	1,584.0(-)	1,182.0(-)

After obtaining these forces, the next step is to proceed with the design of the required sections of the structure, as detailed in the figure below.

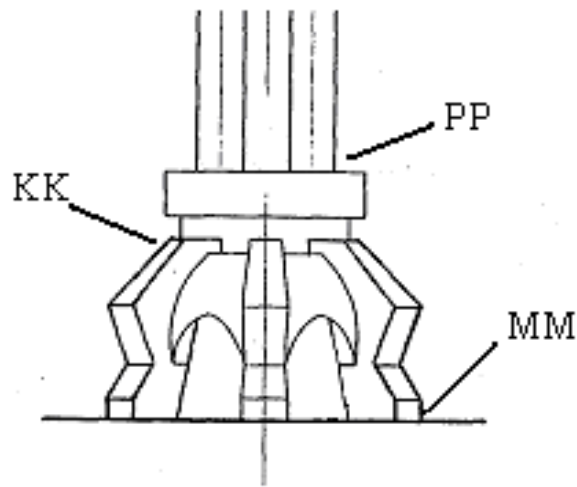


Fig 5.9 Section PP, KK and MM in the monument [18]

5.8.2 Disc region: STM Modeling

In an attempt to represent practically the above axial forces in relation to the actual structure, we may consider the sections X-X and Y-Y from the plan of the region, as shown in fig 5.10.

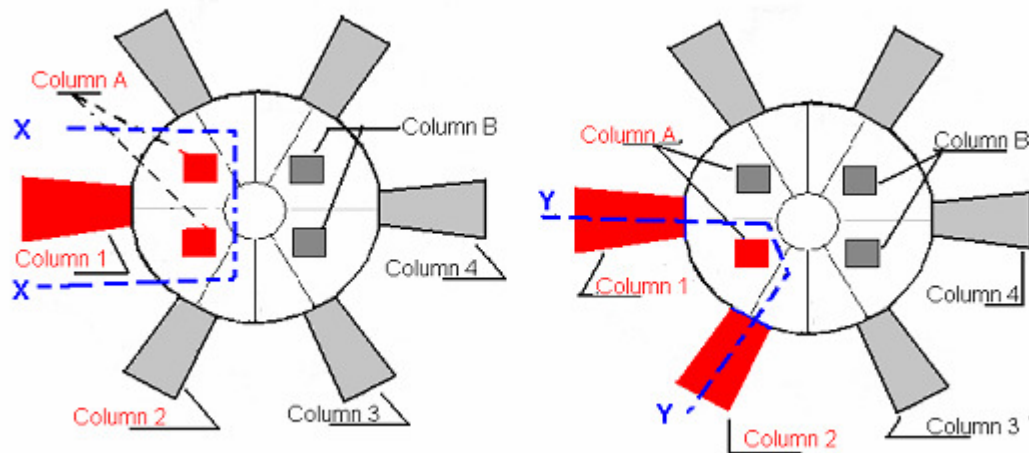


Fig 5.10 plan of the focus area, section X-X and Y-Y [18]

The boundary action acting on the region is shown in figure 5.11a with bending moment and axial forces. The moments are then replaced by equivalent axial forces and summed with the axial force to obtain the net axial force acting on the boundaries. The loads applied at the disk consists of tension and compression forces, which are transmitted to the structure below in two directions each, or trusses. As shown in Fig 5.11b, it forms two trusses, truss abc and truss a'b'c'. In addition to this, a third truss aa'c' is formed to connect the two 2-dimensional STM models. It may be considered as single STM or considered with the other STM models and analyzed as 3-Dimensional truss.

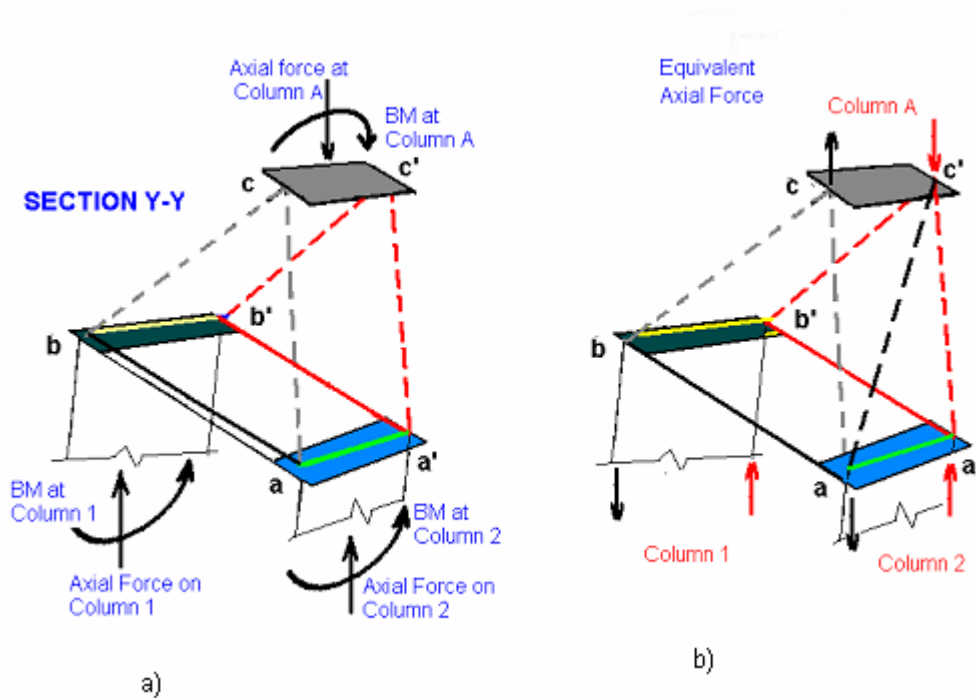


Fig 5.11 Section Y-Y a) boundary actions on the disk region b) Equivalent axial force and STM model of the region

The boundary forces obtained by applying the steps enumerated in this section are shown in the Fig 5.12 below to illustrate the actions on the region. The boundary forces applied are obtained from table 5.2 and 5.3 and we observe that the whole structure is in equilibrium.

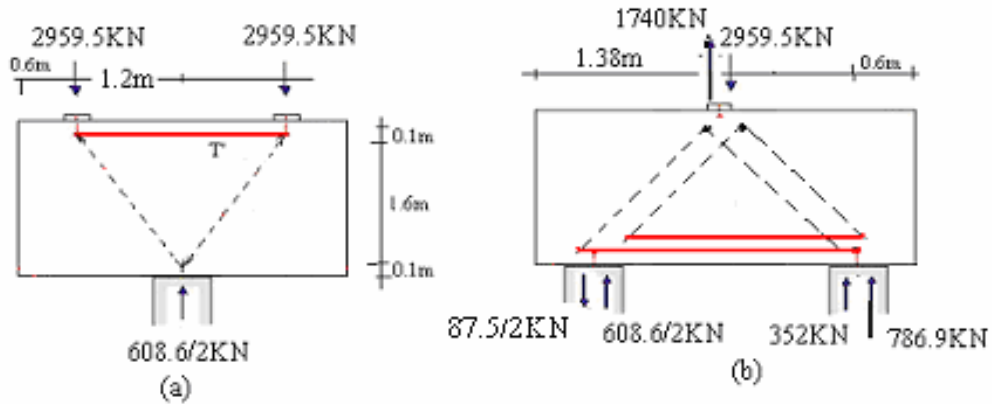


Fig 5. 12 two dimensional representation of region near column A, the boundary force and STM

$$\sum F_V = 0 = 2*(1219 + 1920) - (521.2 + 1139.8 + 2082.3 + 2143.3) = 0$$

Even though the structure as a whole may be in equilibrium we need to check the static equilibrium of a section of the truss that is shown in table 5.2 and 5.3.

$$\sum F_V = 0 \neq 1139.8 + 521.2 - 1219 = 442 \text{ KN}$$

This shows that the unbalanced force is transferred to the other column that is not easily observed in the two dimensional figures.. For simplicity of the analysis of the region each truss is considered alone and later combined to consider the effect of one on the other.

5.8.3 Statical Calculation for Disc Region

1. Statical Calculation for Critical Section Near Column A

i) Region with compressive force on all nodes

The forces on this section of the region are redrawn, below, for clarity and the assumed STM model showing the transverse tension in the compressive strut.

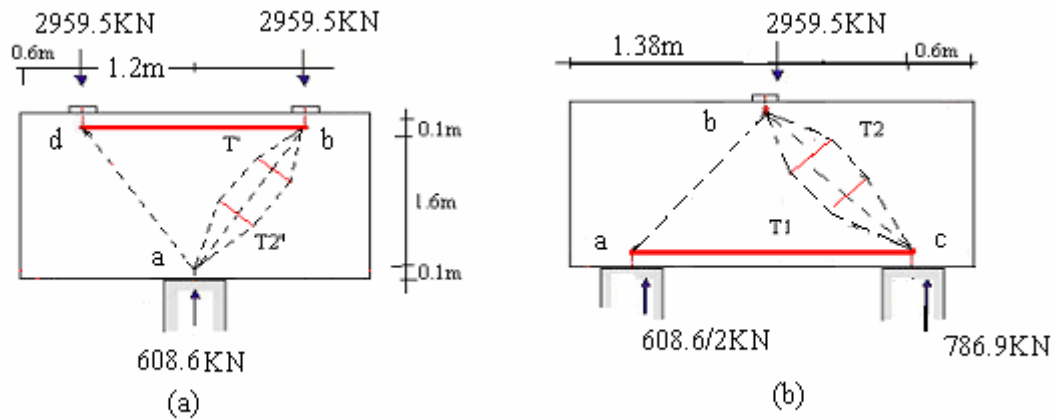


Fig. 5.13 Boundary forces and STM representation of compression section of node

From the equilibrium of the nodes the member force are obtained as follows:

$$C_{ab} = (608.6/2) * \sqrt{(1.62 + 1.2^2)} / 1.6 = 304.3 * 2 / 1.6 = 380.4 \text{ KN}$$

$$T_{bd} = C_{ab} * 1.2 / 2 = 228.24 \text{ KN}$$

$$T2' = 0.25 C_{ab} (1 - a / b_{\text{eff}})$$

$$a = 0.2, \text{ (strut width } a = 0.2)$$

$$b_{\text{eff}} = a + l/6 = 0.2 + 2/6 = 0.53\text{m (well inside the region)}$$

$$T2' = 0.25 * 380.4 * (1 - 0.2 / 0.53) = 59 \text{ KN}$$

From figure (b)

$$C_{cb} = 786.9 * \sqrt{(1.38^2 + 1.6^2)} / 1.6 = 786.9 * 2.11 / 1.6 = 1037.7 \text{ KN}$$

$$T_{ac} = 1037.7 * 1.38 / 2.11 = 678.7 \text{ KN}$$

$$T2 = 0.25 C_{cb} (1 - a / b_{\text{eff}})$$

$$a = 0.4, \text{ (strut width } a = 0.2 \text{ compression width)}$$

$$b_{\text{eff}} = a + l/6 = 0.2 + 2.11/6 = 0.55\text{m (well inside the region)}$$

$$T2 = 0.25 * 1037.7 * (1 - 0.2 / 0.55) = 165 \text{ KN}$$

The reinforcement to be provided in this region is proportioned using the steel property below:

From figure (a)

$$T_{bd} = 228.24 \text{ KN} \quad A_s = 228.24 / 348 = 656 \text{ mm}^2$$

$$T_{2'} = 59 \text{ KN} \quad A_s = 59 / 348 = 170 \text{ mm}^2$$

From figure (b)

$$T_{ac} = 678.7 \text{ KN} \quad A_s = 678.7 / 348 = 1950 \text{ mm}^2$$

$$T_2 = 165 \text{ KN} \quad A_s = 165 / 348 = 475 \text{ mm}^2$$

ii) Region with tensile node force

As can be seen the second STM model consists of tension members, figure below.

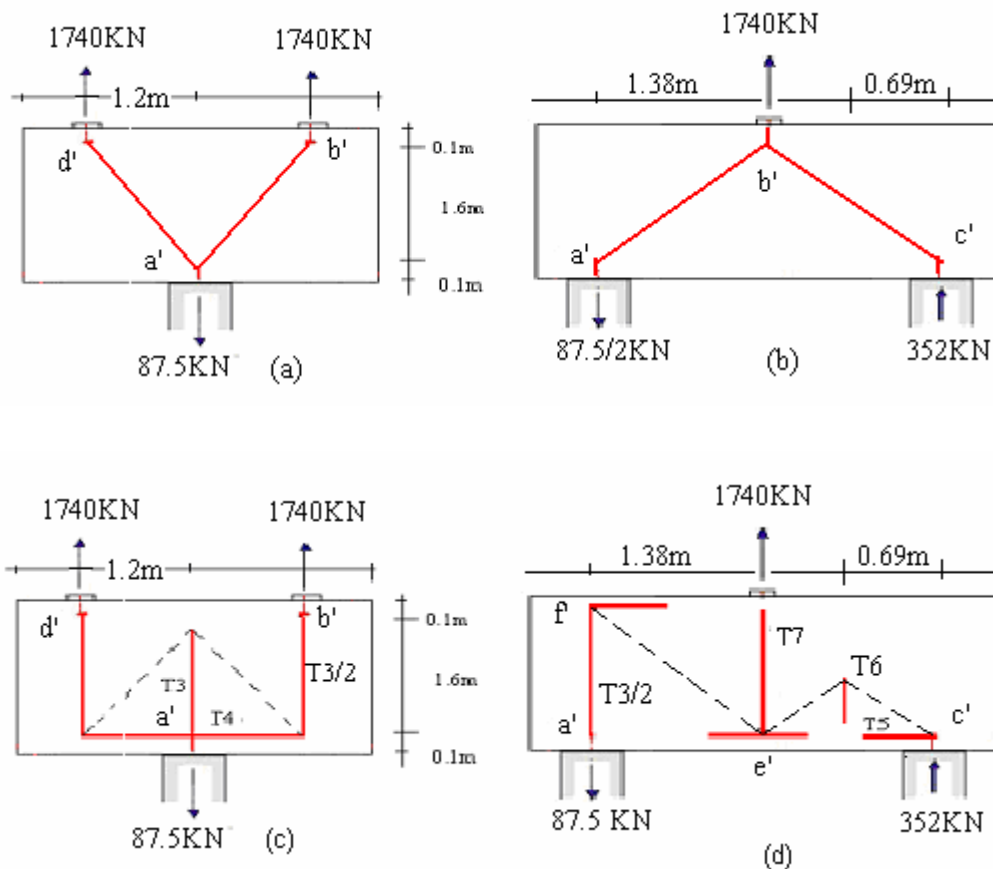


Fig. 5.14 the boundary forces on the tension side of region near column A, a) & b) simple truss c) & d) the refined STM with practical reinforcement layout

However, in order to have a practical reinforcement layout the STM in fig 5.14 a & b are replaced by a refined STM model as in Fig 5.14 c and d.

The member forces are determined from the nodal equilibrium of the region the truss model and the corresponding steel, if necessary shall be provided.

From figure 5.14c

$$T3 = 87.5 \text{ KN}$$

$$T4 = (T3)/2 * (1.2 / 1.6) = 87.5/2 * 1.2/ 1.6 = 33 \text{ KN}$$

The transverse tensile force due to the compressive force $C_a'f'$ is so small that it may be neglected in the analysis and all other STM members forces are determined using the nodal equilibrium and the result is shown below.

From figure 5.14d

$$T5 = 352 * 0.69 / 0.8 = 303.6 \text{ KN}$$

$$T6 = 352 \text{ KN}$$

$$T7 = T3/2 + T6 = 87.5 + 352 = 439.5 \text{ KN}$$

Once again the compressive force in the strut $e'f'$ is so small that the transverse tension developed in the region may be neglected to simplify the analysis but for other members the tension reinforcement is determined from material strength requirements.

$$T3 = 87.5 \text{ KN} \quad A_s 3 = 250 \text{ mm}^2$$

$$T4 = 33 \text{ KN} \quad A_s 4 = 94 \text{ mm}^2$$

$$T5 = 303.6 \text{ KN} \quad A_s 5 = 872 \text{ mm}^2$$

$$T6 = 352 \text{ KN} \quad A_s 6 = 1011 \text{ mm}^2$$

$$T7 = 439.5 \text{ KN} \quad A_s 7 = 1136 \text{ mm}^2$$

iii) Column type action of the two trusses

As we can see, each truss is not in equilibrium in the plane of analysis. In order to obtain the equilibrium the connection of each of the two regions is shown below, one for each bottom direction support. As we can see partial of the top force is transferred to the bottom of figure 5.15a and the other is to B.

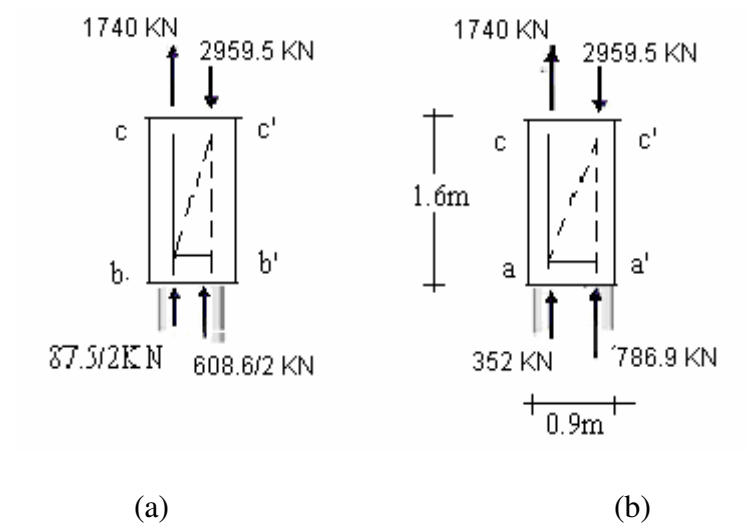


Fig. 5.15 column type truss due to the adjoining simple truss in region near column 1

Assuming that the proportion of the top force for each truss to be proportional to the bottom force,

The force on the top of truss,

$$\text{Ratio of } C_{\text{top}} = (608.6/2) / (608.6/2 + 786.9) = 0.28$$

$$C_{\text{top},b} = 0.28 * 2959.6 = 828.7 \text{ KN}$$

$$C_{\text{top},c} = 2959.6 - 828.9 = 2130.9 \text{ KN}$$

From equilibrium of figure a,

$$C_{ab'} = 828.7 - 608.6/2 = 524.4 \text{ KN}$$

$$T_{aa'} = C_{ab'} (aa' / ab') = 524.4 * (0.9 / \sqrt{(1.6^2 + 0.9^2)}) = 524.4 * 0.9 / 1.84 = 256.5 \text{ KN}$$

$$\text{As } aa' = T_{aa'} = f_{yd} = 256.5 / 348 = 737 \text{ mm}^2$$

From equilibrium of figure b,

$$C_{ac'} = 2130.9 - 786.9 = 1344 \text{ KN}$$

$$T_{aa'} = C_{ac'} (aa' / ac') = 1344 * (0.9 / \sqrt{(1.6^2 + 0.9^2)}) = 1344 * 0.9 / 1.84 = 657.4 \text{ KN}$$

$$A_s = T_{aa'} / f_{yd} = 657.4 / 348 = 1890 \text{ mm}^2$$

The summary of the reinforcement determined from the statical calculation is shown below.

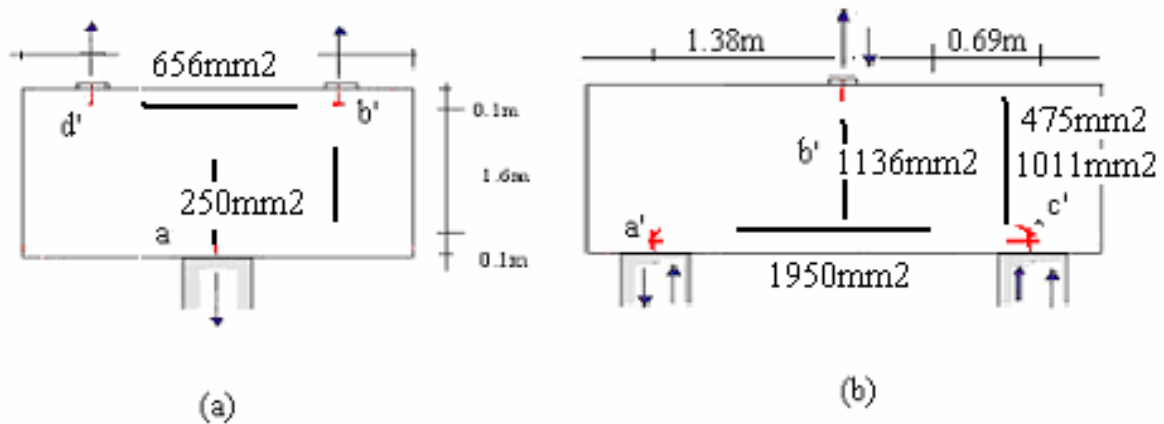


Fig 5. 16 Reinforcement layout of region near column 1

Width in which reinforcement is placed at top for $w_{bd} = 0.9\text{m}$

$$\text{using } \phi 20, \# = 656/314 = 2.1, \quad \text{spacing } s = 1.2/2.1 = 570\text{mm}$$

Width in which reinforcement is placed for $w_{ac} = 0.9\text{m}$

$$\text{using } \phi 20, \# = 1950/314 = 6.2, \quad \text{spacing } s = 0.9 / 6.2 = 145\text{mm}$$

using $\phi 20$ c/c 140mm

Similarly for the column type truss, $w_{aa'} = 1.2\text{m}$

$$\text{Using } \phi 20, \# = (737 + 1890) / 314 = 8.37, \quad \text{spacing } , s = 1.2\text{m} / 8.37 = 143\text{mm}$$

using $\phi 20$ c/c 145mm

The vertical reinforcement is given by arithmetic sum of the right hand side bar,

$$A_s = 475 + 1011 = 1486 \text{ mm}^2$$

Using $\phi 12$, $\# = 1480 / 113 = 13$ on one side of the member or in 0.9×1.38 i.e. the placing $\phi 12$ c./c 300mm

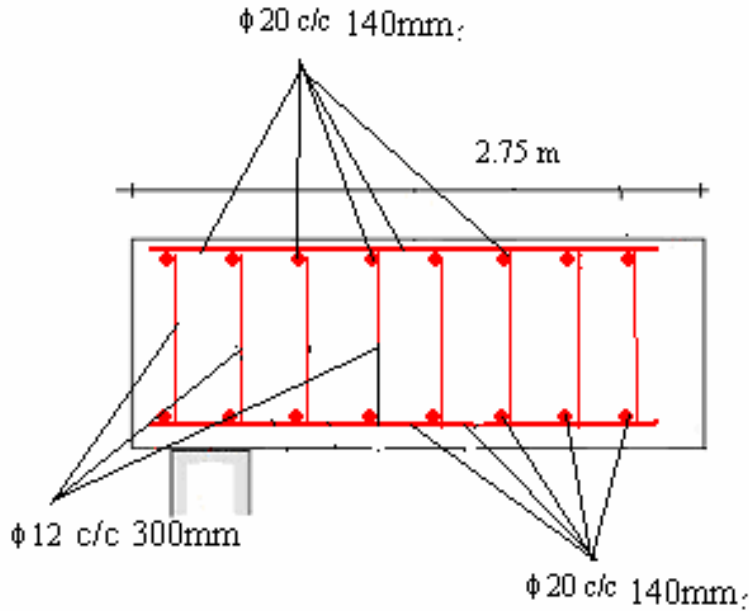


Fig 5.17 Reinforcement layout of the Disk near Column A

2. Static Calculation for Critical Section near Column B

The forces in the region near column B are shown in the figure below.

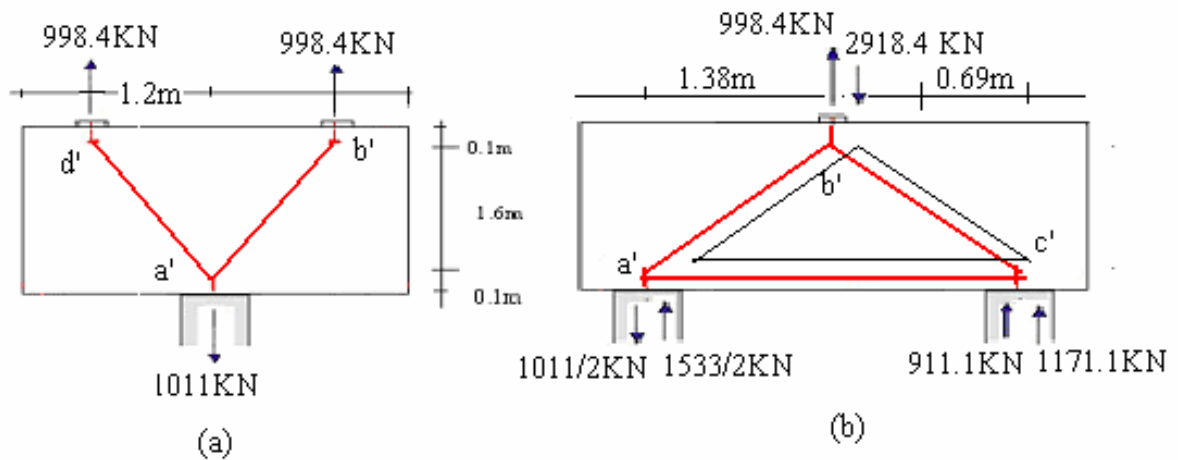


Fig. 5.18 Boundary forces and STM representation of compression section of node near column 4

As shown in the figure above, the forces on the top are connected to the bottom in truss model.

The vertical force equilibrium is checked:

$$\sum F_v = 0 \neq 2082.3 + 2543.9/2 - 1920$$

This shows that the unbalanced force is transferred to the other column that is not shown in the figure. For simplicity of the analysis, each truss of the region is considered alone and later combined to consider the effect of one on the other.

iv) Region with all compressive node forces

The forces on this section of the region are redrawn, below, for clarity and the assumed STM model and try to show the transverse tension in the compressive strut.

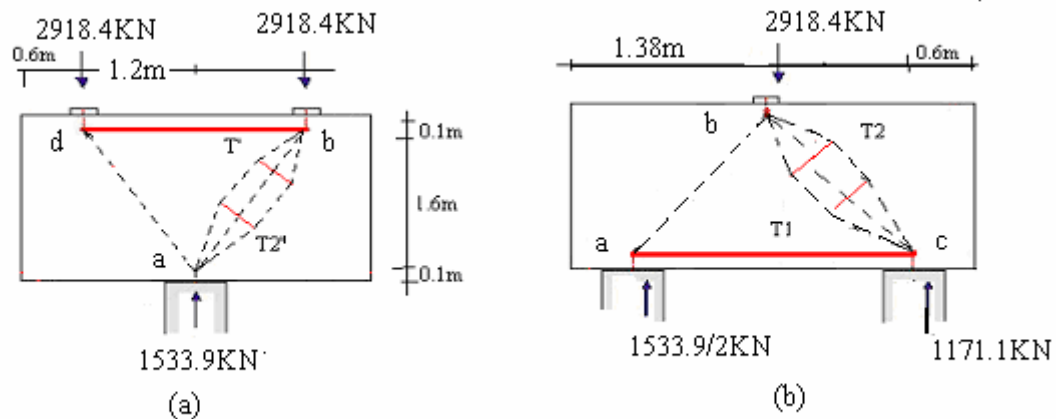


Fig 5.19 Boundary forces and STM representation of compression section near column B

From the equilibrium of the nodes the member force are obtained as follows:

$$C_{ab} = (1533.9/2) * \sqrt{(1.6^2 + 1.2^2)} / 1.6 = 767 * 2 / 1.6 = 959 \text{ kN}$$

$$T_{bd} = C_{ab} * 1.2 / 2 = 959 * 1.2 / 2 = 575.4 \text{ KN}$$

$$T_2' = 0.25 C_{ab} (1 - a / b_{eff})$$

$$a = 0.2, \text{ (strut width } a = 0.2)$$

$$b_{eff} = a + l/6 = 0.2 + 2/6 = 0.53\text{m (well inside the region)}$$

$$T_2' = 0.25 * 959 * (1 - 0.2 / 0.53) = 150 \text{ KN}$$

From figure (b)

$$C_{cb} = (1171.1 -) * \sqrt{(1.38^2 + 1.6^2)} / 1.6 = 11171.1 * 2.11 / 1.6 = 1544 \text{ KN}$$

$$T_{ac} = 1544 * 1.38 / 2.11 = 1009 \text{ KN}$$

$$T_2 = 0.25 C_{cb} (1 - a / b_{eff})$$

$$a = 0.4, \text{ (strut width } a = 0.2 \text{ compression width)}$$

$$b_{eff} = a + l/6 = 0.2 + 2.11/6 = 0.55\text{m (well inside the region)}$$

$$T_2 = 0.25 * 1629 * (1 - 0.2 / 0.55) = 245 \text{ KN}$$

The reinforcement to be provided in this region is proportioned using the steel property and as shown;

From figure (a)

$$T_{bd} = 575.4 \text{ KN} \quad A_s = 575.4 / 348 = 1620\text{mm}^2$$

$$T_2' = 150 \text{ KN} \quad A_s = 150 / 348 = 431\text{mm}^2$$

From figure (b)

$$T_{ac} = 1009 \text{ KN} \quad A_s = 1009 / 348 = 2890\text{mm}^2$$

$$T_2 = 245 \text{ KN} \quad A_s = 245 / 348 = 704 \text{ mm}^2$$

v) Region with tension node force

As can be seen the second STM model consists of tension members as shown in the figure below.

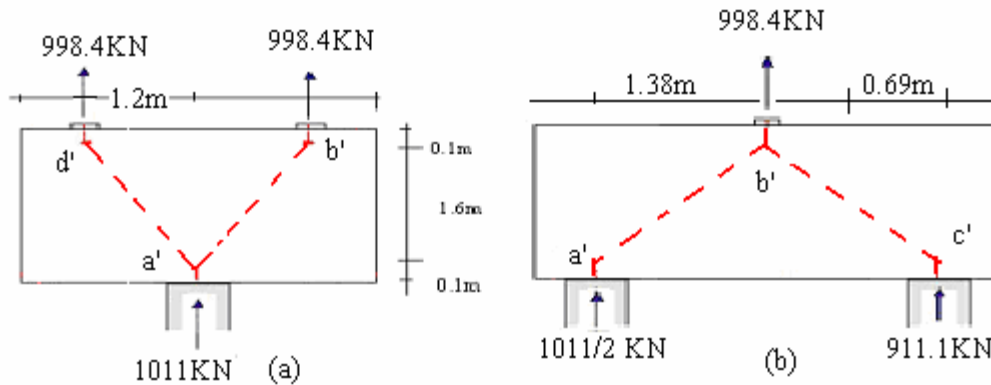


Fig. 5.20 Boundary forces and STM model representation for tension forces

From the figure, it can be seen that the region is not in equilibrium with these forces but a force in the third direction is necessary for the truss to be stable. Due to the presence of compressive force in the third direction and the practical reinforcement layout the STM will be refined as shown below.

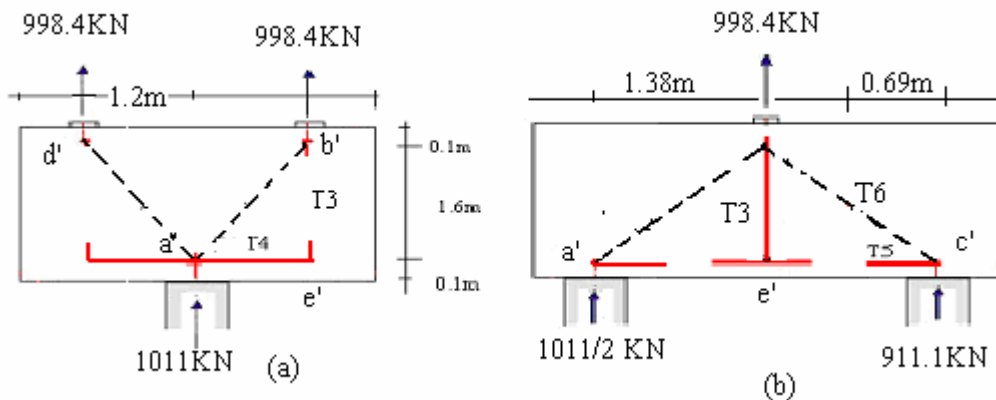


Fig. 5.21 Boundary forces and refined STM model for tension forces

The member forces are determined from the nodal equilibrium of the region.

From figure a

$$T3 = 998.4 \text{ KN}$$

$$T4 = (1011/2) * (1.2 / 1.6) = 379 \text{ KN}$$

The transverse tensile force due to the compressive force $C_{b'c'}$ is so small that can be neglected in the analysis. From figure 5.21b

$$T_5 = 911.1 * 1.38 / 1.6 = 785.6 \text{ KN}$$

$$T_6 = 0.25 C_{b'c'} (1 - a / b_{eff})$$

$$C_{b'c'} = 911.1 * 2.11 / 1.6 = 1201 \text{ KN}$$

$$a = 0.2, \text{ (strut width } a = 0.2)$$

$$b_{eff} = a + l/6 = 0.2 + 2.11/6 = 0.55\text{m (well inside the region)}$$

$$T_6 = 0.25 * 1201 * (1 - 0.2 / 0.55) = 191 \text{ KN}$$

The transverse tension due to the compressive force $C_{a'b'}$ is assumed to be equal to T_6 .

The reinforcement required is as shown below.

$$T_3 = 998.4 \text{ KN} \quad A_{s3} = 2870 \text{ mm}^2$$

$$T_4 = 379 \text{ KN} \quad A_{s4} = 1080 \text{ mm}^2$$

$$T_5 = 785.6 \text{ KN} \quad A_{s5} = 2257 \text{ mm}^2$$

$$T_6 = 191 \text{ KN} \quad A_{s6} = 550 \text{ mm}^2$$

vi) Column type action of the two trusses

As we can see, each truss is not in equilibrium in the plane of analysis. In order to obtain the equilibrium the connection of each of the two regions is shown below, one for each bottom direction support. As we can see partial of the top force is transferred to the bottom of figure 5.22a and the other to 5.22b.

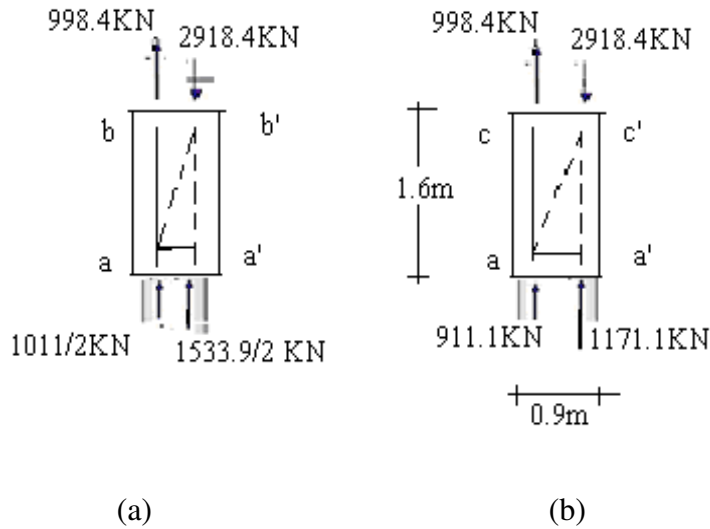


Fig. 5.22 Boundary forces and STM representation of compression section of node

Assuming that the proportion of the top force for each truss to be proportional to the bottom force, The force on the top of truss in a,

$$\text{Ratio of } C_{\text{top}} = (1533.9/2) / (1533.9/2 + 1171.1) = 0.40$$

$$C_{\text{top},a} = 0.40 * 2918.4 = 1167 \text{ KN}$$

$$C_{\text{top},b} = 2918.6 - 1167 = 1751.6 \text{ KN}$$

From equilibrium of figure 5.22a,

$$\text{Vertical component of } C_{ab'} = 1167 - 1533.9/2 = 400 \text{ KN}$$

$$C_{ab'} = 400 * \sqrt{(1.6^2 + 0.9^2)} / 1.6 = 460 \text{ KN}$$

$$T_{aa'} = C_{ab'} (aa' / ab') = 460 * (0.9 / \sqrt{(1.6^2 + 0.9^2)}) = 460 * 0.9 / 1.84 = 225 \text{ KN}$$

$$\text{As } aa' = T_{aa'} / f_{yd} = 225 / 348 = 647 \text{ mm}^2$$

From equilibrium of figure 5.22b,

$$\text{Vertical component of } C_{ac'} = 1751.6 - 1171 = 580 \text{ KN}$$

$$T_{aa'} = C_{ac'} (aa' / ac') = 580 * (0.9 / 1.6) = 326.3 \text{ KN}$$

$$\text{As } aa' = T_{aa'} / f_{yd} = 326.3 / 348 = 940 \text{ mm}^2$$

The summary of the reinforcement is shown in the figure below.

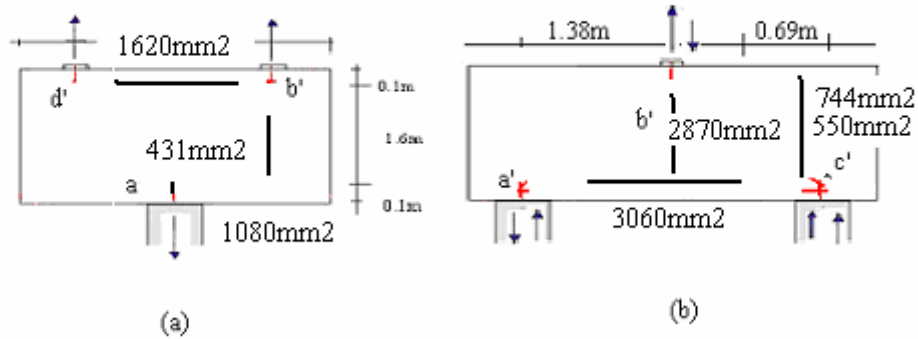


Fig. 5.23 Reinforcement of Disc region near Column B

Width in which the reinforcement is placed at top for $w_{bd} = 0.9m$

$$\text{Using } \phi 20, \# = 1620/314 = 5.2, \quad \text{top \& bottom spacing } s = 1.2/5.2 = 230mm$$

Width in which reinforcement is placed for $w_{ac} = 0.9m$

$$\text{Using } \phi 20, \# = 3060/314 = 9.7, \quad \text{spacing } s = 0.9 / 9.7 = 145mm$$

Using $\phi 20$ c/c 140mm

Similarly for the column type truss, $w_{aa'} = 1.2m$

$$\text{Using } \phi 20, \# = (647 + 940) / 314 = 5.1, \quad \text{spacing, } s = 1.2m / 5.1 = 230mm$$

Using $\phi 20$ c/c 230mm

The vertical reinforcement is given by arithmetic sum of the right hand side bar,

$$A_s = 704 + 550 = 1486 \text{ mm}^2$$

Using $\phi 12, \# = 1486 / 113 = 13.1$ on one side of the member or in $0.9 * 1.38$ i.e. the placing $\phi 12$ c/c 300mm

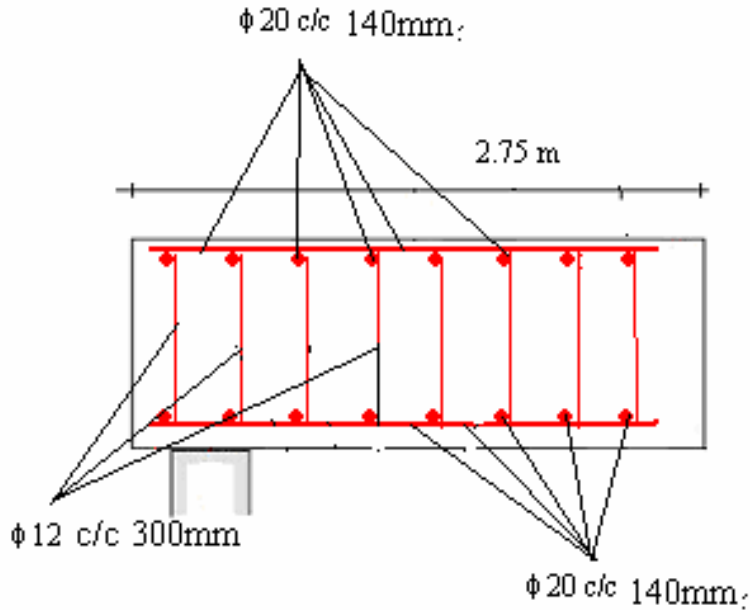


Fig. 5.24 Reinforcement layout for the region near Column 1

5.8.4 Inclined Column STM model and Statical Calculations

On area of focus of the thesis is the inclined column with variable cross-sections along the height. We will attempt to design the inclined column using the STM method. The boundary forces on each of the six-inclined column is as shown in table 5.2c. Only two inclined columns, column 1 and column 4 handled, because they are the most critically loaded.

Design procedure

Step 1 - Determine boundary forces from the overall analysis

The boundary forces are obtained from the overall analysis that are tabulated in table 5.3 & table 5.4 and magnitude and orientation is as shown in the figure below.

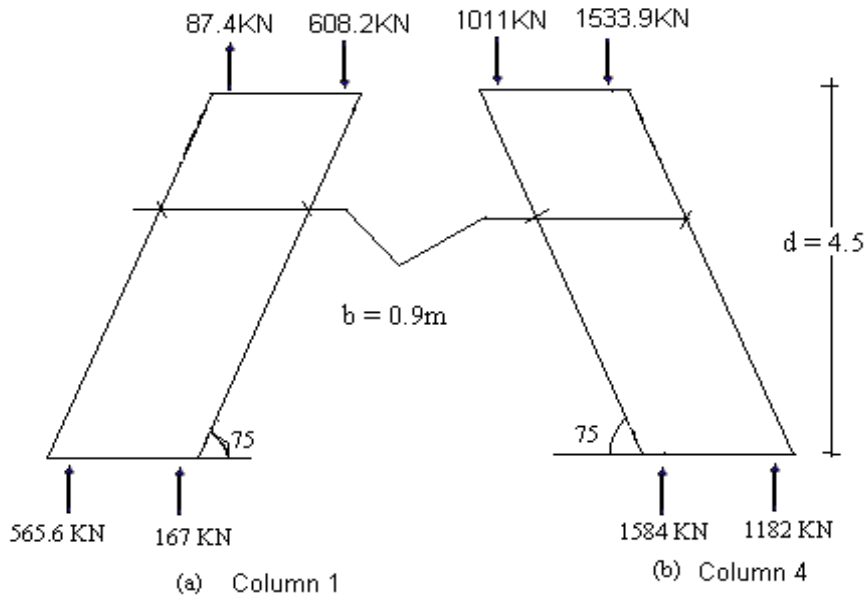


Fig 5.25 the boundary force on the inclined Column 1 and Column 4

Step 2: Divide the structure in to B & D region

The inclined column is variable in cross section through out the height and it may be replaced by a number of uniform sections or by single section. For this structure, we model the inclined column having constant equivalent dimension. This section is obtained by considering the stress developed at the boundary.

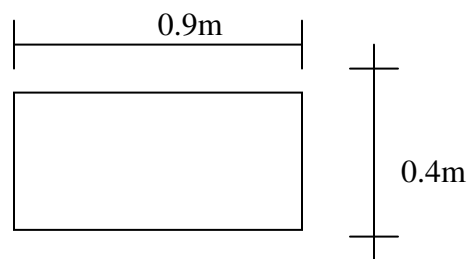


Fig 5.26 Uniform column dimension for design of the truss model

We will check of the section for the worst boundary force condition, with maximum force for the reduce area.

$$\begin{aligned} \sigma &= P/A \\ &= (1584+1182) / (0.4*0.9)= 7.69\text{MPa} < 13.6 \text{ MPa} = f_{cd} \end{aligned}$$

Step 3: Equilibrium of the inclined column

The equilibrium of the section is checked in order to understand the flow of forces in the region.

For the Column 1: $\Sigma F_V = 0 \neq 608.6 - (87.4 + 565.6 + 167) = -211.4 \text{ KN}$

For the Column 4: $\Sigma F_V = 0 \neq 1533.9 + 1011 - (1584 + 1182) = -221. \text{ KN}$

The bottom boundary force is larger than the top one due to the inclusion of the own weight of the inclined column, cumulatively added to the bottom. To balance this, adding a fictitious force at the top will give us equilibrium member forces.

Step 4: Determination of Truss member forces

The trial truss for both columns is obtained by considering a diagonal strut Cd at an inclination of 45° from the base of the column. From the geometry of the column, width is 0.9m and column height is 4.5 m, we will have five diagonal struts. From the equilibrium of nodes a horizontal tension develops for which reinforcement shall be provided to resist them, see figure below.

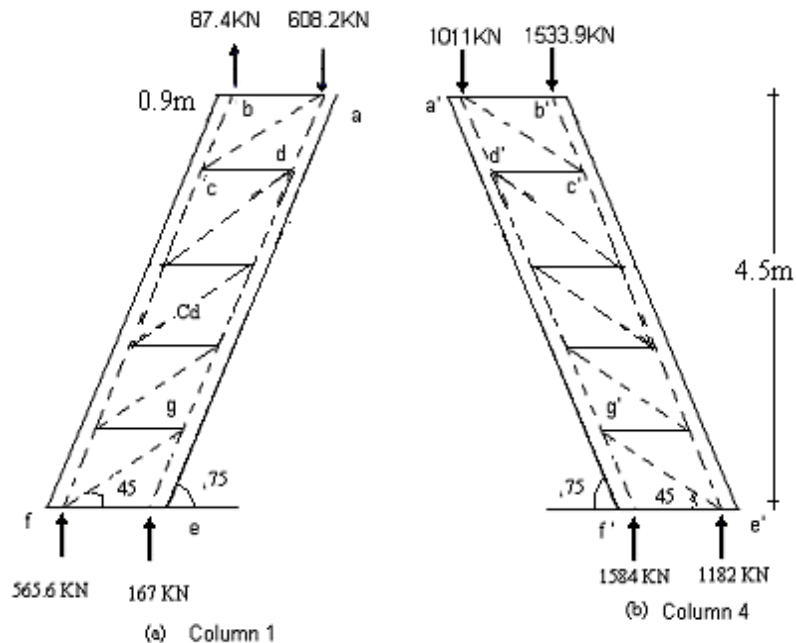


Fig 5.27 Inclined columns with STM model, diagonal strut at 45° and horizontal tension

Step 5: Diagonal compression force

The diagonal compression in this section is constant from geometry and so the variation in the vertical force is equally shared in every section.

$$\text{For column 1: } C_d = (565.6 - 87.4) / 4 = 119.6 \text{ KN}$$

$$\text{For column 4: } C_d = (1584 - 1011) / 4 = 143.2 \text{ KN}$$

The horizontal force in the horizontal direction is obtained from geometry, $C_{d_v} = C_{d_H}$. The balancing tension in the section shall be

$$T = C_{d_H} = 143.2 \text{ KN}$$

$$A_s = T / f_{yd} = 143.2 / 348 = 411 \text{ mm}^2 \text{ (per width of the regions, 0.9m)}$$

$$A_{s \text{ net}} = a_s / 0.9 = 411 / 0.9 = 457 \text{ mm}^2$$

Since we use a closed stirrup of $\phi 10 \text{mm}$, $\# = 457 / (2 \times 78) = 2.9$

Hence use closed stirrup, 3 $\phi 10$ /m or use $\phi 10$ c/c 300mm. Fro each inclined column.

Step 6: Main reinforcement

Apart from very small tension on the top of column 1 ($T = 87.4 \text{KN}$), all other boundary forces are compressive. As a result, the column is in compression and the section may not be provided tension reinforcement. However, EBCS-2 recommends a minimum reinforcement ratio of 0.008 for column and a maximum of 0.04. Therefore, we shall provide the minimum reinforcement.

$$A_s = 0.008 A_c, \quad A_c = \text{area of concrete}$$

$$A_c = (0.8 + 1.2) / 2 * 1.38 = 1.38 \text{mm}^2$$

$$A_s = 0.008 * 1,380,000 = 11040 \text{ mm}^2$$

For the sake of comparison we use $\phi 28$, $A_{s \text{ bar}} = 615 \text{ mm}^2$

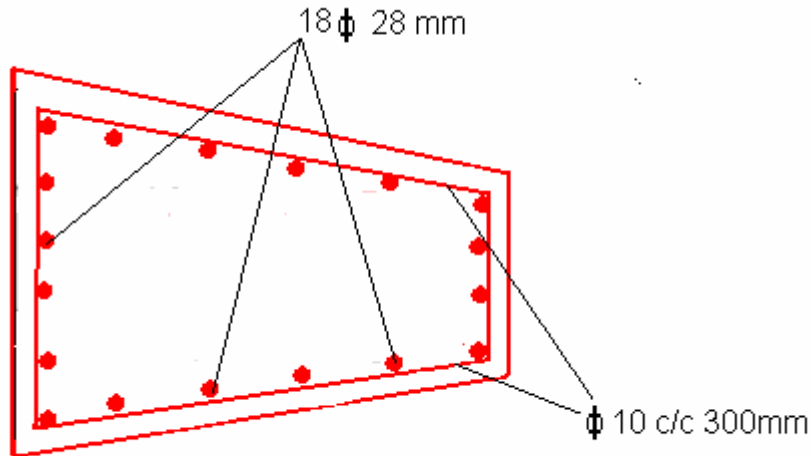


Fig 5.28 Reinforcement layout of inclined column.

5.8.5 Reinforcement Summary

The final outputs of both approaches, that is the initial modeling and analysis using stress analysis [18] and that of the STM analysis, is compared by considering the reinforcement amounts and spacing for both regions, see the detailed in the table 5.5 below.

Table 5.5 Reinforcement layouts for the Disk and Column regions

Region	Reinforcement types	STM Method	Stress Analysis
Disc region	Main reinforcement	$\phi 20$ c/c 140 mm	$\phi 20$ c/c 140 mm
	Transverse reinforcement	$\phi 20$ c/c 140 mm	$\phi 20$ c/c 140 mm
	Vertical	$\phi 12$ c/c 300 mm	$\phi 12$ c/c 150 mm
Column region	Main reinforcement	18 $\phi 28$ mm	18 $\phi 28$ mm
	Stirrup	Single $\phi 10$ c/c 300	$\phi 10$ c/c 200

CHAPTER 6

6.1 Conclusion

As the above discussion indicates, the STM method is a simple analysis and has quite a wide application to many types as well as parts of structures. As an alternative method of analysis, it may also be used as a counter check to other types of analysis.

Two types of structures have been addressed in this approach, the first one being simply supported deep beam and the second one a corbel. The deep beam analysis using the STM method has yielded results that are same with other methods of analysis.

In the instance of the corbel, the STM analysis has resulted in the determination of higher transverse tension reinforcement amounts that are not even addressed by the code, indicating a more detailed analysis result.

As was shown earlier, modeling of the obelisk at Bahir Dar using STM has resulted in a close checking of the structure, demonstrating its validity and practical application. In this check, it has been demonstrated that the reinforcement quantities obtained for the obelisk are nearly the same for both methods. Except in one area where the reinforcement was rather higher. This is true because the STM method uses the lower bound principle which gives a conservative result. In addition to this, the STM method's simplicity in modeling and analysis makes it a handy tool that may be used by almost every one beginning from students to practicing engineers. The application of this approach also gives a preliminary prediction of the amount and intensity of the stresses that may be inherent in a system; hence, designers are aware of the outcome ahead of time.

As we have seen previously the STM method is a powerful analysis approach particularly for discontinuous or D regions, even though its application may cover all section of a member. In addition to this, the STM method facilitates a clear vision in areas of critical sections that shall be addressed with great attention when designing and construction. Hence, as an alternative stress check mechanism the STM method offers a powerful means.

6.2 Recommendations

The Strut-and-Tie method of modeling and analysis, as seen from previous discussion, is a handy tool that can be applied to every part of a structure. However, in the thesis, only two-dimensional modeling and analysis of the monument (sample structure) was carried out in order to simplify analysis even though the internal stress have three dimensions behavior, which a limitations of the thesis. The other limitation is replacing the irregular shaped inclined column by a single uniform section, which would have been better if it was replaced by a number of uniform sections. In this line, the thesis does not show in a systematic way what length of the structure shall be replaced by a single uniform section.

One may attempt to solve these limitations by developing computer software that will be used in estimating the actual pattern of the stress trajectories and the respective point of application of the lumped force in the area, which are location of the struts and ties as well as the nodes of the STM model. The result has to be justified either by laboratory test results or from detailed non-linear stress analysis of the respective structures.

The STM method of modeling by it nature gives usually conservative reinforcement in structure. Hence, this is also one area where further research has to be carried to obtain an efficient and minimized reinforcement.

Annex

Annex 1

The monument was analyzed using line and shell element model for the SAP 2000N. Partial results that is the axial force, shear force and bending moment in both axis for both models is shown in the figures below, from Fig A1 to Fig A6.

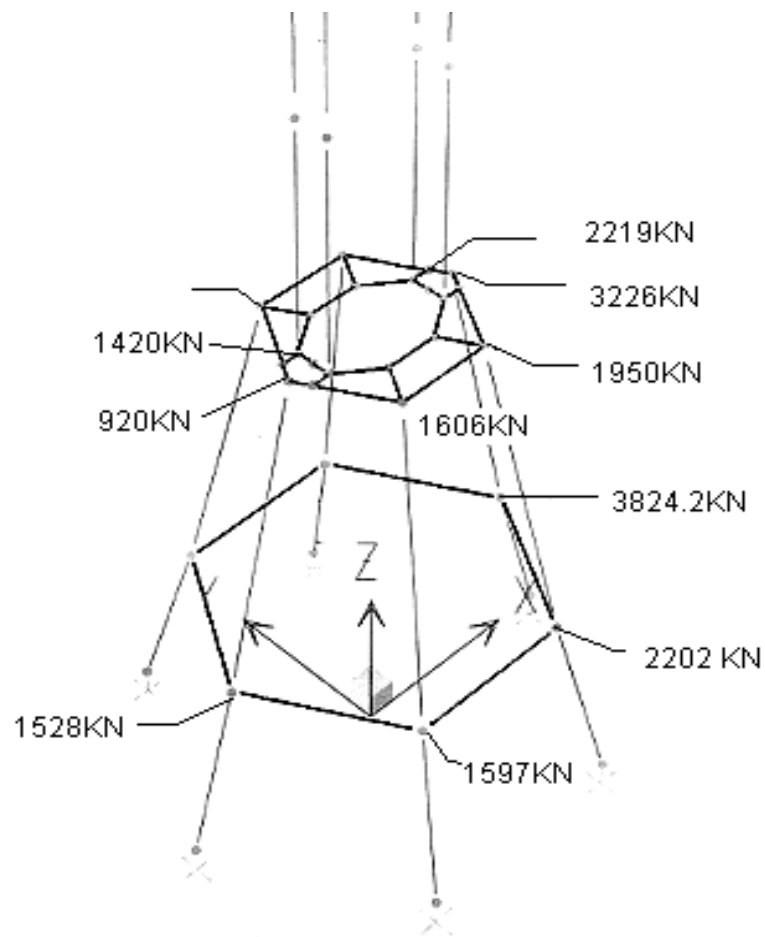


Fig. A1. SAP 2000N – File Trus_thesis4 – Axial Force Diagram (Comb 1)- KN-m Units

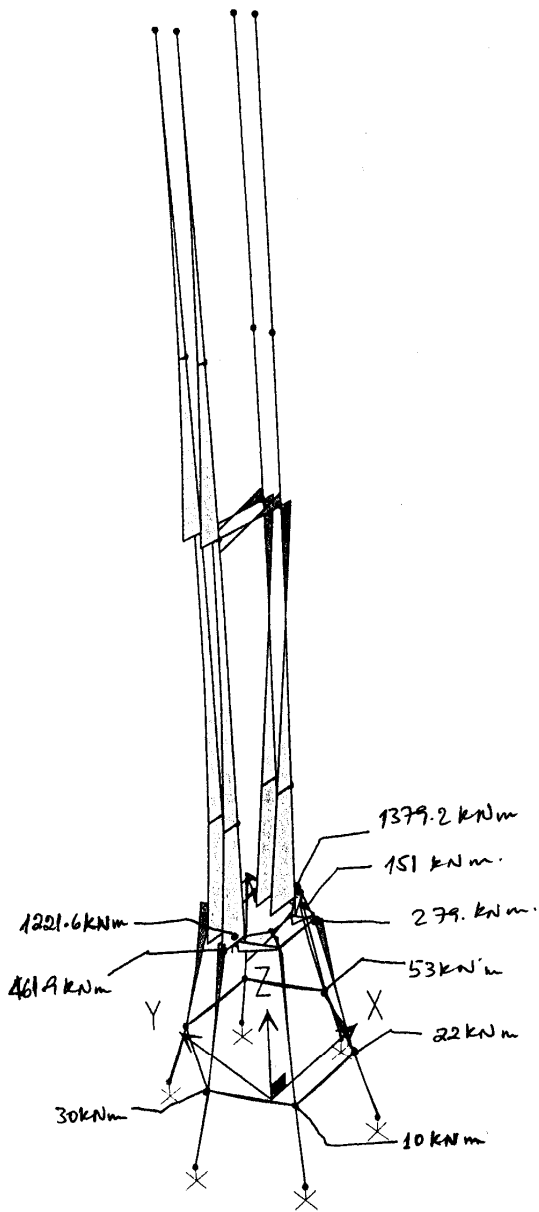


Fig. A2. SAP 2000N – File Trus_thesis4 - Moment 3-3 Diagram (Comb 1)- KN-m Units

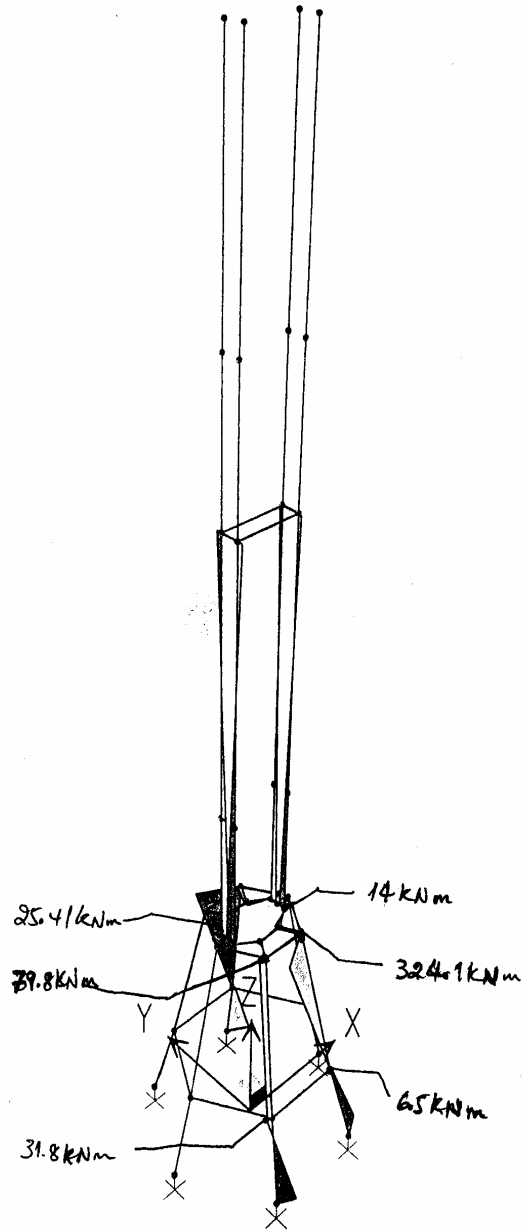


Fig. A3. SAP 2000N – File Trus_thesis4 - Moment 2-3 Diagram (Comb 1)- KN-m Units

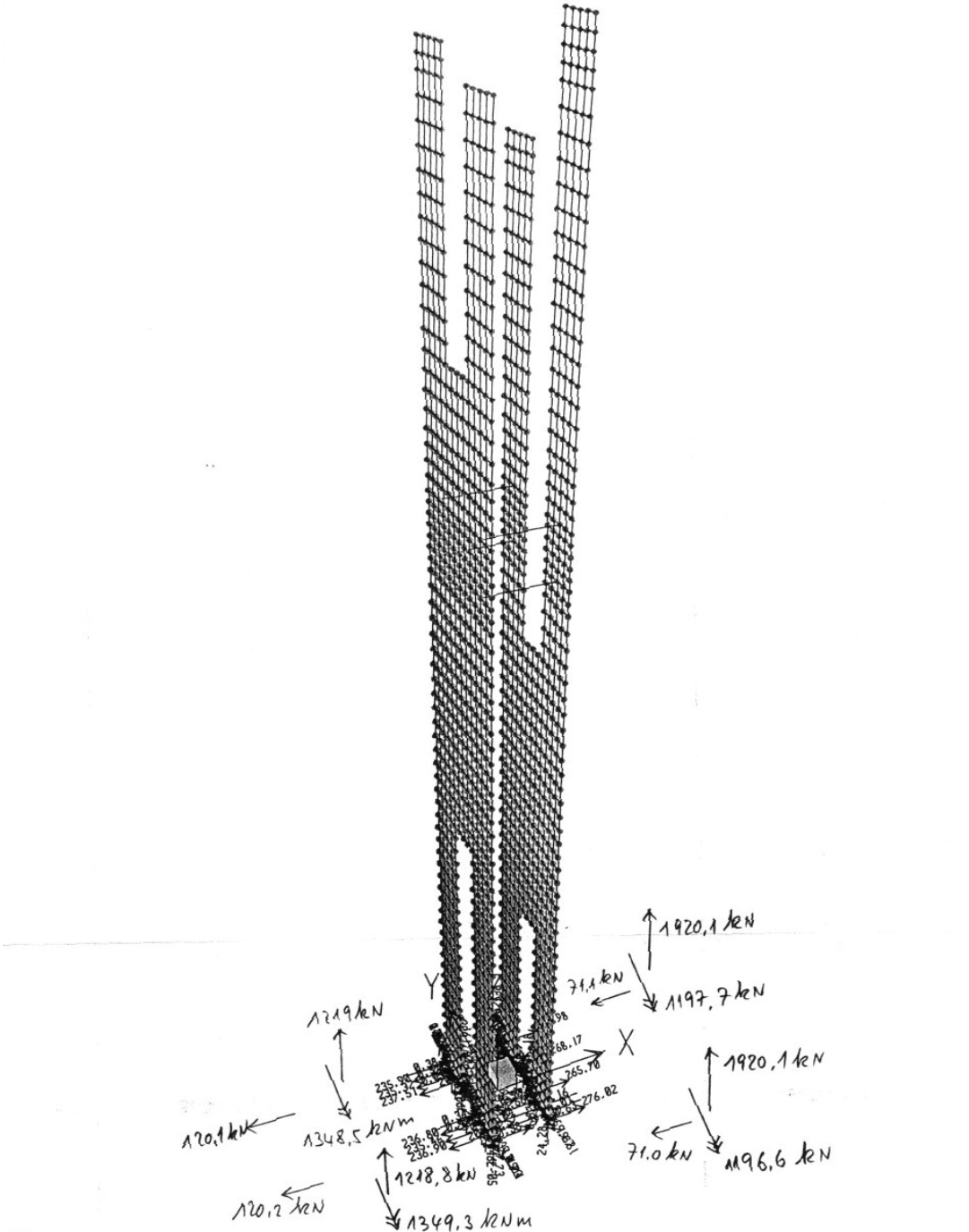


Fig. A4. SAP 2000N v7.21 – Restraint Reactions (COMB 1) – KN-m Units [18]

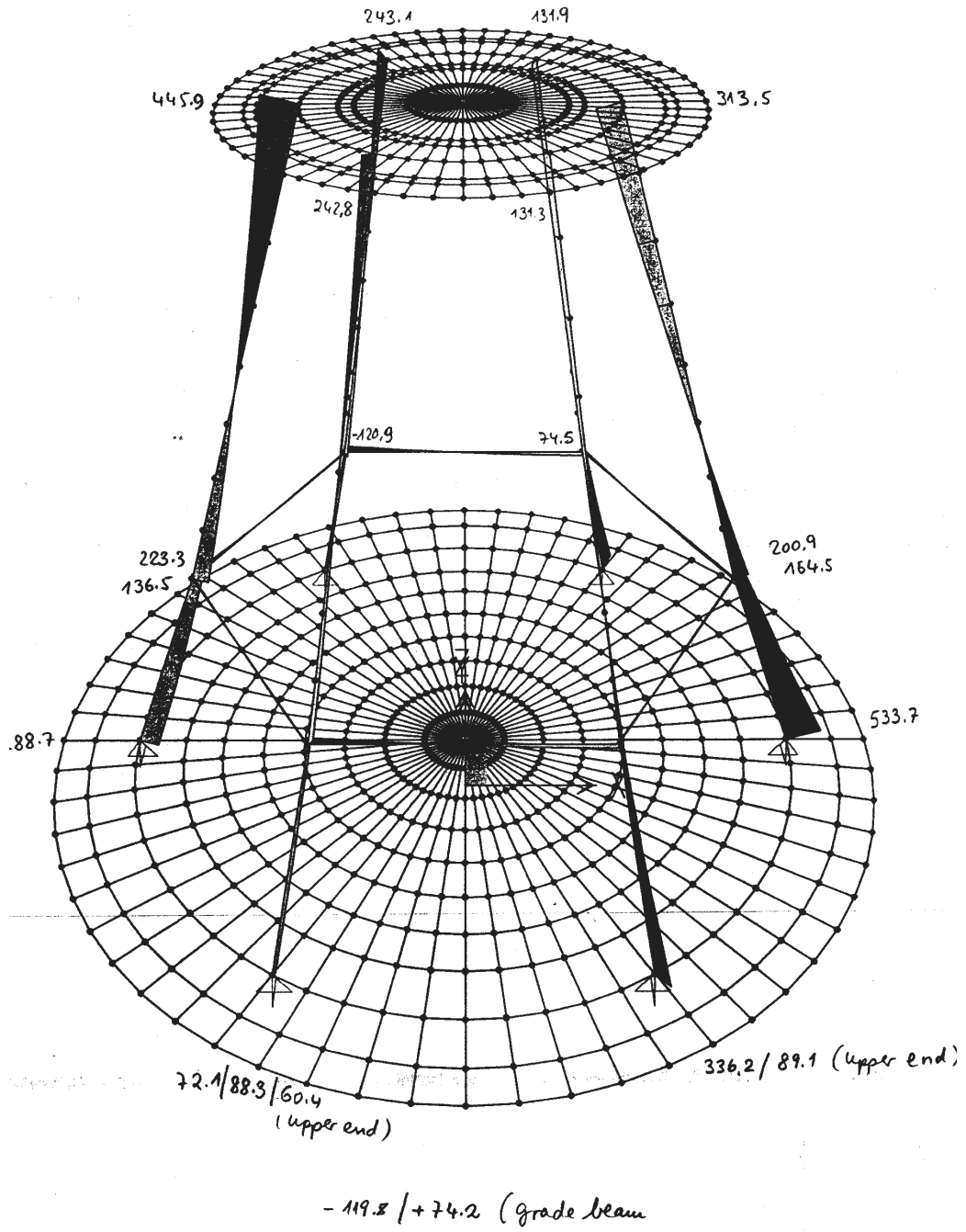


Fig. A4. SAP 2000N v7.21 – Moment 3-3 Diagram (COMB 1) – KN-m Units [18]

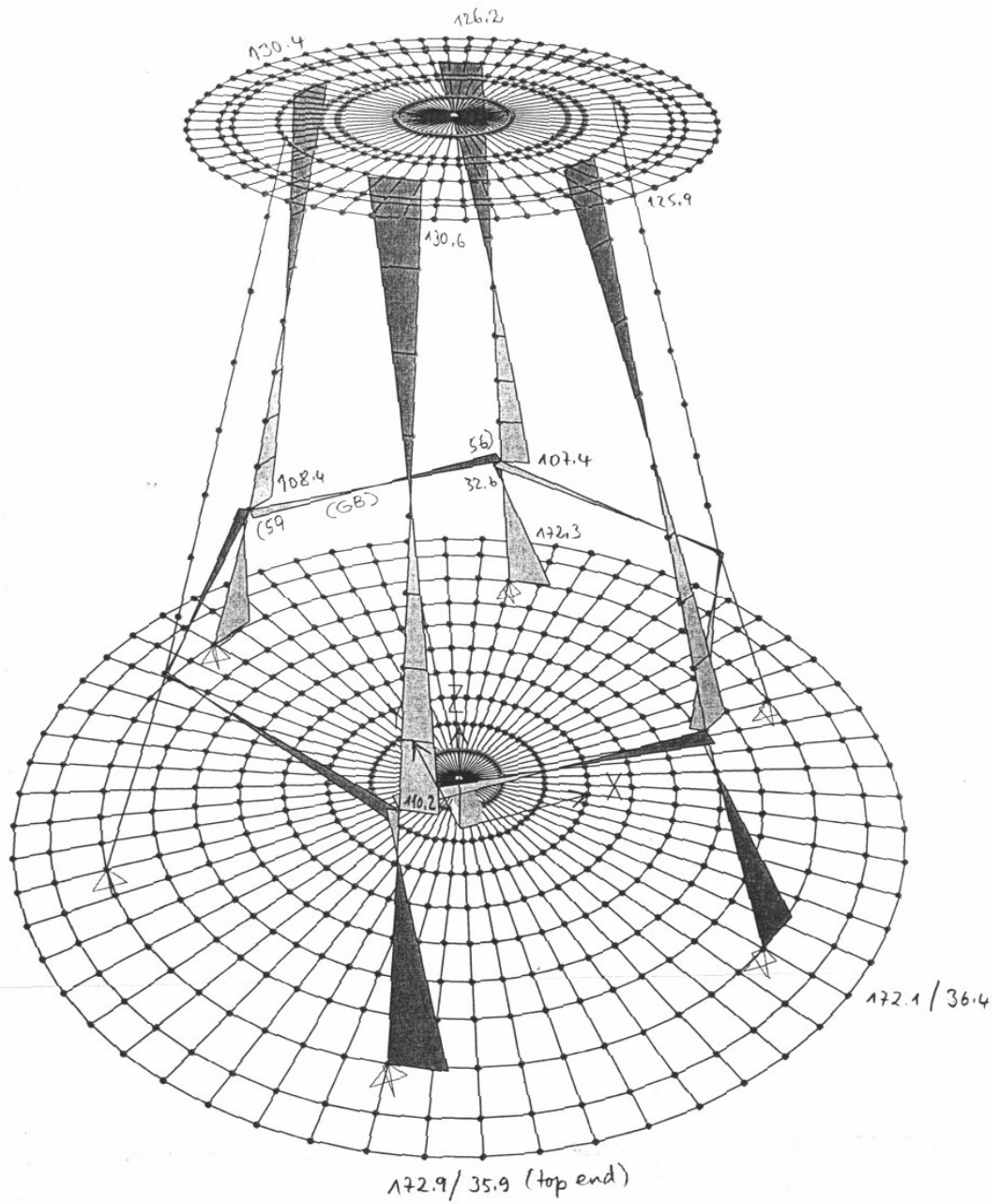


Fig. A5. SAP 2000N v7.21 – Moment 2-2 Diagram (COMB 1) – KN-m Units [18]

References

1. Jorg Schlaich, Kurt Schaefer, and Mattias Jennewein, "Towards a Consistent Design of Structural Concrete" journal of the Prestressed Concrete Institute, Vol.32, No 3, May –June 1987, pp 77-150
2. Schlaich, J., Schafer, K., "Konstruieren im Stahlbetonbau" (Design and Detailing of Structural Concrete), Beton-Kalender 1984, Part 11, W. Ernest & Sohn, Berlin-Munchen, pp.787-1005
3. Schlaich J., and Weischede, D., "Einpraktisches Verfahren Zum Methodischen Bemessen Und Konstruieren Im Stahlbetonbau" (A Practical Method For The Design And Detailing Of Structural Concrete), Bulletin D' Information No. 150, Comite Euro-International Du Beton, Paris, March 1982.
4. Ritter, W., "Die Bauweise Hennwbique" (The Hennebique System), Schweizerische Bauzeitung, Bd, XXXIII, No. 7, January 1899.
5. Morsch, E., "Der Eisenbetonbique, Seine Theorie Und Anwendung" (Reinforced Concrete, Theory and Application), Verlag Konrad Wittwer, Stuttgart, 1912.
6. Macgregor J. G, "Reinforced Concrete Mechanics and Design," 2nd edition, Prentice-Hall International Limited Inc., 1988.
7. Marti, P., "Basic Tools of Reinforced Concrete Beam Design," ACI Journal, V. 82, No 1, January-February 1985, Pp. 46-56.
8. Leonhardt, F., "Reducing The Shear Reinforcement In Reinforced Concrete Beams And Slabs," Magazine Of Concrete Research, V. 17, No. 53, December 1965, P. 187.
9. Rusch, H., "Uber Die Grenzen Der Anwendbarkeit Der Fachwerkanalogie Bei Der Berechnung Der Schubfestigkeit Von Stahlbetonbalken" (On The Limitation Of

- Applicability Of The Truss Analog For The Shear Design Of Reinforced Concrete Beams), Festschrift F. Campus "Amici Et Alumni," Universite De Liege, 1964.
10. Kupfer, H., "Erweiterung Der Morsch' Schen Fachwerkanalogie Mit Hilfe Des Prinzips Vom Minimum Der for Manderungsarbeit" (Expansion of Morsch's Truss Analog by Application of the Principle of Minimum Strain Energy), CEB-Bulletin 40, Paris, 1964.
 11. Thurlimann, B., Marti, P., Pralong, J., Ritz, P., And Zimmerli, B., "Vorlesung Zum Fortbildungskurs Fur Bauingeniure" (Advanced Lecture For Civil Engineers), Institute Fur Baustatik Und Konstruktion, ETH Zurich, 1983 (See Further Reference Here).
 12. Mueller, P., "Plastische Berechnung Von Stahlbetonscheiben Und Balken" (Plastic Analysis Of Reinforced Concrete Deep Beams and Beams), Bericht No. 83, Institute Fur Baustatik Und Konstruktion, Eth Zurich, July 1978.
 13. Cook, W. D.; Michell, D.: Studies of Disturbed Regions near Discontinuities In Reinforced Concrete Members. ACI Structural Journal, Vol. 85, No. 2, March-April 1988, P.206-216.
 14. Prof. S.P. Timoshenko, and Prof. J. N. Goodier, "Theory of Elasticity," 3rd Edition, B & Jo Enterprise Pvt Ltd, Singapore, 1974.
 15. Collins, M. P., and Mitchell, D., "Shear and Torsion Design of Prestressed and Non-prestressed Concrete Beams," PCI Journal, V. 25 No. 5, September-October 1980, Pp. 32-100.
 16. Ministry of Work & Urban Development, "Ethiopian Building Code Standard Part 2: Structural Use of Concrete," EBCS part 2, 1995.
 17. Euro code Nr. 2, "Design of Concrete Structure, Part 1," General Rules and Rules for Buildings. Commission of the European Communities, 1992.
 18. Dr Ing Girma Zerayohannes, et al., "Design of Reinforced Concrete Monument at Bahir Dar," Analysis and Design calculation, 2002.